University of Stavanger

Faculty of Science and Technology

MASTER'S THESIS

Study program/ Specialization: Petroleum Engineering / Drilling Technology	Fall semester, 2015 Open
Writer: Henrik Stenstrøm	……………………………………… (Writer's signature)
Faculty supervisor: Mesfin Belayneh	
Thesis title **Nano silica treated water based drilling fluid formulation and analysis in various polymers and salts systems**	
Credits (ECTS): 30	
Key words: Salts Polymers: XC, PAC, DUOVIS, CMC Drispac Nano Silica Bentonite Rheology Filtrate Hydraulics Viscoelasticity	Pages: ………118………… + enclosure: ……32…… Stavanger, …21/12/2015…………….. Date/year

Abstract

This thesis presents the formulation of nano silica particle based water drilling fluid, its characterization and performance simulation study. A total of ten test matrix fluid systems were designed to investigate the impact of single and combined additives such as salts, polymers and Nano silica on the drilling fluid properties. The fluids have been characterized through their rheology, pH, and filtrate loss. Further the viscoelasticity of the selected nano based fluid systems were analysed. The performances of the fluids are also simulated through hole-cleaning and hydraulics behaviours. Several observations have been discussed in the main report.

Among others, one formulation which allows 2.81ppb (8.0 kg/m^3) KCl is a DUO-VIS and CMC polymer system. Fluid 1 is a nano based drilling fluid. When fluid 1 is treated with an ex-situ *0.3g Na_2CO_3 salt*, the rheology improved greatly. The composition of the best Nano-silica based is:

- **Fluid 1**: = *500g H_2O + 0.1g Nano silica + 4g KCl + 0.75g Na_2CO_3 + 0.95g DUOVIS + 0.35g CMC + 25g Bentonite*

- **Fluid 2** = Fluid 1 + *0.3g Na_2CO_3 (ex-situ)*

Finally, this thesis comes to the conclusion that the application of nano silica has shown positive and negative results. The negative results can be improved by treating with polymers, which creates a positive synergy. A positive effect nano is the result of using the right concentration in a given salt and polymer system. In addition, the performance of KCl in nano treated system could be improved with other salts such as NaCl and Na_2CO_3.

Acknowledgment

First of all, I want to thank my supervisor Mesfin Belayneh for his never-ending engagement, guidance and knowledge, and for always being there for the students. You’re a good man.

Then I would like to thank the University of Stavanger for letting me use their facilities for my thesis, and letting me do it in the fall semester.

Finally I would like to thank my friends and family for the moral support throughout the entire process.

Contents

1 Introduction

Drilling fluids are used to drill oil & gas wells. The commonly used drilling fluid types are water based (WBM) and oil based (OBM) fluid systems. In terms of performance such as low friction coefficient and shale swelling avoidance, the application of oil based mud system is better than water based mud system. However, due to cost and environmental susceptible area, the common practice is to use inhibitive water based drilling fluid system. The basic composition of a drilling fluid contains shale inhibitive control additives, filtrate loss control polymers; viscosities control additives, and weighting agents. However, the conventional ''inhibitive'' WBM is not a 100% solution for shale swelling problem.

In an oil industry, nano technology research results have shown an improving performance on drilling fluid [1-3], cement [4], and enhanced oil recovery [5,6].

This thesis presents the formulation, characterization and performance simulation studies of nano-silica treated drilling fluid system.

The work presents an investigation of the effect of nano on polymer (PAC, DUOVIS, CMC, XC, & Drispac) based bentonite mud system. Several conventional (without nano) and nano based WBM systems were formulated and tested. The salt types used are: Na_2CO_3, $NaHCO_3$, NaCl, Na_2SO_4, and KCl.

The primary objective is to formulate and to evaluate the rheology, filtrate and pH properties nano fluid systems. The fluids will then be tested for their viscoelasticity properties. In addition, the hydraulic and hole cleaning efficiency of the system will also be simulated.

1.1 Background

As illustrated in Figure 1.1, a rotary drilling operation uses a continuous circulation of the drilling fluid when drilling a hole. Among many others, the main functions of drilling fluid are to (a) carry cuttings from downhole to the surface, and b) to keep well pressures within a desired safe window. Other functions are to cool and lubricate the bit [7]. For these purposes, it is important to formulate the right drilling fluid.

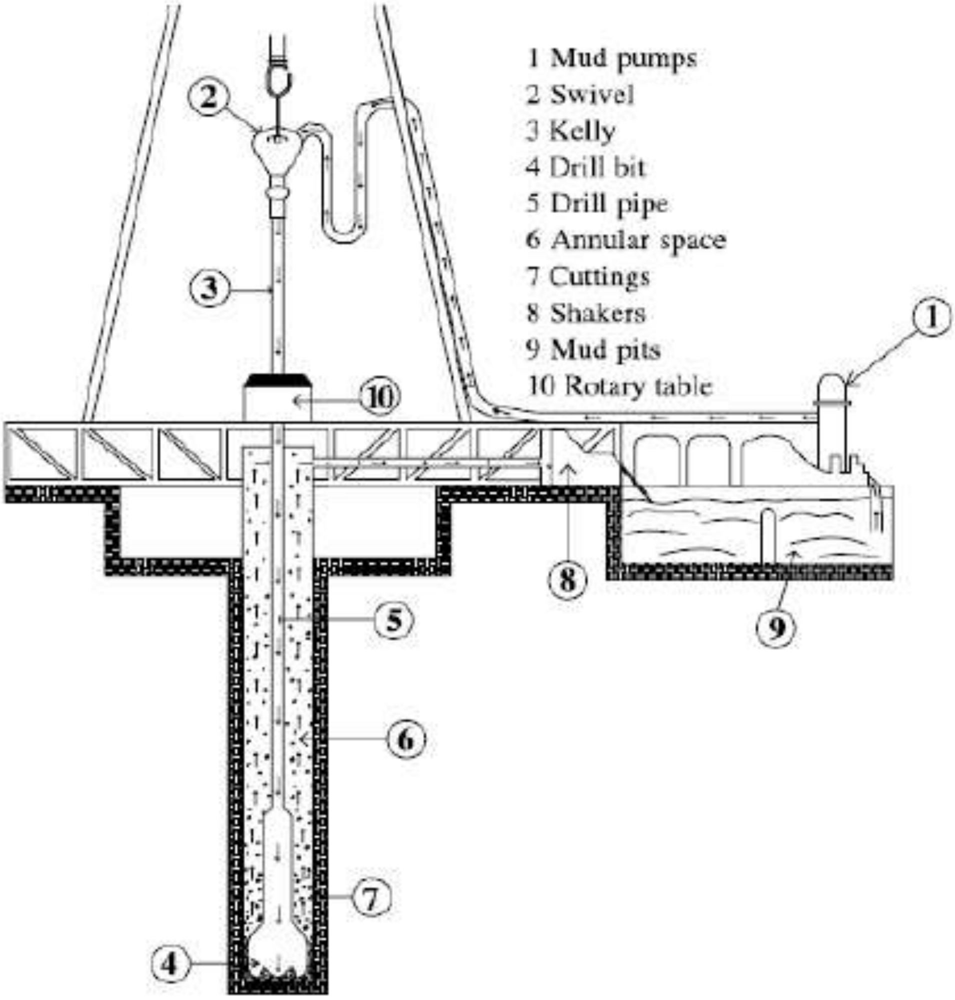

Figure 1.1: Drilling system [8].

A wrongly formulated drilling fluid causes undesired problems, such as formation damage, which reduces productivity; fluid filtrate into a formation influences the well log data and finally would be a reason for wrong interpretation of results. Therefore, it is important to formulate an appropriate fluid system and characterize its property and performance efficiency.

A properly designed fluid makes good filter cake, which is thin, firm and impenetrable, on the walls of the hole, which prevents too much drilling fluid to go into the formation. These properties increase the well strength and avoid well instability problems.

When the well pressure is exceed or lower than this window, well fracturing and well collapse occurs. The problems result in a huge fluid loss into a formation and drill string sticking respectively. The overall consequence is an expenditure of a large amount of money due to operational cost and non-productive time as well. As illustrated in Figure 1.2, designing a well pressure between well collapse and well fracturing pressure controls well instability problems.

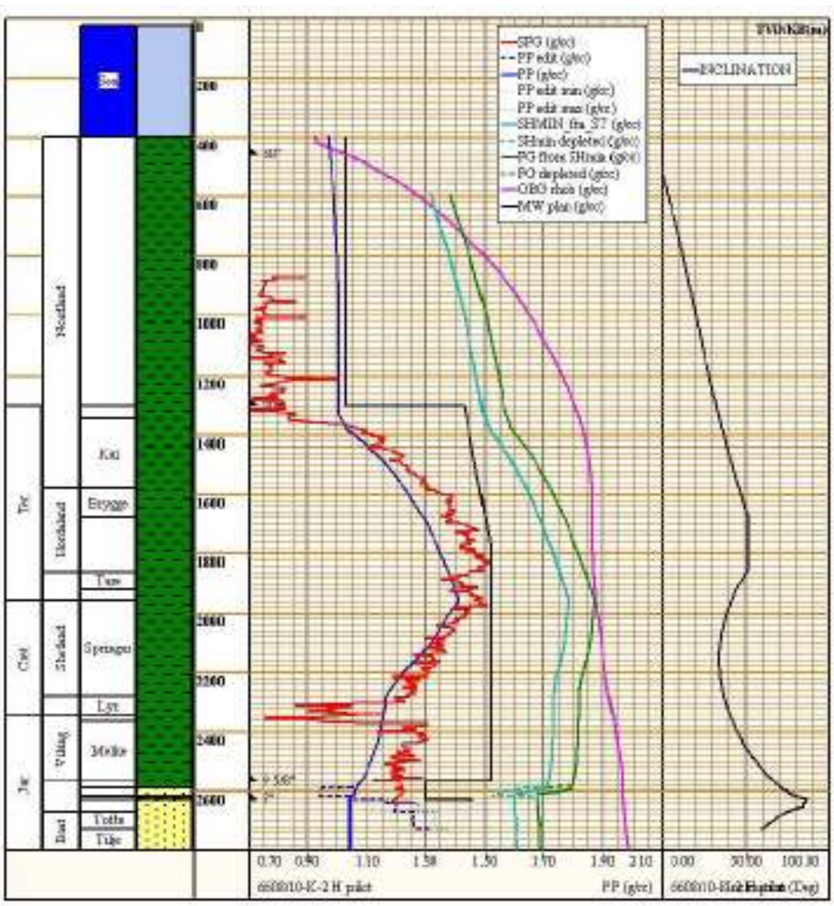

Figure 1.2: Well program [9].

When drilling in a reservoir section with a well pressure lower than the formation pressure, formation fluid influx will occur. The appropriate mud pressure is determined by equivalent circulation density, which is the sum of hydrostatic and friction pressure loss given as [10]

$$ECD = \rho_{st} + \frac{\Delta P_{annulus}}{0.052 \cdot TVD} \qquad 1.1$$

Where:

- ρ_{st} = Static mud density (ppg).
- $\Delta P_{annulus}$ = Pressure loss (psi).
- TVD = True vertical depth (ft).

The friction part of the ECD is a function of fluid rheology properties, flow rate and well geometry.

Therefore, the knowledge of drilling fluid is very important to predict the hydraulics, hole-cleaning, well stability and formation damage control behavior

1.2 Problem Formulation

Several authors have shown the effect of Nano in oil based mud system and water based mud system. The performance of Nano silica in cement has shown good improvement in mechanical strength.

This thesis work address issues such as the impact of nano in various salt and polymer systems in terms of:

- Rheology of drilling fluid
- Filtrate loss control
- pH
- Viscoelastic behavior of fluid system
- Hydraulics and hole cleaning performances

1.3 Scope and objective of the thesis

The primary objective of the work is to formulate and assess nano SiO_2 in salt and polymer treated bentonite fluid system. The scope of the thesis is limited to experimental and simulation studies. The activities are:

- Review the properties of drilling fluid ingredients to be used for the formulation
- To review rheology and hydraulics model to be used for evaluation of the formulated drilling fluid
- To formulate Nano based drilling fluid and characterize their rheological, filtrate, pH and viscoelastic behavior
- To perform hole cleaning and hydraulic simulation studies

2 Literature study

This chapter presents literature studies on properties of the drilling fluid ingredients used in this thesis work.

2.1 Drilling fluids and functions

The most commonly used drilling fluids are two types; Water based mud (WBM), and Oil based mud (OBM). Due to environmental issues, instead of OBM, the application of an inhibitive WBM is common. OBM lubricates the bit better than WBM, and can provide a higher drilling rate. OBM is also more expensive than WBM.

WBM is more environmental friendly, and cheaper. It consists often of water or seawater, salts, weight materials like barite or bentonite, and different polymers.

A Drilling fluid has several functions. Among others, the primary functions can be mentioned [7, 11, 12].

1. Prevent formation fluids from getting into the borehole
2. Maintain well pressure so that it prevents fluid flow in to a well and prevents well collapse.
3. Remove cuttings from the bottom of the well and transport it to the surface.
4. Form a thin, firm and impenetrable filter cake on the walls of the hole, which prevents too much drilling fluid to go into the formation

During drilling, an applied energy on drill bit to crush rocks causes quite high temperature on the drill bit. If this temperature is not cooled down, it could damage the bit. Therefore, drilling fluids prevents this from happening.

2.2 Loss circulation problems and solutions

One of the critical problems in the industry is loss circulation. It is defined as the loss of drilling fluid into a formation. This occurs when drilling through in naturally fractured and drilling induced over pressure. When this occurs, the driller needs to solve the problem. Together with operational cost, non-productive time is also a cost factor for the industry. Figure 2.1 illustrates the four different types of drilling loss formation.

It is experimentally shown that different drilling fluids have different well fracturing strengths. Good mud cake, which consists of particles at the gate of a fracture, helps to hinder a huge mud loss and increase the strength of the wellbore. To characterize the bridging performance of a drilling fluid along with the loss circulation additives, one need to do laboratory studies before using for application [13, 14, 20]

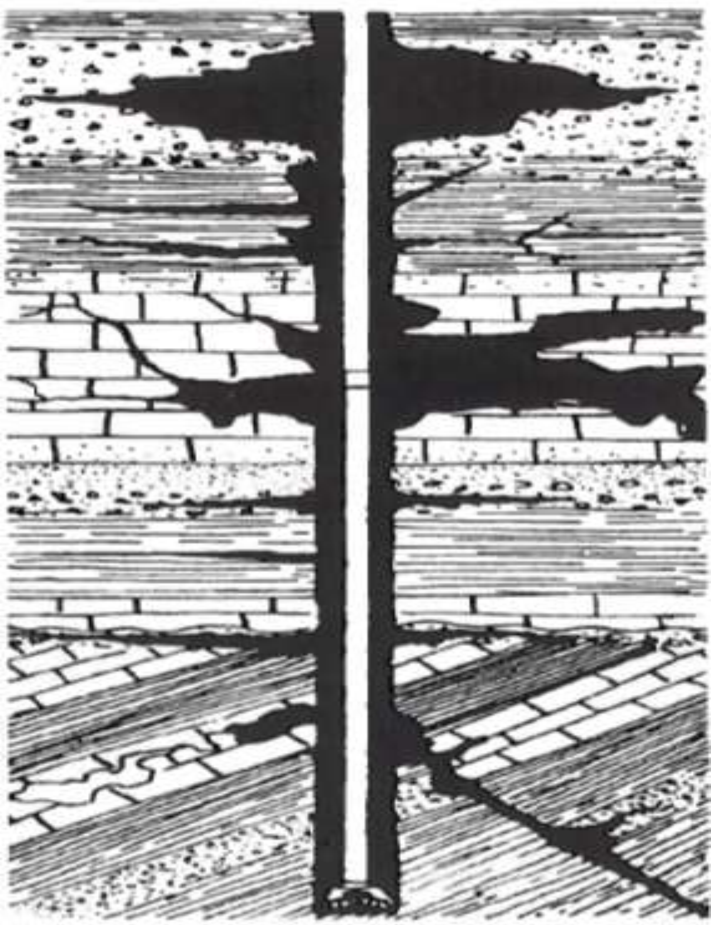

Figure 2.1: Types of loss circulation formations [15].

2.3 Dynamic filtration

During dynamic filtration, filter cake formation and growth are influenced by erosive action drilling fluid stream, drill string rotation and dynamic well pressure. Initially as the fluid exposed to the surface of rock strata, the filtration is very high, and the cake grows rapidly. Later the growth rate decreases, and thereafter the thickness of the cake become constant. The dynamic filter cakes differ from static filter cakes.

Darcy's law governs the rate of filtration. It depends on the thickness, permeability of the cake and the viscosity of filtrate [16]:

$$v_f = \frac{k \cdot A \cdot \Delta p \cdot t}{\mu \cdot h_{mc}} \qquad 2.1$$

Where, k is permeability of mud cake, A is surface area of cake, ΔP is differential pressure across mud cake, t is time of filtrate testing, μ is viscosity of filtrate, h_{mc} is the thickness of mud cake

Because of erosion, unlike static filter cake, the soft surface layer of are not present in the dynamic cake. The degree of surface erosion depends on the shear stress provided by the hydrodynamic force of the mud stream applied surface of cake.

The property of mud cake is characterized by several parameters such as: the solid particles size & shape, compressibility, lubricity, clay particle flocculation and thickness. Comparing the static conditions, the dynamic condition mud cake is characterized by optimum-sized particles, and a lower permeability. These properties results in a lower filtrate rate per unit thickness [17].

Figure 2.2 illustrates a typical accumulated fluid loss vs time [18]. The curve shows the behavior of fluid losses during dynamic and static conditions. As shown, the first phase of the fluid losses at a higher rate. The second part of the curve shows a period during which circulation stopped. The static mud builds upon the dynamic cake. As shown, the loss rate is lower. The third part of the curve illustrates the dynamic condition. The deposited cake during static period will be eroded fully or partially or sometimes not at all [19].

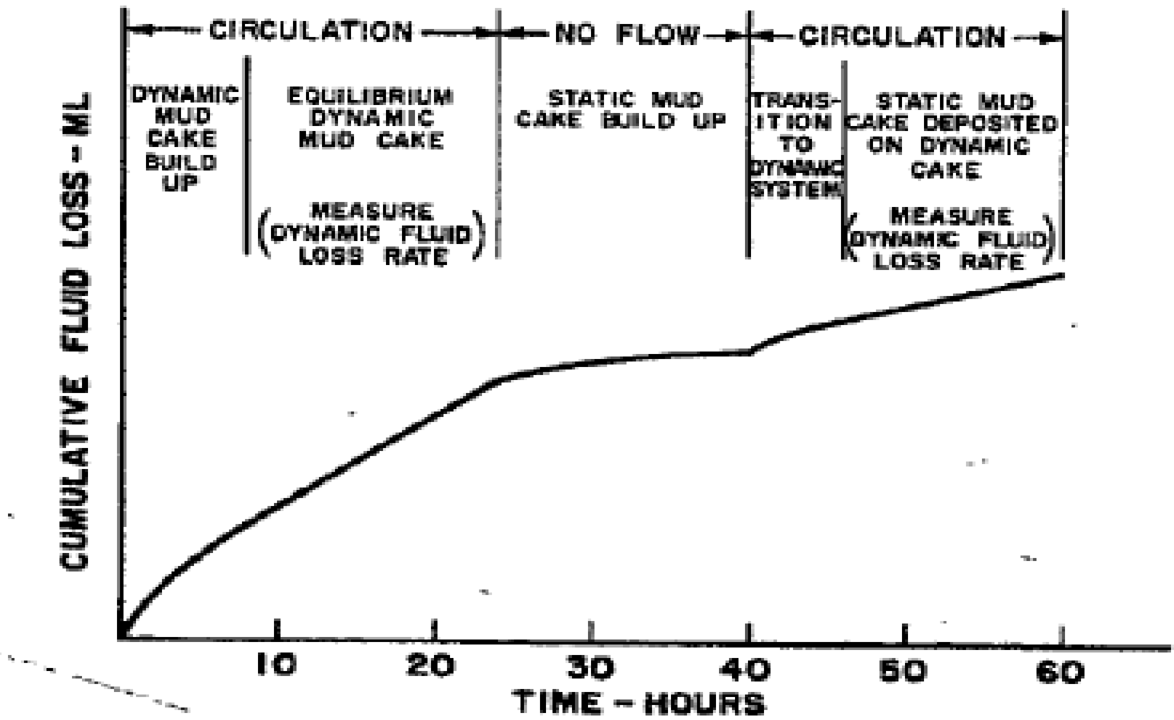

Figure 2.2: Typical cumulative fluid loss curve during dynamic test [18].

Figure 2.3 shows the experimental dynamic filtration cumulative per unit area. The model described in Equation 2.2 consists of three terms. [19]

$$V_c = V_{sp} + A\sqrt{t} + Bt \qquad 2.2$$

Where:

- V_C = Cumulative filtrate volume per unit area
- t = time
- V_{sp} = spurt loss
- A = static leak-off
- B = dynamic leak-off

The terms presented in Equation 2.2 are the stages in the leak off process. The first term is spurt loss, the second term is the buildup of filter cake, and the third term is erosion of filter cake.

It is experimentally shown that V_{sp} and A are independent of the shear rate. The dynamic component, B, varies with the shear rate.

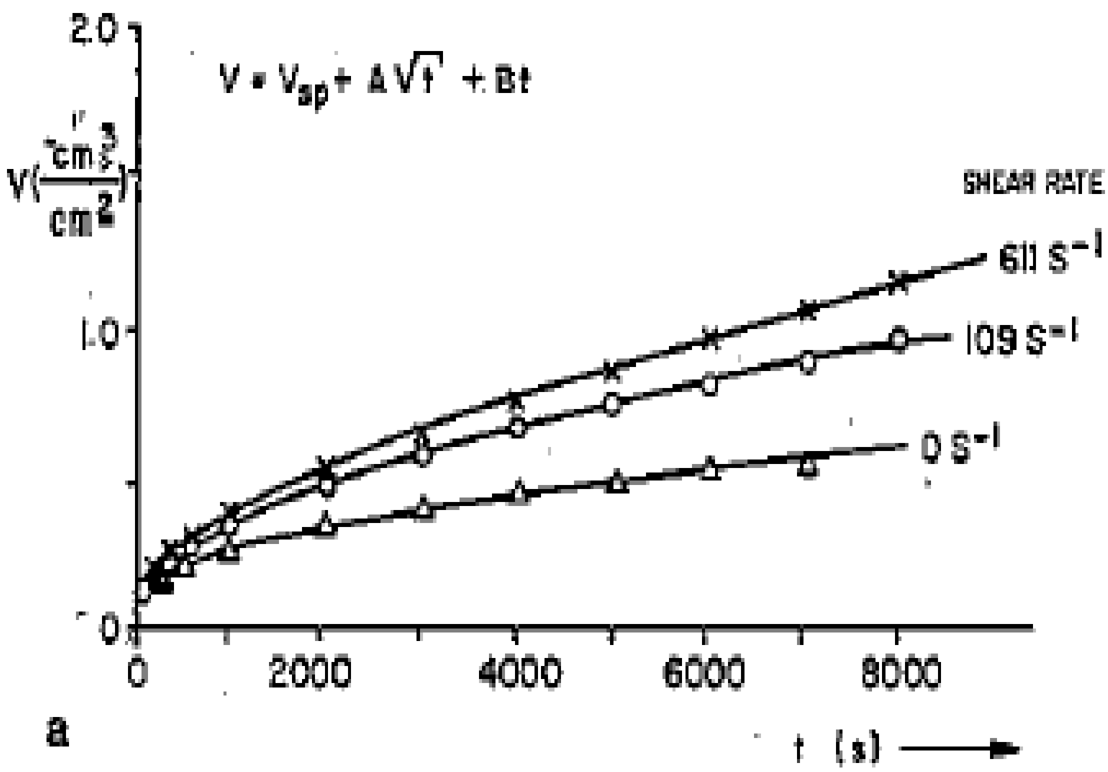

Figure 2.3: Fluid loss through a micro porous porcelain disk [19].

2.4 Static filtration

Static filtration occurs when drilling mud is at rest. The filter cake will grow over time. Control of static filtering is necessary to control the filter cake deposited on the hole wall. The lower permeability, the thinner thickness and strong and stiff characterize good quality filtrate cake. These properties results in lower filtrate loss.

Filter cake thickness increases with increasing filtrate loss. For static case, the filtrate loss volume is directly proportional to the square room of time given as [19]

$$V_c = V_p + m\sqrt{t} \qquad 2.3$$

Where, the V_p is the spurt loss.

Fig 2.4 shows fluid loss through porous disc under stat condition.

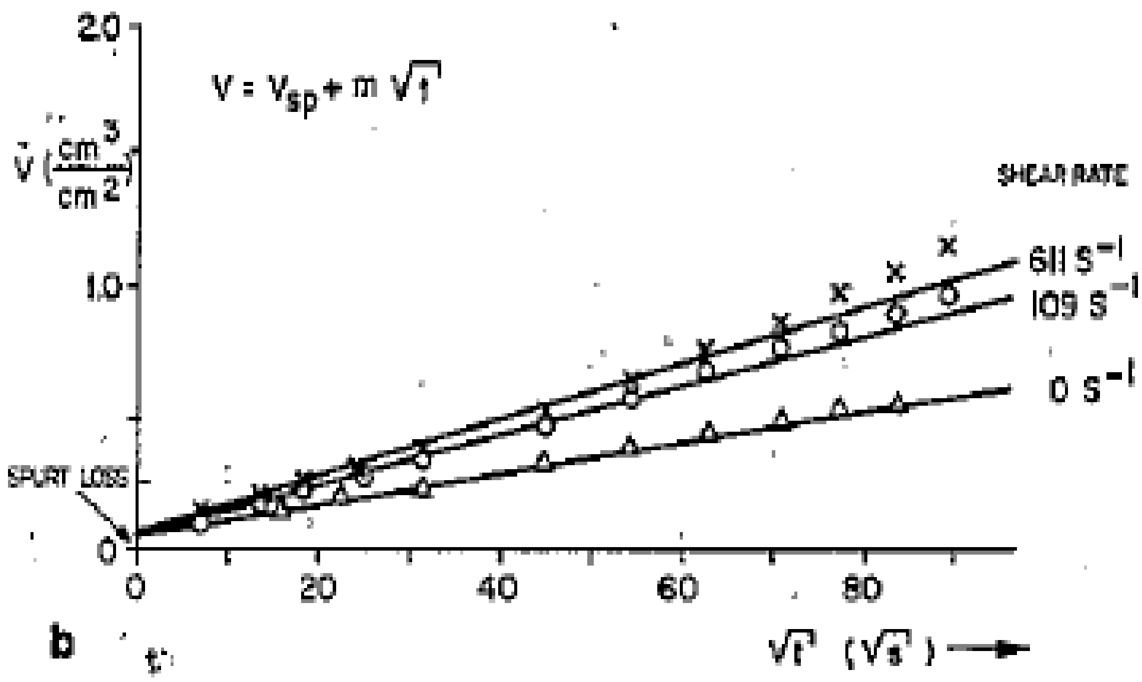

Figure 2.4 Fluid losses through a micro porous porcelain disk [19]

2.5 Filter cake-bridging process

The mud spurt loss is the filtrate at time zero that appears on filter paper before filtration test properly begins. After wards, as shown in Figure 2.4, the filtrate volume becomes proportional to the square root of the time.

Since drilling formation is more porous and permeable, the spurt loss in drilling well is much larger in this particular formation. A continuous loss into a formation may occur if the drilling fluid contains a particle size smaller than the size of the pore. Thus, to establish a good bridging performance, good petro-physical and mechanical properties of filter cake is required.

Several bridging experimental studies were carried out at the University of Stavanger. The results show that the D_{50} size of particle is higher or equal to the fracture/pore size and form a good bridging [13, 14, 20]

Figure 2.5 illustrates the process of bridging. At first, the primary bridge is established. Then, the smaller particles are trapped between the particles.
As shown on the figure, three zones are established at the near face of a wellbore [16]

- An external filter cake.
- An internal filter cake
- A zone invaded by the fine particles during the mud spurt period

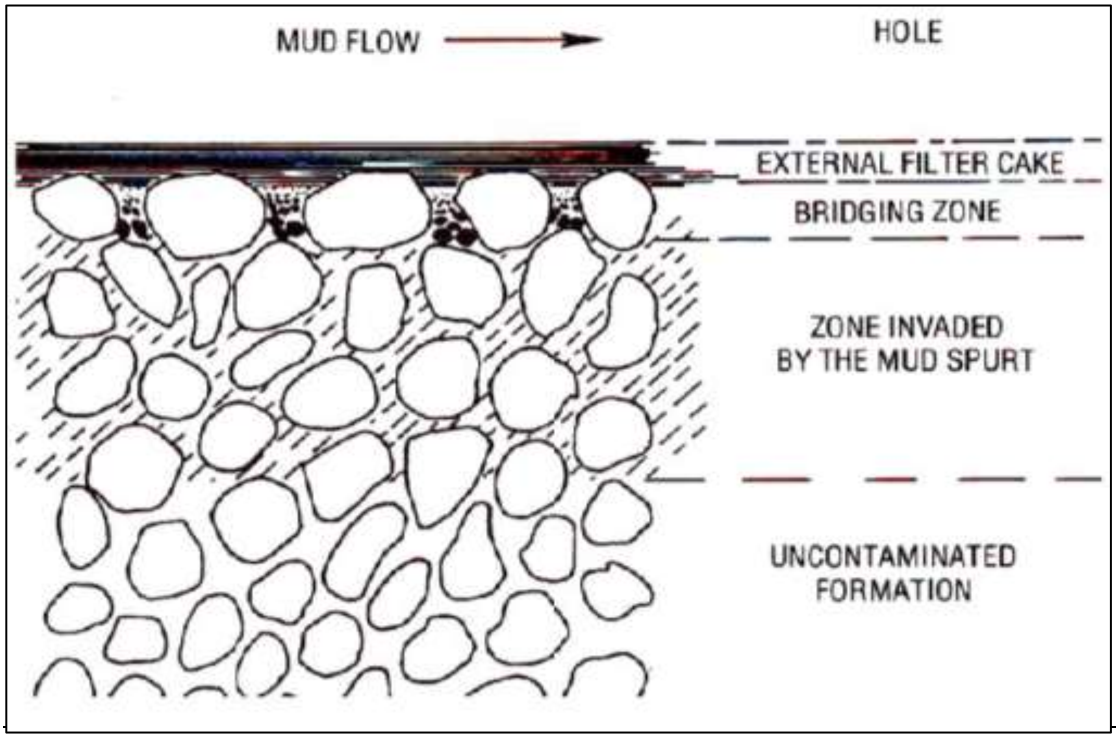

Figure 2.5: Invasion of a permeable formation by mud solids [16].

Poor mud properly characterized by more invasion and poor bridging performance. This results in formation damage and huge mud losses.

2.6 Components of water based muds

The components of drilling fluid used in this thesis are freshwater, bentonite, various salts, polymers and nano silica. In this section, the behavior of these additives will be presented.

2.6.1 Fresh water

For the drilling fluid preparation, fresh water from tap was used. The chemistry of the tap water is not available. However, it is shown that the polymer and salt untreated tap water swells the bentonite pellet.

2.6.2 Bentonite

The word Bentonite was first used for a plastic clay found in Wyoming, USA. Bentonite swells up when it is immersed in water. A small amount of bentonite mixed with water could create a thixotropic gel structure in water. The most dominant mineral in bentonite is montmorillonite; other minerals in bentonite can be illite and kaolinite, which can make up to 50% of the clay minerals in bentonite. None-clay minerals can also be found in bentonite and can represent 10-30% of the bentonite. Bentonite has a specific gravity of 2.5. The hardness in a Mohs scale is 1 to 1.5.

Clay is commonly used for filtration control in water-based fluids. Bentonite is one of the most used and the microscopic structure consists of sheets (Figure 2.6) [21]. Moreover bentonite also increases viscosity since it swells in presence of water. Table 2.1 shows the chemical composition of commercial bentonite [22].

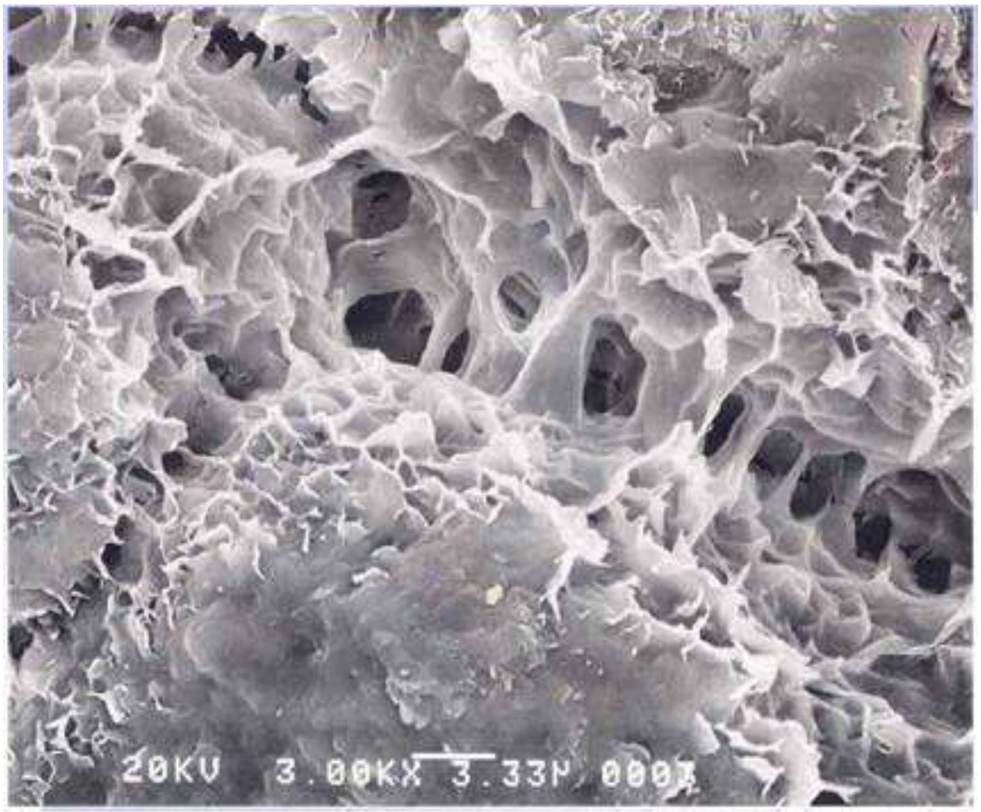

Figure 2.6: SEM picture of bentonite [21].

Chemical composition in %			
	Wyoming "Volclay"	*Panther Creek Mississippi*	*Ponza, Italy*
Silica, SiO_2	64.32	64.00	67.42
Alumina, Al_2O_3	20.74	17.10	15.83
Ferric oxide, Fe_2O_3	3.03	} 4.70 {	0.88
Ferous oxide, FeO	0.46		-
Titanium dioxide, TiO_2	0.14	1.50	-
Lime, CaO	0.50	3.80	2.64
Magnesia, MgO	2.30	0.50	1.09
Potash, K_2O	0.39	0.20	}1.09
Soda, Na_2O	2.59	-	
Phosphoric anhydride, P_2O_5	0.01	-	-
Sulfuric anhydride, SO_3	0.35	0.20	0.01
Other minor constituents	0.01	8.00	-
Combined water	5.14	64.00	10.88

Table 2.1: Chemical component of commercial bentonite [22].

2.6.2.1 Structures of bentonite

The fundamental structures of clay minerals are octahedral layer and tetrahedral layer.

Octahedral layer

Figure 2.7 illustrates the crustal structure of octahedral. The octahedral layer is made up of two planes, which are packed with oxygen or hydroxyls molecules (OH) that aluminum (Al) is surrounded in between.

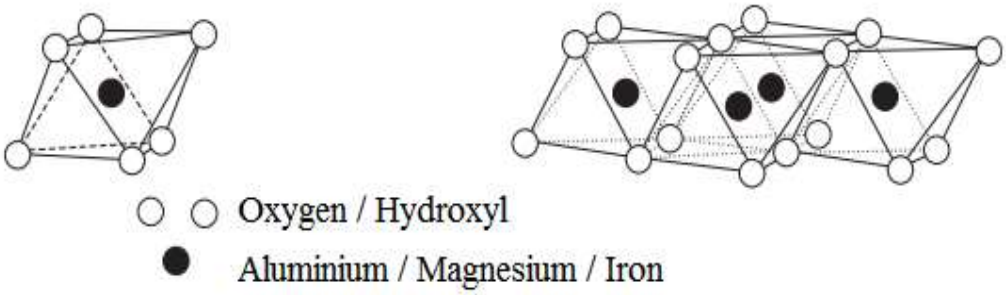

Figure 2.7: Crystalline structure for octahedral sheet [23].

Tetrahedral layer

Figure 2.8 illustrates the crystal structure of tetrahedral layer, which consist of four oxygen / hydroxyl and a silicon molecule. As shown on Figure 2.9, six tetrahedral layers are packed in a hexagonal structure and share an oxygen/ hydroxyl molecule. The thin clay layers of this structure like mica can be separated from each other.

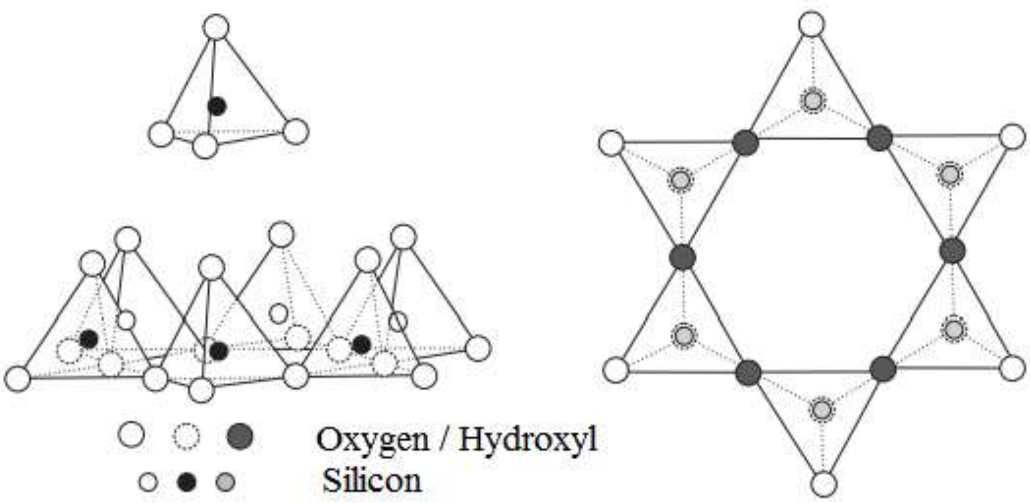

Figure 2.8: Crystalline structure for tetrahedral sheet [23].

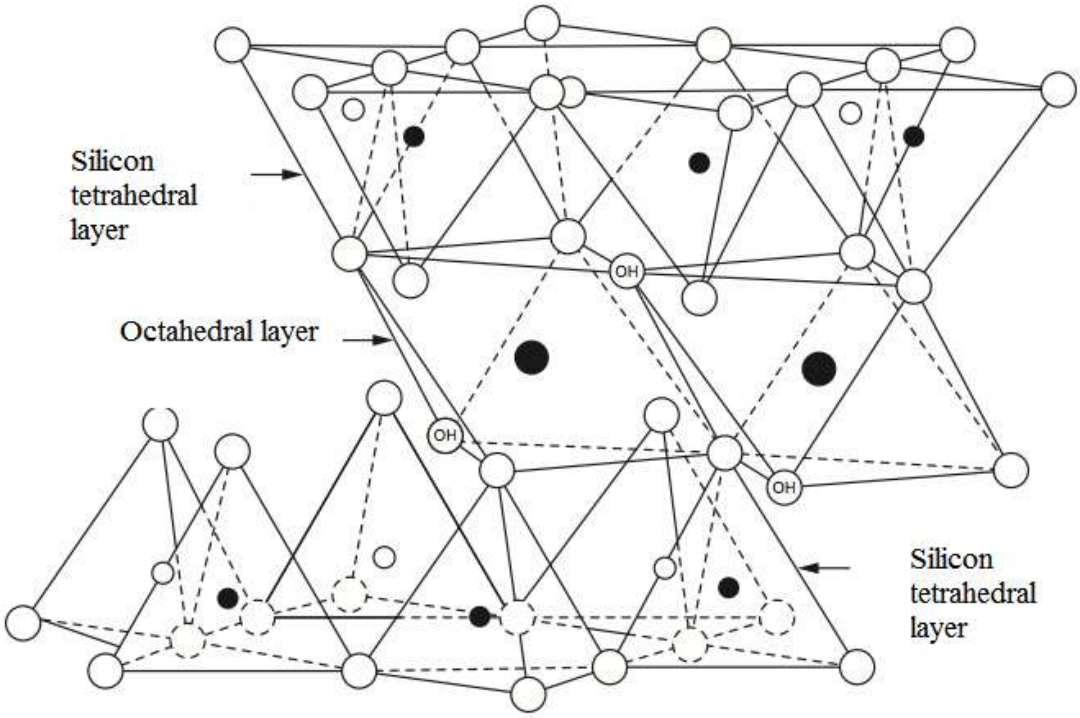

Figure 2.9: Crystalline structure of Montmorillonite mineral [23].

2.6.2.2 Particle associations

The arrangement of clay particles has an impact on the rheological and fluid loss properties of the drilling fluid. These arrangements are described as the following four states and also shown in Figure 2.10:

Flocculated Systems:

In the flocculated systems, the clay particles are formed in clustered form connected end-to-surface due to the existence of a net attractive force.

Deflocculated:

In this system, by the addition of deflocculates neutralize the particle and disperse the clay plates takes place in the drilling fluid system. This can also be obtained by creating a system of the same charge, which the system becomes under repulse force between particles. Alkaline conditions create a net negative charge.

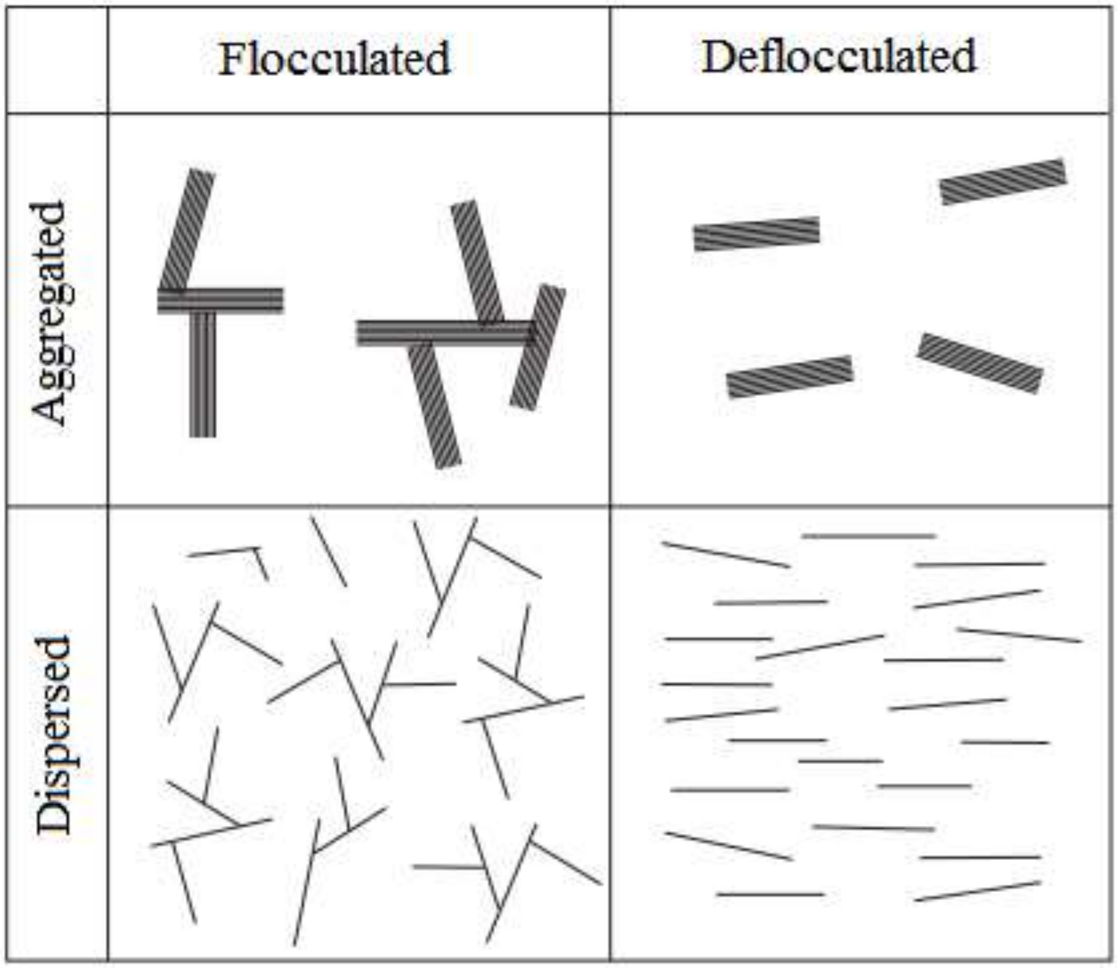

Figure 2.10: Arrangement of clay particles in drilling fluid [23].

Aggregated Systems:
Clay's sheet structure are assembled and packed together one upon the other. As the clay in contact with water, the fluid adsorbed between the swelling clay montmorillonite. The aggregated assemblage of clay sheets disaggregated by means of hydration mechanical shear. As a result, the aggregates sheet could be in state of flocculated or deflocculated as shown in the Figure.

Dispersed System:
The packing of the aggregated or the deflocculated systems break down due to the pH and charges. This system is known as dispersed.

2.6.3 Polymers

The primary functions of polymers are to give sufficient viscosity. In this thesis, drilling fluids were formulated in the presence of the commonly used polymers in the oil industry. These are: PAC (Poly-anionic Cellulose), CMC, Drispac, Xanthan (XC) and DUO-VIS. The performance of nano-silica was tested in the mixtures of these polymers and six different salt types. The single and combined effect of salts and polymers in nano systems are analyzed.

2.6.3.1 Polyanionic Cellulose (PAC)

PAC stands for poly-anionic cellulose, which is water-soluble cellulose. It is derived from natural cellulose. PAC is widely used in oil drilling. Polyanionic Cellulose is nontoxic and has excellent heat-resistant stability, and has strong antibacterial activity. Figure 2.11 is the chemical formula [24]

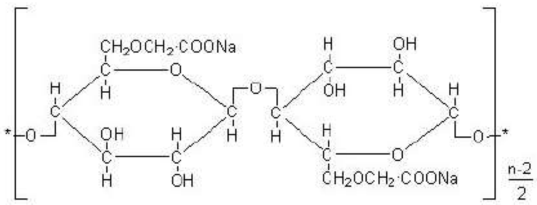

Figure 2.11: Poly-anionic Cellulose (PAC) chemical structure [24].

2.6.3.2 Drispac

Drispac polymer is polyanionic cellulose polymers and has high-quality. The primary function of this polymer is used for swelling inhibition, fluid loss and viscosity control in water–based muds [25]. According this reference, the polymers work well at any salinity.

2.6.3.3 DUO-VIS/Super-VIS

DUO-VIS/SUPER-VIS is a viscosifier xanthan gum. It is a high-molecular-weight biopolymer. It is used in water based mud system, which improves the carrying capacity of the fluid system. DUO-VIS/SUPER-VIS biopolymer produces in the fluid system to have highly shear-thinning and thixotropic properties.

2.6.4 Salts

Andreas 2015 [26] has analyzed six salts in cement slurry along with nano-silica. The author has investigated influence of these salts system on the mechanical strength of cement plug. This thesis work also tries to investigate the single and combined effect of these salts in drilling fluid.

Formation water obtained from pore fluid composition of Pierre II shale taken from deep water in the USA [27]. Table 2.2 shows the salt types and concentration. In this thesis work, only 2g of the each salts provided in the table and in addition KCl was analyzed in 25gBentonite/500gH_2O.

Salt	Content g/l
$NaHCO_3$	15.6
Na_2SO_4	7.3
NaCl	3.86
Na_2CO_3	3.3
$MgSO_4$	0.62
$CaSO_4$	0.42
Total	31.1

Table 2.2: Formation water salt compositions [27].

2.6.4.1 Sodium bicarbonate $NaHCO_3$

Sodium bicarbonate has the chemical formula $NaHCO_3$. It is widely used; the salt has related names such as baking soda, and bicarbonate of soda [28].

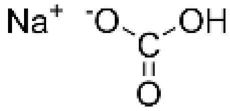

When baking soda combined with moisture and acidic ingredient, the chemical reactions result in producing CO_2 bubbles**.**

The salt has the effect of neutralization when mixed with acids. The salt is harmless and commonly used to increase the pH.

2.6.4.2 Sodium carbonate Na_2CO_3

Sodium carbonate is known as soda ash**.** It is water-soluble sodium salt. Pure sodium carbonate forms a strongly alkaline water solution. It is synthetically produced from sodium chloride salt and limestone [28].

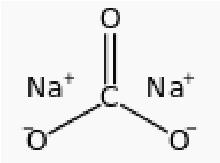

Sodium carbonate forms carbonic acid and sodium hydroxide are formed when Na_2CO_3 dissolves in water. Sodium hydroxide control pH. It neutralizes acid and acting as an antacid

2.6.4.3 Sodium sulfate Na_2SO_4

Sodium sulfate is the sodium salt of sulfuric acid. It is regarded as non-toxic. Sodium sulfate is used for the manufacture of detergents and paper pulping. It is used in water treatment as an oxygen scavenger agent [28].

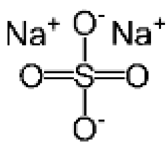

2.6.4.4 Potassium chloride KCl

The desired amount of potassium chloride drilling mud is normally determined by any prior knowledge of the formation to be drilled through. Such information about the crystal structure of slate of clay, a few including is from electron diffraction measurement.

It may in some cases be of importance that KCl concentration is kept within 10-20% of the desired level. There is a reliable and accurate method to determine the potassium content, namely by means of a flame photometer. However, neither drilling fluid company nor operating company is willing to hold such an instrument on a rig. Instead, it is common to use a primitive and inaccurate centrifuge method for determination of potassium concentration [12, 29].

2.6.4.5 Sodium chloride NaCl

Routine control of the chlorine content of the drilling mud is particularly important in areas where salt formation may contaminate the drilling fluid. Salinity has great influence on the behavior of clay. The clay hydrating capacity decreases rapidly with increasing chlorine content. Water used for pre-hydration should be checked for chlorine content and only used for Cl <10 000 mg/l [12,30].

2.6.5 Weight material

In this thesis, Barite ($BaSO_4$) was not used in the formulated drilling fluids. However, the following presents just to describe its property. Barite is the most commonly used weight substance for increasing the density of drilling fluids. Barite is 98.5% pure barium sulfate. The density is about 4200 kg/m^3. Barite has little chemical interaction with other substances. [7].

3 Theory

For the analysis of experimental data, the relevant theories are reviewed and presented in this chapter. The theories are rheology, hydraulic, viscoelasticity and hole-cleaning related information.

3.1 Rheology

Rheology is the term used to define the study of flow and deformation. Flow deals with type and pattern and deformation deals with the shear stress and shear rate relation. The flow pattern depends on several parameters and characterized by Reynolds number. The flow behavior has a strong impact on drilling process like ROP and cuttings transport. To ensure these qualities it is significant that we control the rheological abilities.

The rheological flow properties are very important for the muds functions. Some examples are:

- Cuttings transport
- The mud must be able to hold on to the cuttings and weight materials even in a suspension (stop in circulation)
- Protect/minimum damage of the drilled formations

3.1.1 Reynolds number

Reynolds number is dimensionless number, which is named after an English Physicist. The parameter is defined by the ratio of fluid's inertia forces and its viscous forces. It is used to identify type of flow regimes, such as laminar, transitional or turbulent flow. Reynolds number is given as [31]:

$$R_e = \frac{\rho \cdot \bar{V} \cdot D}{\mu} \qquad 3.1$$

Where:

- D = Hydraulic diameter of the pipe (m)
- $\bar{V}$ =Mean fluid velocity (m/s)
- μ = Dynamic viscosity of the fluid (Pa·s or N·s/m² or kg/m·s)
- ρ =Density of the fluid (kg/m³)

3.1.2 Flow regime

A fluid flow is said to be a laminar flow when the fluid flow pattern is parallel to the flow direction. Laminar flow can be described as a telescopic flow. The flow velocity is higher at the center and getting lower (at point A) and zero (at the wall). The laminar flow is distinguished by a smooth pattern and the profile is a parabolic. This is illustrated in Figure 3.1.

This type of flow occurs when the Reynolds number typically lower than 2000. Laminar flow occurs when the flow velocity is low, hydraulic diameter is wider and lower fluid density.

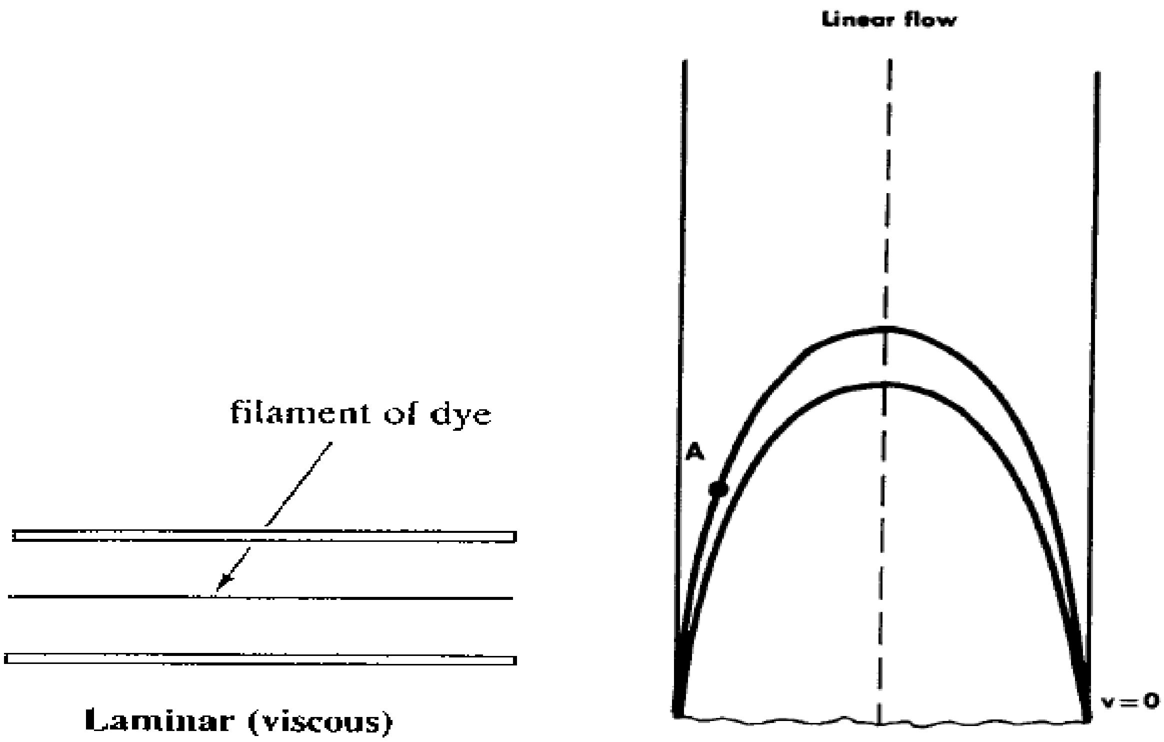

Figure 3.1: Illustration of Laminar flow [31, 32].

Turbulent flow

Turbulent flow is characterized by random/chaotic flow patterns of drilling fluid. The Reynolds number associated with turbulent flow is typically greater than 4000.

The flow pattern is illustrated on Figure 3.2. This flow pattern occurs at high velocities, narrower hydraulic diameter. As the degree of turbulence increase, the pressure loss also increases.

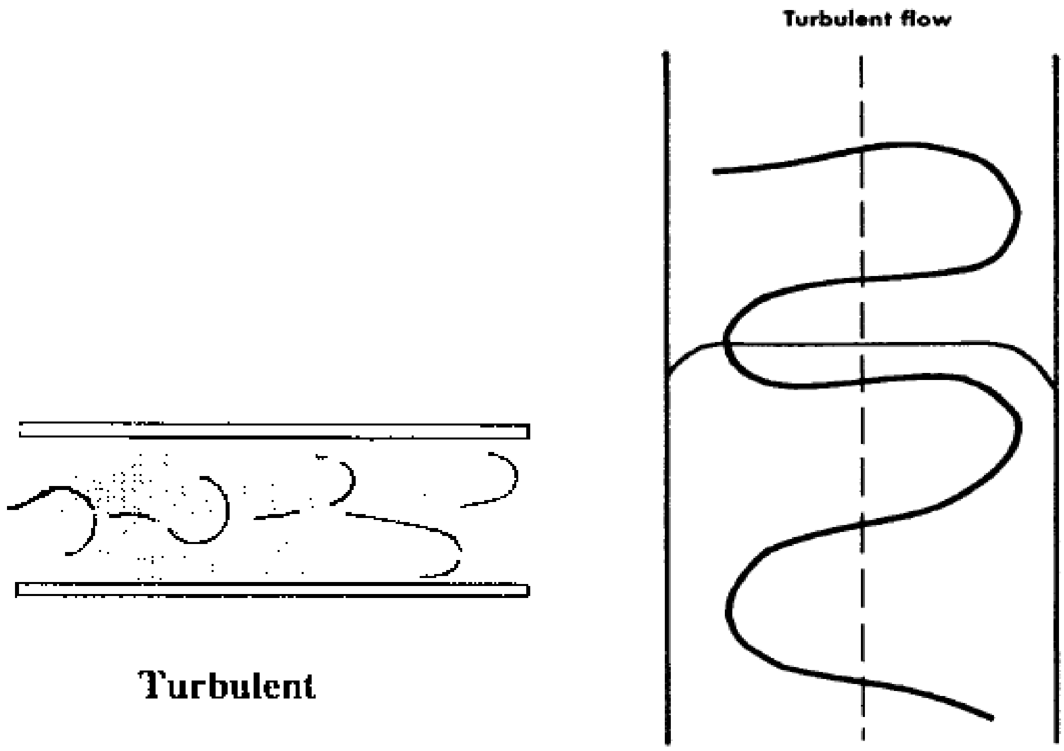

Figure 3.2: Illustration of turbulent flow [31, 32].

Transitional flow

As flow velocity increases, there exists a transition period that the flow pattern changes from uniform to chaotic. The Reynolds number associated with this transition flow is between 2000 and 4000. The flow pattern is a kind of wavy and Figure 3.3 illustrates this type.

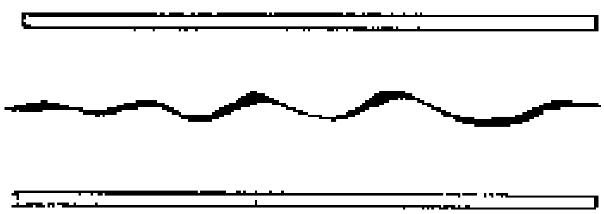

Figure 3.3: Illustration of transitional flow [31].

3.1.3 Viscosities and gel strengths

Drilling fluids to be formulated and tested are going to be characterized based on viscosity and gel strength. The following presents the description of the parameters [32].

Plastic viscosity (PV):
Drilling fluid's flow resistance is created due to mechanical friction between particles and fluids. This part of fluid resistance is described by a term called plastic viscosity. The magnitude of plastic viscosity depends on the additives in a drilling fluid.

Yield point (YP):

Yield stress is part of flow resistance created due to an electrostatic attractive force between particles contained in a drilling fluid. In order to initiate flow, an applied pressure should exceed the yield strength of the fluid.

Gel-strength (gel):
The gel strength of a drilling fluid is an important property for holding solids in suspension. Gel structure also helps prevent fluid invasion into a formation and loss circulation [33]. Gel structure is formed when fluid is at rest. The attractive forces between particles determine the gel strength. Gel strength is the measure of the drilling fluid to develop and retain gel form.

3.2 Rheological models

Rheological model are categorized as Newtonian and non-Newtonian. For the non-Newtonian, there are several models available in literatures. The models relate shear stress with shear rate. The most commonly used non-Newtonian models are Bingham Plastic, Power Law, Robertson & Stiff, Unified, and Herschel-Buckley. From the measured data and the models, one can extract flow viscosity and gel strength. These parameters determine the hole-cleaning and flow behavior of drilling fluid. For the analysis of the models, the Fann-35 data provided in Table 3.1 is used.

Table 3.1: Viscometer Fann-35 data used for the analysis.

RPM	Dial Reading
R_{600}	78
R_{300}	47
R_{200}	36
R_{100}	24
R_{6}	8
R_{3}	7

3.2.1 Newtonian fluids

A constant viscosity for any shear rate characterizes Newtonian fluids. These fluids do not contain particle additives for instance gases, water and high-gravity oils. The Newtonian model is described by. [7. 34]:

$$\tau = \mu \cdot \gamma \qquad 3.2$$

Where:

- μ = Viscosity
- γ = Shear rate
- τ = Shear stress

Figure 3.4 illustrates the comparisons between the model and the rheology data provided in Table 3.1.

The Newtonian viscosity in field units (cP) can be estimated by multiplying the slope as:

μ =47880xSlop/100 =
47880x0.0884/100 = 42.33cP

As can be seen from the figure, the model does not capture the data and hence Newtonian model is not good enough to describe the fluid behavior.

The absolute value average sum % deviation between model and data is 44.119%.

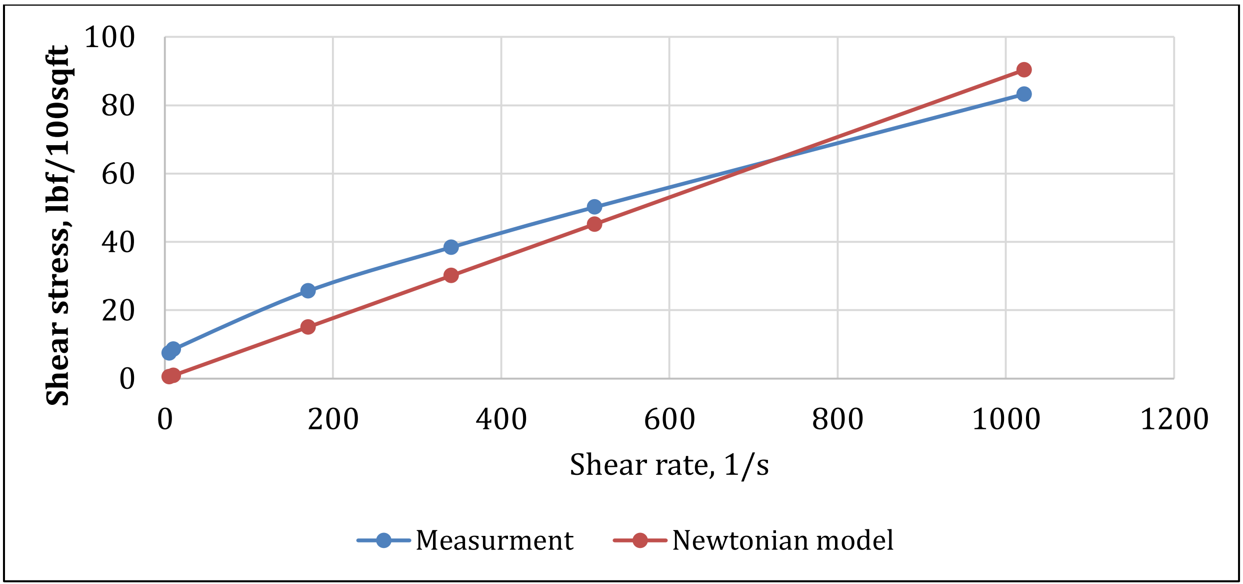

Figure 3.4: Illustration of Newtonian fluid model.

Model	Equation	μ_p, slope	μ_p,cP	% Deviation
Newtonian	0.0884*γ	0.0884	42.32592	44.11

3.2.2 Non Newtonian fluids

Most drilling fluids are non – Newtonian. The fluids are described by two or more parameters model.

3.2.2.1 Bingham plastic

Bingham rheology model is characterized by a linear shear stress (τ)-shear rate (γ) relation flow. According to the model, flow is initiated when the applied pressure exceeds the yield strength of the fluid. The flow behaviour also states that the plastic viscosity is constant for any shear rate. The model is given as [7. 34]:

$$\tau = \mu_p \cdot \gamma + \tau_y \qquad 3.3$$

Where:

- τ_y = Yield point
- μ_p = Plastic viscosity

The plastic viscosity and Yield stress are determined from the measured Fann viscometer data using equations 3.4 and 3.5 respectively.

$$\mu_p = PV\ [cP] = R_{600} - R_{300} \qquad 3.4$$

$$\tau_y = YS\ [lbf/100sqft] = R_{300} - PV \qquad 3.5$$

Figure 3.5 shows the comparison between Bingham model prediction and viscometer data. The absolute value average sum % deviation between model and data is 15.99%.

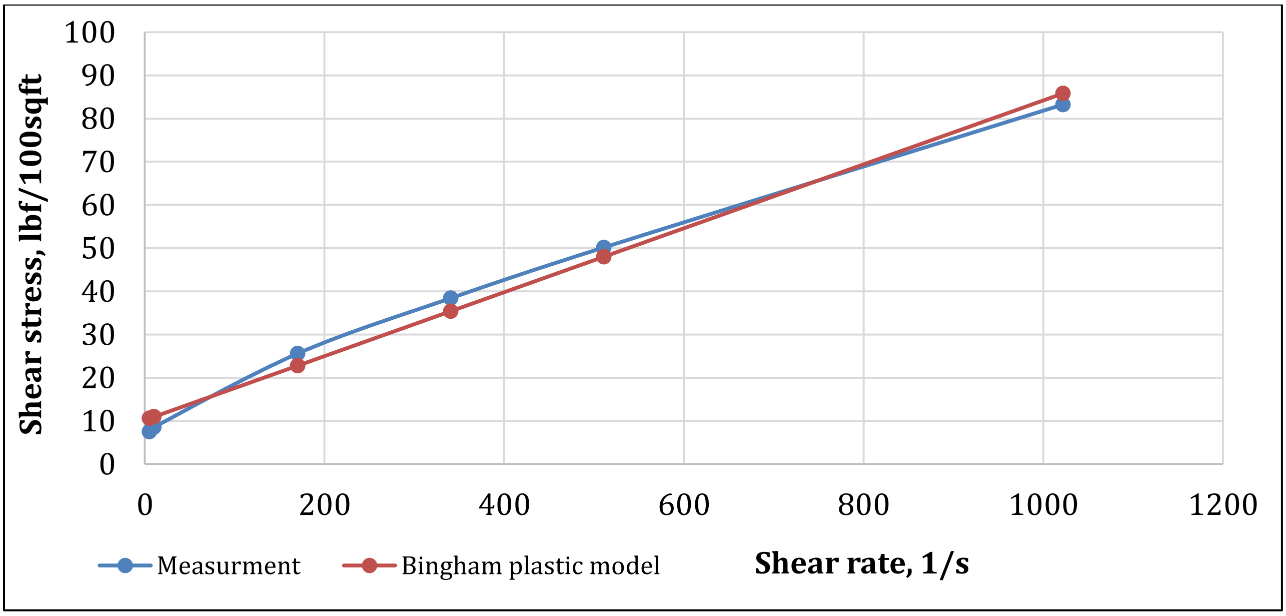

Figure 3.5: Illustration of Bingham model prediction.

Model	Equation	τy	µp,slope	µp, cP	% Deviation
Bingham	0.074*γ+10.188	10.188	0.074	35.4312	15.99

3.2.2.2 Power Law

Power-law fluid is characterized by two parameters. The shear stress, τ, is given by [7. 34]:

$$\tau = k \cdot \gamma^n \qquad 3.6$$

Where:

- k (lbf/100sqft) = Consistency index and
- n = Flow behaviour index.

The Power-law parameters can be estimated from following equations:

$$n = 3.32 \log\left(\frac{R_{600}}{R_{300}}\right) \tag{3.7}$$

$$k = \frac{R_{300}}{511^n} = \frac{R_{600}}{1022^n} \tag{3.8}$$

The Power-law model can represent more than one fluid, i.e when:

- n < 1 a pseudo plastic fluid
- n = 1 a Newtonian fluid
- n > 1 a dilatant fluid

When the n-value less than one, the effective viscosity would decrease with increasing shear rate. This is called shear thinning plastic fluid. This is typical behavior for drilling fluid. The dilatant fluid is less common and is not exhibited by drilling fluid.

Figure 3.5 shows the comparison between Power law prediction and viscometer data (Table 3.1). The absolute value average sum % deviation between model and data is 10.79%.

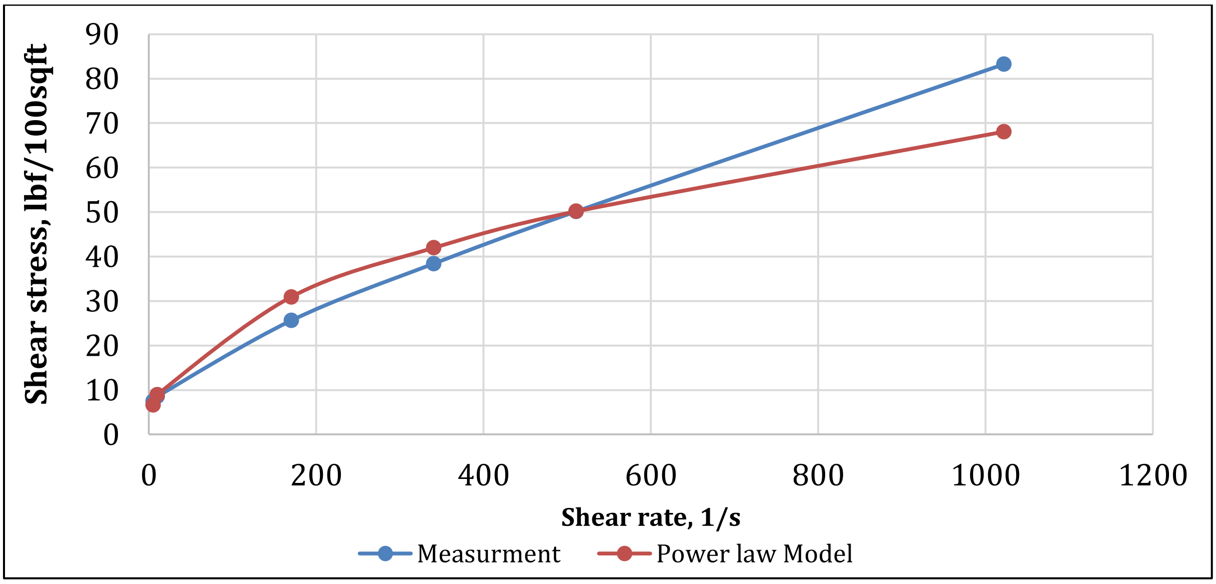

Figure 3.5: Illustration of Power law model prediction.

Model	Equation	k	n	% Deviation
Power Law	$3.2178*\gamma^{0.4404}$	3.2178	0.4404	10.79

3.2.2.3 Herschel-Buckley

Herschel-Buckley (H-B) is a modified yield Power law, which describes the mud rheology better than power law or Bingham model [35]. The model states that fluid requires an external pressure to initiate flow at zero shear strain and as the shear rate increases the viscosity decreases.

The model is described by three parameters as follows [36, 49]:

$$\tau = \tau_0 + k \cdot \dot{\gamma}^n \qquad 3.9$$

Where

τ (lbf/100sqft) = shear stress
τ_0 (lbf/100sqft) = yield stress
k (lbf/100sqft) = consistency factor
$\dot{\gamma}$ (1/s) = shear rate
n = flow index, a power law exponent.

The n and k values can be determined graphically.

τ_o can be determined as: [36]

$$\tau_o = \frac{{\tau^*}^2 - \tau_{min}\tau_{max}}{2\tau^* - \tau_{min} - \tau_{max}} \qquad 3.10$$

Where:
The parameter τ^* is determined from the corresponding geometric mean of the shear rate, γ^*, and can be determined as:

$$\gamma^* = \sqrt{\gamma_{min}\gamma_{max}} \qquad 3.11$$

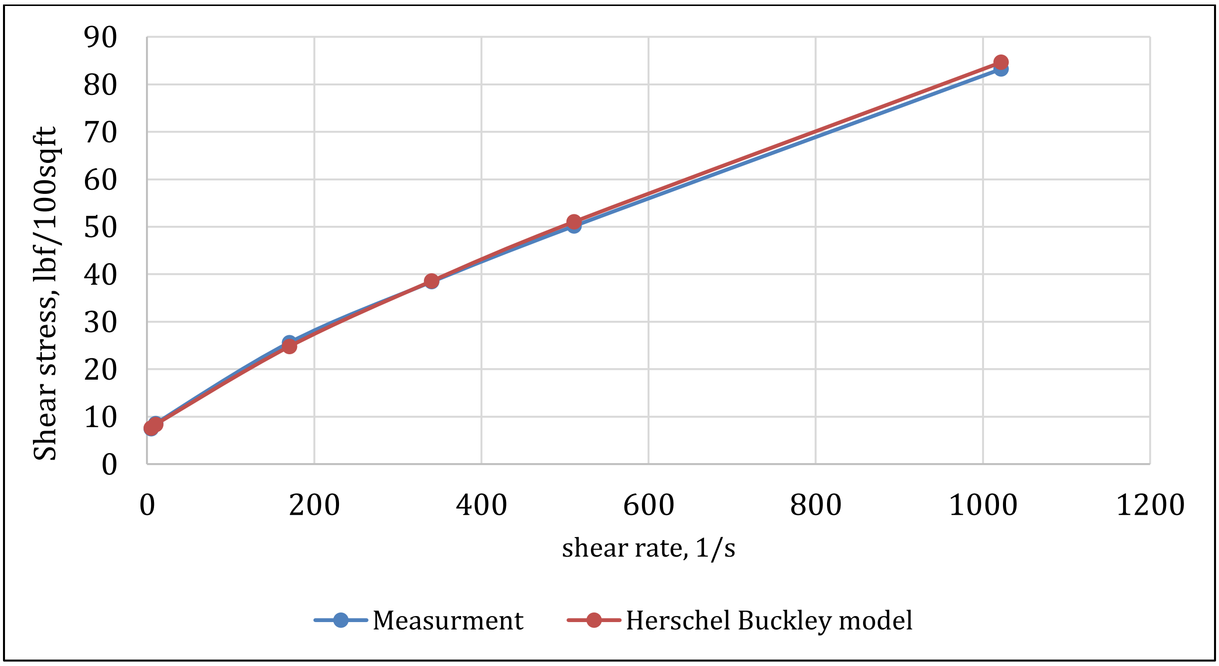

Figure 3.6: Illustration of Herschel-Buckley model prediction.

Model	Equation	Parameters			% Deviation
		τ_o	k	n	
Herschel Buclkley	$0.2845*\gamma^{0.8104} + 6.492$	6.492	0.2845	0.81040	1.72

3.2.2.4 Robertson and Stiff

Robertson-Stiff (R & S) model is a shear stress corrected power law model. The model is used for describing drilling fluid and cement slurries. The model is given as equation 3.12: [36]

$$\tau = A(\gamma + C)^B \qquad 3.12$$

Where, the model parameters A and B correspond to k and n in power law model. The parameter C is shear rate correction factor given as: [36].

$$C = \frac{\left(\gamma_{min}\gamma_{max} - \gamma^{*2}\right)}{2\gamma^* - \gamma_{min}\gamma_{max}} \qquad 3.13$$

Where, the parameter γ^* is determined by interpolation, which corresponds to the geometrical shear stress given as:

$$\tau = \sqrt{\tau min * \tau max}$$

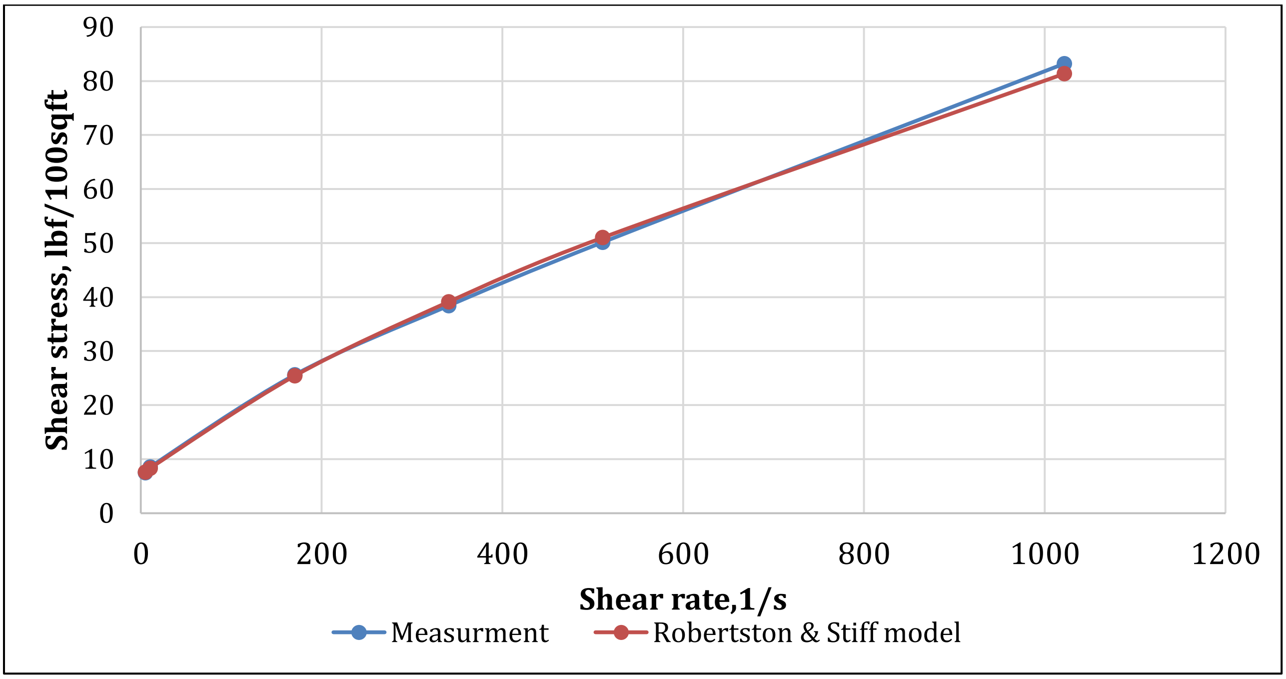

Figure 3.7: Illustration of Robertson and Stiff model prediction.

Model	Equation	Parameters			% Deviation
		A	C	B	
Robertson and Stiff	$0.6101*(30.993+\gamma)^{0.7031}$	0.6101	30.9930	0.7031	1.76

3.2.2.5 Unified

Unified model is a modified yield power law model, which is another version of Herschel-Buckley. Unlike the Herschel-Buckley mode, Unified model uses yield stress point derived from the Fann data (6 and 3-RPM reading). The model is given as [37]

$$\tau = \tau_{yL} + k \cdot \gamma^n \qquad 3.14$$

Where:

$$\tau_{yL}(lbf/100sqft) = (2 \cdot R_3 - R_6) \cdot 1.066 \qquad 3.15$$

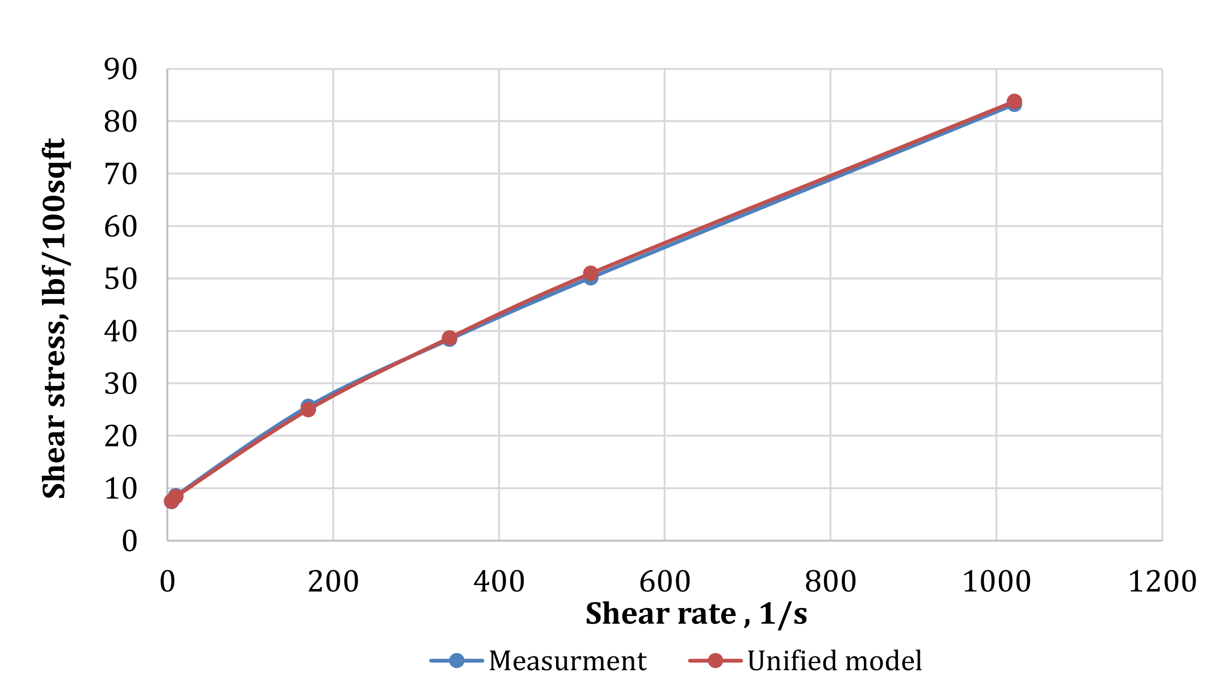

Figure 3.8: Illustration of Unified model prediction

Model	Equation	Parameters			% Deviation
		τ_o	k	n	
Unified	$6.402+0.3125*\gamma^{0.7954}$	6.402	0.3125	0.7954	1.36

The last three models (HB, R&S and Unified) show quite good fit with the measured data with % deviation rate of 1.72, 1.76 and 1.36 respectively.

3.3 Viscoelasticity

A viscoelastic material is a material that behaves partly viscous and partly elastic. It is a time dependent material response to a sinusoidally varying strain shown on Figure 3.9.

Drilling fluids shows viscous and elastic responses. Characterization and quantification of the viscoelastic properties of drilling fluids helps to evaluate gel structure, gel strength, barite sag, and solid suspension phenomenon [38].

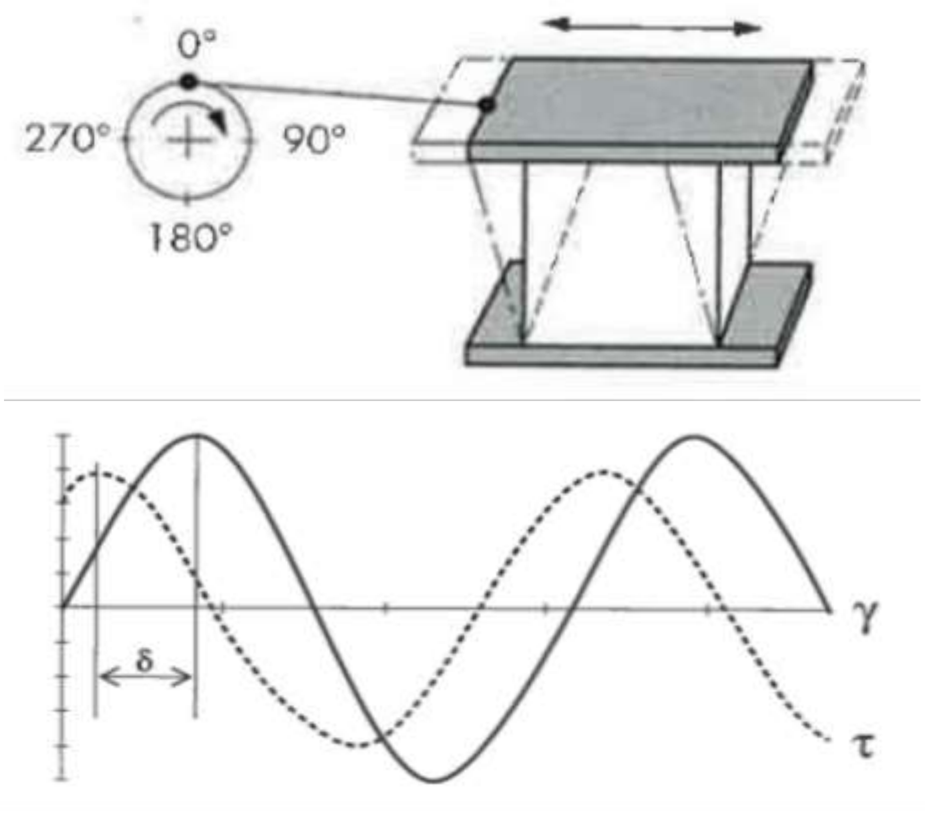

Figure 3.9: Sinusoidal loading by two plate and deformation [38].

The flow behavior and pressure drop influenced by the elastic property of drilling fluids. Pressure transient or pressure delay phenomenon is due to the viscoelasticity and gel structure formation of drilling fluids.

Gel structure formed when the drilling fluid is under static condition. Good gel may suspend solid components and reduces particle depositions.

The viscoelasticity properties of drilling fluid is quantified by measuring the elastic modulus (G') and the viscous modulus (G")

The term elastic modulus, G' describes the energy stored and hence termed as storage modulus. The viscous modulus "G" describes the energy lost and it is also known as the loss modulus [38].
The viscoelastic behavior the selected nano fluid systems (in Chapter 4) will be examined. Therefore, this section presents the theory of viscoelasticity, which is useful to interpret the measured data.

3.3.1 Viscoelastic theory

During viscoelasticity experiment, drilling fluid sinusoidal deformation and the stress response are measured. Shear stress can be written in term of strain as [33]:

$$\tau(t) = \gamma_o\left[\left(\frac{\tau_o}{\gamma_o}\cos\delta\right)\sin(\omega t) + \left(\frac{\tau_o}{\gamma_o}\sin\delta\right)\cos(\omega t)\right] \qquad 3.16$$

$$\tau(t) = \gamma_o\left[G^{'}\sin(\omega t) + G^{''}\cos(\omega t)\right] \qquad 3.17$$

$$G^{'} = \left(\frac{\tau_o}{\gamma_o}\cos\delta\right) \qquad 3.18$$

$$G^{''} = \left(\frac{\tau_o}{\gamma_o}\sin\delta\right) \qquad 3.19$$

$$\tan\delta = \left(\frac{G^{''}}{G^{'}}\right) \qquad 3.20$$

For a purely viscous fluid, the phase angle (δ) is equal to 90. For a purely elastic material, the phase angel is equal to 0. And for a viscoelastic material, the phase angle has values between 0 and 90. [38]

Phase angle	$\delta = 0$	$\delta = 45$	$\delta = 90$
Behavior	Elastic	transition	Viscous
G' and G''	G' > G''	G' = G''	G' < G''

Table 3.3: Viscoelastic parameters.

3.3.2 Viscoelasticity measurement

In this thesis, we will use two types of viscoelastic tests, namely oscillatory amplitude sweep and frequency sweep. From the amplitude sweep measurement, we will determine the linear viscoelastic region (LVER). The LVER is used to determine the stability of a fluid system. The length of LVER of the elastic modulus (G') describes the degree of the sample dispersion and stability [38].

3.3.3 Oscillatory amplitude sweep test

The first oscillatory test to be performed is an amplitude sweep test. During an amplitude sweep test, the amplitude of the shear stress is varied for a constant frequency. Figure 3.10 illustrates the test result, which display the storage modulus G' in red and the loss modulus G'' in blue as a function of shear rate [39].

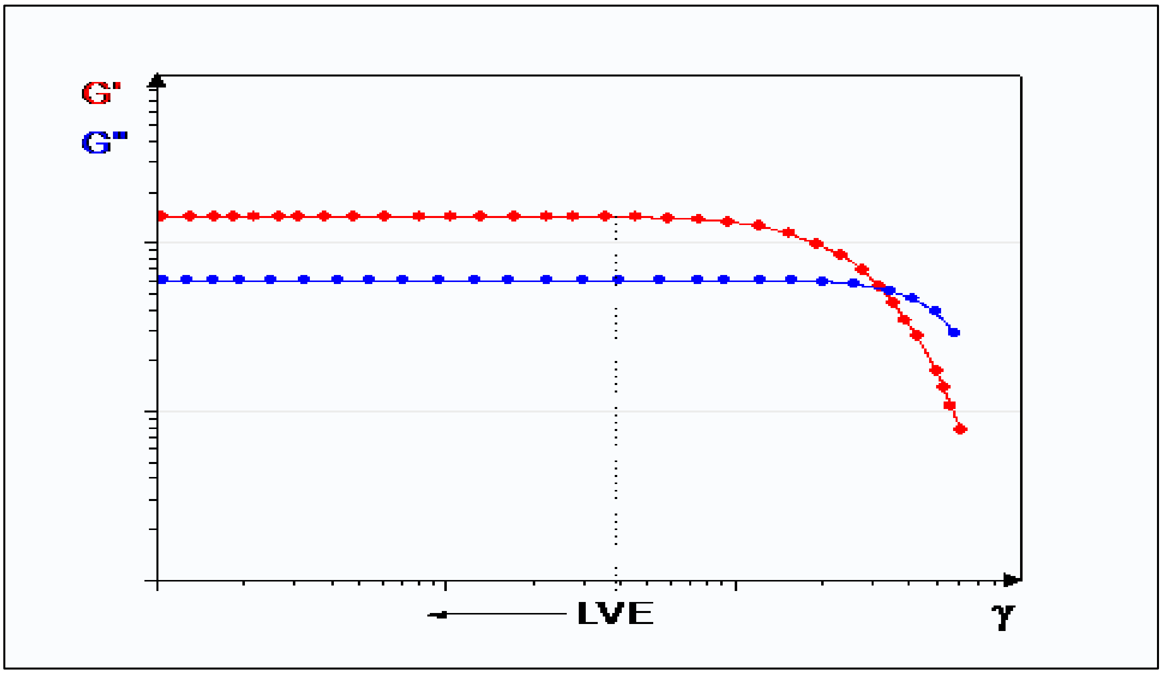

Figure 3.10: Amplitude Test G' and G'' moduli plotted against the deformation [39]

As shown on the figure, at the lower shear rate, the G' and G'' are constant. Physically, this is interpreted as the fluid structure is undisturbed. The horizontal region before being deviated is called linear-viscoelastic (LVE). As the loss and storage moduli begin decreasing, the structure is being disturbed.

From the amplitude sweep test, the yield point is the point at which the storage modulus deviates from the horizontal line. This point shows the end of the lower viscoelastic region. When the G' and G'' lines intersect, this point is called flow point, where the system becomes equally viscous and elastic. The phase angle becomes 45 deg. After flow point the fluid becomes more viscos dominated.

3.3.4 Oscillatory frequency sweep test

The second viscoelasticity measurement is the frequency sweep. During measurement, keeping the amplitude constant the frequency is varied from zero to 100 cycles. This type of test is good for characterization of polymer fluids. The test results indicate the fluid sedimentation stability. Figure 3.11 shows an illustration of frequency sweep-test result for a polymer fluid system [39].

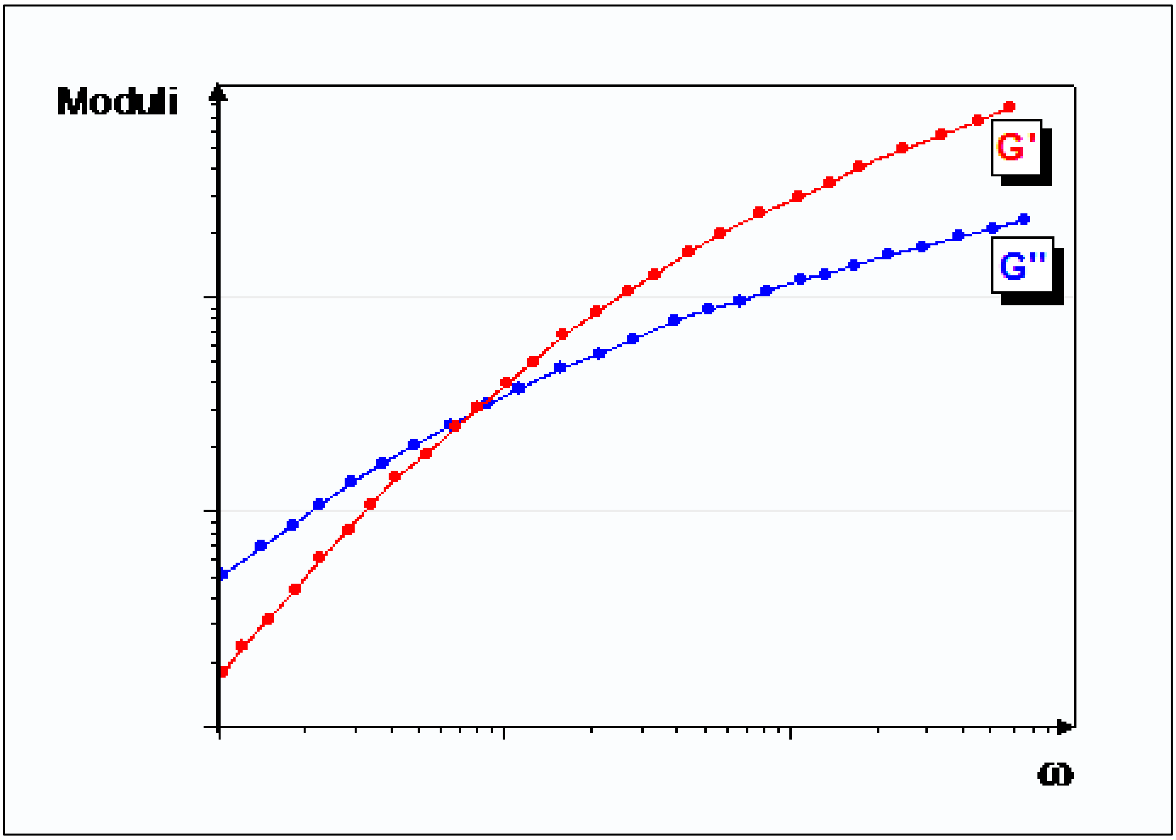

Figure 3.11: The Frequency Sweep Test [39].

3.4 Hydraulic model

Hydraulics is concerned mainly with the dynamics of moving liquids. This is concerned with matters such as friction in pipe, annulus, and surface equipment and through nozzles.

Figure 3.12 illustrates drilling fluid circulation system. During fluid circulation through the system, pressure is lost.

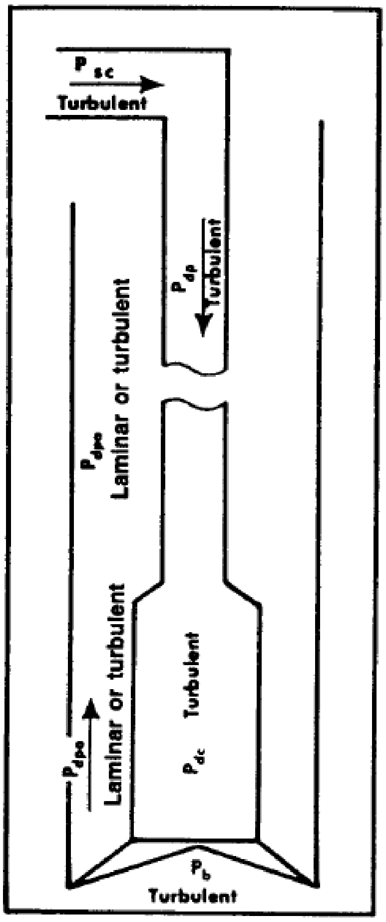

Figure 3.12: Hydraulic system and pressure drops [32].

The surface rig pump therefore overcomes all pressure losses. These are:

- Surface pressure loss as flows thorough the surface equipment like swivel and pipes ΔP_s
- Flows through drill string ΔP_{ds} and drilling collar ΔP_{dc}
- Flows through the nozzles of drilling bitΔP_b
- Flows through annulus spaces ΔP_{ac}
- Flows through annular spaces between drilling string and riser ΔP_{ads}

The total pressure loss is the sum of the mentioned pressure drops.

$$\Delta P_{Total} = \Delta P_s + \Delta P_{dc} + \Delta P_{ds} + \Delta P_b + \Delta P_{ac} + \Delta P_{ads} \qquad 3.21$$

Bit nozzle pressure loss

The pressure drop across a bit is calculated by [40, 41]

$$\Delta P_b = \frac{\rho q^2}{12034.7 A^2 {C_d}^2} \tag{3.22}$$

Where

ΔP_b pressure drop across the bit nozzle , q is the volumetric flow rate across the bit nozzles (GPM), ρ is the density of the drilling fluid (ppg), A is the sum area of the bit nozzles (in^2) and C_d is the bit discharge coefficient which is normally set equal to 0.95.

In literature, there are several hydraulics models available. These are Bingham plastic and power law model, Herschel-Buckley, Unified, Robertson & Stiff and other.

The main objective of the thesis is to characterize (through measurement) and performance simulation studies to evaluate the cutting transport efficiency and hydraulics of the considered drilling fluids.

To analyze the hydraulics performance of the drilling fluids, we considered only Unified model. Why we used this model in Chapter 5? The following was the reason.

Sadigov (2013)[42] has analyzed the hydraulics of drilling fluid-A and drilling fluid-B. The author compared the predictive power of several hydraulic models among others Unified and Herschel-Buckley. As shown on Figure 3.13, Unified model captured the measured data better than the Herschel-Buckley model for drilling fluid-A when flowing in annulus.

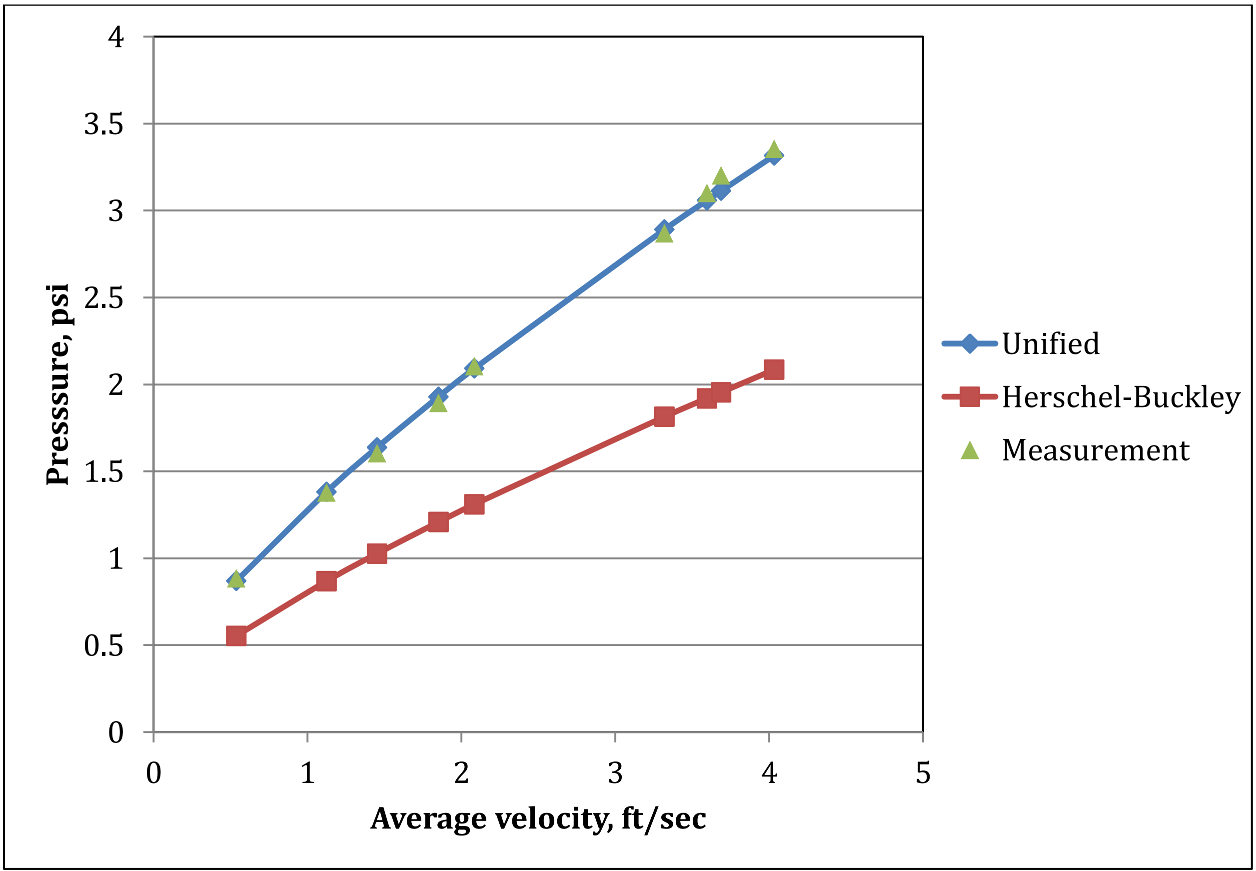

Figure 3.13: Prediction of Herschel-Buckley and Unified model in annuls flow for fluid type A [42].

The author also analyzed drilling fluid-B when flowing through pipe. As shown in Figure 3.14, the Herschel-Buckley model predicts better than the than Unified model. This illustrate that different drilling fluids behave differently with different models.

Similarly, fluid type B was also analyzed in annulus flow. As shown on Figure 3.15, both of the models do not perfectly predict the measured hydraulic pressure. However, comparing the two models, the Unified model is nearly closer to the measured data than the Herschel-Buckley model.

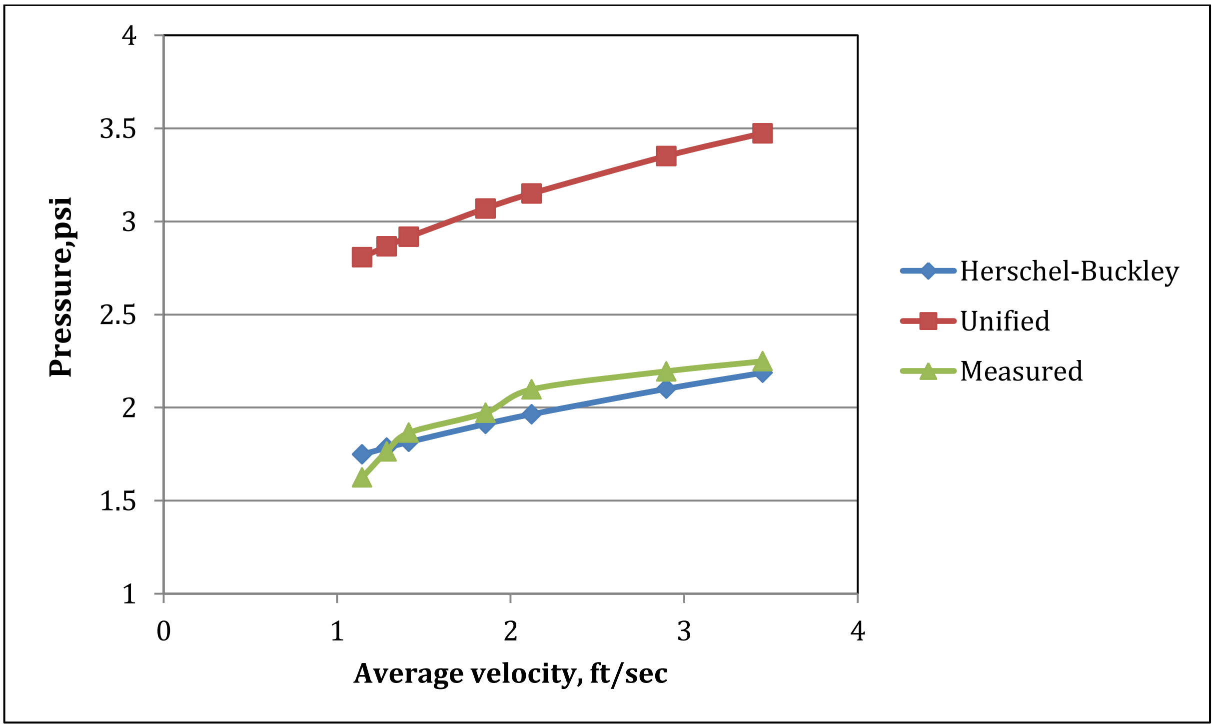

Figure 3.14: Comparison of Herschel-Buckley and Unified model in pipe flow for fluid type B [42]

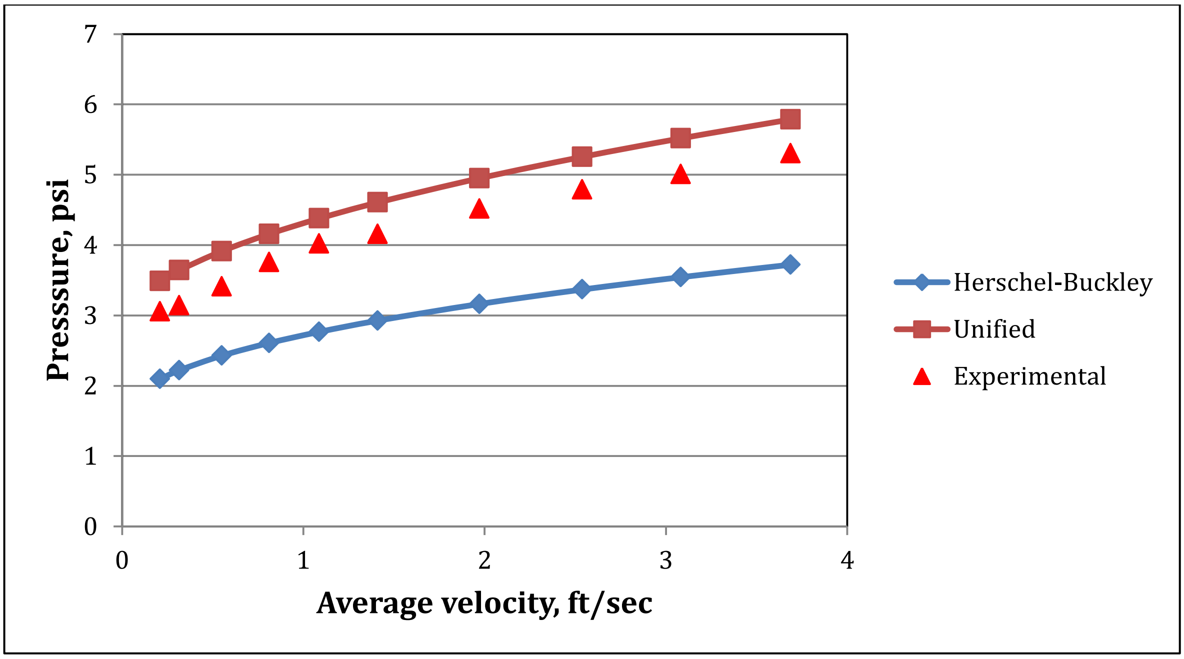

Figure 3.15: Prediction of Herschel-Buckley and Unified model in annulus flow for fluid type B [42].

Based on the above presented reviewed information, we can observe that the Unified model works well. Therefore, in this thesis work to evaluate the drilling fluids formulated in Chapter 4, the Unified model has been chosen.

Table 3.4 shows the summary of the models [50]. The parameters are listed on the list of symbols.

Table 3.4: Unified hydraulic model [50]

<table>
<tr><th colspan="2">Unified model</th></tr>
<tr><th>Pipe Flow</th><th>Annular flow</th></tr>
<tr><td colspan="2">$\mu_p = R_{600} - R_{300}, [cP] \quad \tau_y = R_{300} - \mu_p, [lbf/100ft^2] \quad \tau_0 = 1.066 \cdot (2 \cdot R_3 - R_6)$</td></tr>
<tr><td>$n_p = 3.32 \cdot log\left(\frac{2 \cdot \mu_p + \tau_y}{\mu_p + \tau_y}\right)$
$k_p = 1.066\left(\frac{\mu_p + \tau_y}{511^{n_p}}\right)$</td><td>$n_a = 3.32 \cdot log\left(\frac{2 \cdot \mu_p + \tau_{y-\tau_y}}{\mu_p + \tau_{y-\tau_y}}\right)$
$k_a = 1.066\left(\frac{\mu_p + \tau_y - \tau_0}{511^{n_a}}\right)$
$k = [lbf \cdot sec^n/100ft^2]$</td></tr>
<tr><td colspan="2">$G = \left(\frac{(3-\alpha)n + 1}{(4-\alpha)n}\right) \cdot \left(1 + \frac{\alpha}{2}\right)$
$\alpha = 1\ for\ pipe \quad \alpha = 1\ for\ annuli$</td></tr>
<tr><td>$v_p = \frac{24.51 \cdot q}{D_P^2}$</td><td>$v_a = \frac{24.51 \cdot q}{D_2^2 - D_1^2}$
$v = [ft/min]$</td></tr>
<tr><td colspan="2">$\gamma_w = \frac{1.6 \cdot G \cdot v}{D_R} = [sec^{-1}]$</td></tr>
<tr><td colspan="2">$\tau_w = \left[\left(\frac{4-\alpha}{3-\alpha}\right)^n \tau_0 + (k \cdot \gamma_w^n)\right] = [lbf/100ft^2]$</td></tr>
<tr><td>$N_{Re} = \frac{\rho \cdot v_p^2}{19.36 \cdot \tau_w}$</td><td>$N_{Re} = \frac{\rho \cdot v_a^2}{19.36 \cdot \tau_w}$</td></tr>
<tr><td>$f_{laminar} = \frac{16}{N_{Re}}$
$f_{transient} = \frac{16 \cdot N_{Re}}{(3470 - 1370 \cdot n_p)^2}$
Turbulent:
$f_{turbulent} = \frac{a}{N_{Re}^b}$
$a = \frac{\log(n) + 3.93}{50} \quad b = \frac{1.75 - \log(n)}{7}$</td><td>$f_{laminar} = \frac{24}{N_{Re}}$
$f_{transient} = \frac{16 \cdot N_{Re}}{(3470 - 1370 \cdot n_a)^2}$
Turbulent:
$f_{turbulent} = \frac{a}{N_{Re}^b}$
$a = \frac{\log(n) + 3.93}{50} \quad b = \frac{1.75 - \log(n)}{7}$</td></tr>
<tr><td colspan="2">$f_{partial} = ({f_{transient}}^{-8} + {f_{turbulent}}^{-8})^{-1/8}$</td></tr>
<tr><td>$f_p = ({f_{partial}}^{12} + {f_{laminar}}^{12})^{1/12}$</td><td>$f_a = ({f_{partial}}^{12} + {f_{laminar}}^{12})^{1/12}$</td></tr>
<tr><td>$\left(\frac{dp}{dL}\right) = 1.076 \cdot \frac{f_p \cdot v_p^2 \cdot \rho}{10^5 \cdot D_p} = [psi/ft]$
$\Delta p = \left(\frac{dp}{dL}\right) \cdot \Delta L = [psi]$</td><td>$\left(\frac{dp}{dL}\right) = 1.076 \cdot \frac{f_a \cdot v_a^2 \cdot \rho}{10^5 \cdot (D_2 - D_1)} = [psi/ft]$
$\Delta p = \left(\frac{dp}{dL}\right) \cdot \Delta L = [psi]$</td></tr>
<tr><td colspan="2">$\Delta p_{Nozzles} = \frac{156 \cdot \rho \cdot q^2}{({D_{N1}}^2 - {D_{N2}}^2 - {D_{N3}}^2)^2} = [psi]$</td></tr>
</table>

3.5 Hole cleaning

During drilling, drill bit crushes rock formation into pieces. These pieces of rock are called cutting. One of the functions of drilling fluid is to carry out cutting from a well to surface. Figure 3.16 illustrates cutting transport phenomenon in laminar flow. Cuttings transport rates depends on several parameters such as on particle size and density, drilling fluid density and viscosities, flow rate, flow regimes, well inclination, operational parameters such ROP , RPM. [44]

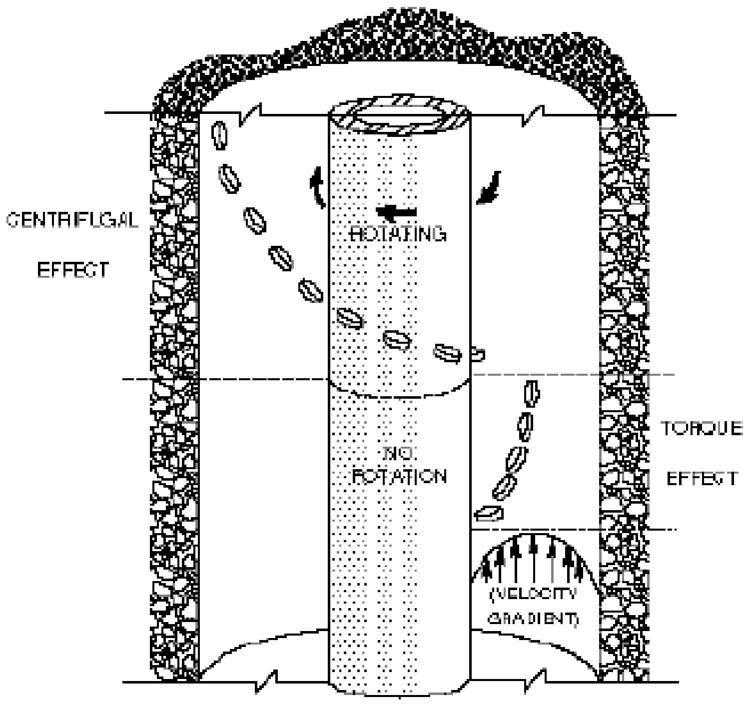

Figure 3.16: Illustration of cutting transport in laminar flow [45]

Poor hole cleaning can cause drilling related problems. There are to mention, drill pipe sticking, and high torque and drag [44].

During planning phase, it is important to perform a hole cleaning simulation study to predict the minimum flow velocity to bring cutting to surface. There are several hole-cleaning models documented in literatures. However, in this thesis we will use WellPlan™ software [46] to analyze the cutting transport performance of the formulated drilling fluids.

4 Experimental study

In this thesis work, drilling fluids were prepared and tested to investigate the effect of nano, polymer and salts in a bentonite treated WBM system. The formulated drilling fluids are going to be characterized through their rheological properties, filtrate loss, and pH. Since weight material was not added, the drilling fluids do have the same density.

The rheology was measured by a Fann-35 viscometer, and the filtrate loss was tested with an API Filter press. We measure 8 Fann readings at 600, 300, 200, 100, 60, 30, 6 and 3 RPM. Graph for shear stress vs shear rate were generated, and rheological parameters of the mud systems were calculated.

4.1 Selection of bentonite content

To determine the amount of bentonite to be used in the drilling fluid, a literature study was performed. As shown in Figure 4.1, the amount of bentonite used in drilling mud varied up to 14% and the most of the studies used 6% of bentonite. [47] The average is 5% out of the considered field data. Therefore, in this thesis 5% Bentonite out of was the fluid content used for experimental work. That means, 25g bentonite treated with 500g H_2O.

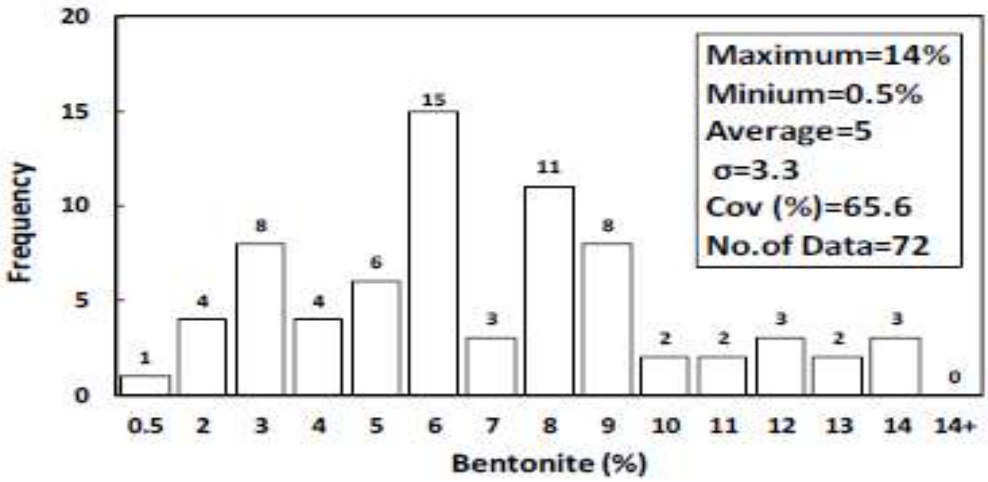

Figure 4.1: Histogram for percent of Bentonite used in drilling fluid [47].

4.2 Description of Nano silica (SiO_2)

15nm sized Nano no-silica particle was used in this thesis work. The particle was obtained from EPRUI Nanoparticles and Microspheres Co. Ltd, China. [48] The purity and the structure of the particle were analysed through imaging Scanning Electron Microscopy (SEM) (Figure 4.2) and Elemental Dispersive Spectroscopy (EDS) (Figure 4.3). As shown on the figure, nano – silica particle contain: Silicon (Si), Oxygen (O) and some Carbon (C) elements. Since the particle has been coated with Palladium (Pd, it is shown on EDS plot, which is not part of the system.

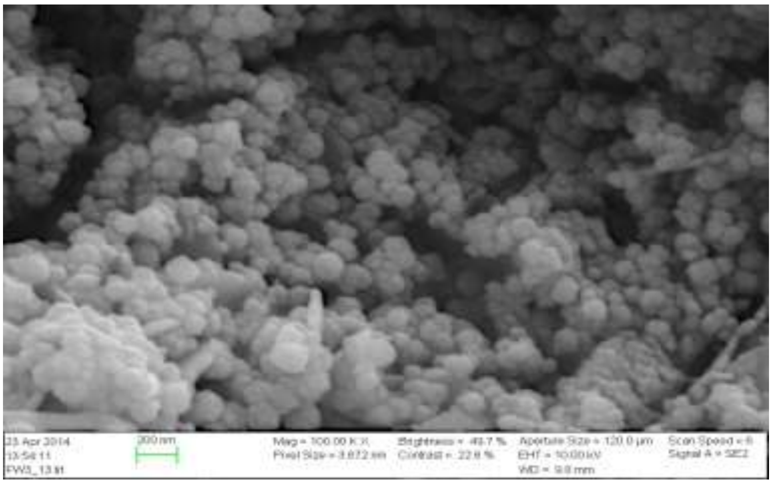

Figure 4.2: SEM picture of Nano- Silica.

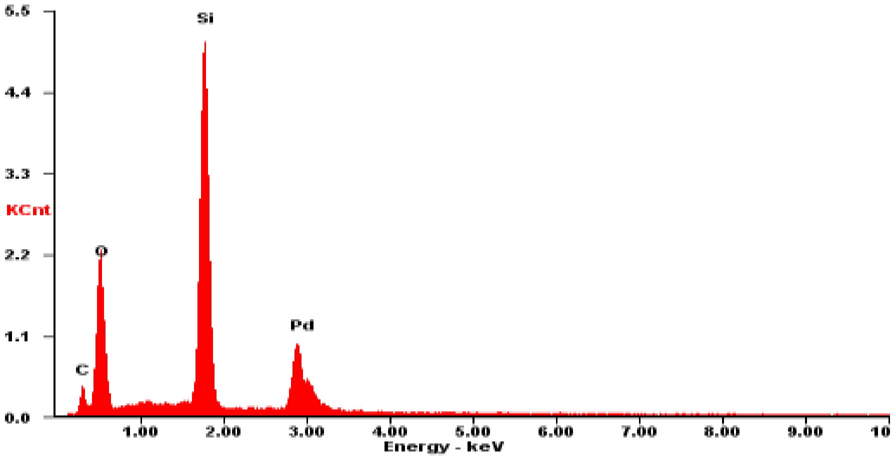

Figure 4.3: Element analysis of Nano- Silica.

4.3 Experimental test matrix designs summary

Table 4.1 illustrates the summary of drilling fluid design and comparisons to learn the effect of additives such as salt, polymer and Nano. For instance, test program #1 is considered as a base case. The objective of this base case is to study the effect of various salts in bentonite drilling fluid. Test program #2 was designed to study how 0.095% wt PAC influences the base case. Test #3 designed based on the result obtained Test #2 and test #4 designed based on the result obtained from Test #5 and so on. This design is believed to systematically investigate the effect of additive and to compare with the base case as well.

Test program	Test design	Additives	Objective of test program	Comparison
#1	Effect of salts	Na_2CO_3, $NaHCO_3$, NaCl, Na_2SO_4, and KCl	Study effect of salts on simple bentonite mud system Used as reference so that the other test matrixes will be compared with	-
#2	Effect of 0.38 wt% Salts types in 0.095 wt% PAC treated drilling fluid	PAC #1 salts	Study effect of PAC with different salts on simple bentonite mud system	#1
#3	Effect of 0.38 wt% salts types in 0.038 wt% Nano Silica treated drilling fluid	Nano Silica #1 salts	Study effect of nano silica on bentonite and salt mud systems	#1
#4	Effect of salts types in 0.038 wt% Nano Silica and 0.095 wt% PAC system	Nano Silica PAC #1 salts	Study combined effect of PAC and Nano Silica on bentonite and salt mud systems	#1, #2, #3
#5	Effect of salts mixtures in 0.038% Nano Silica and 0.038% PAC system	Nano Silica PAC KCl, NaCl, Na_2CO_3, and Na_2SO_4	To study salt mixture effect in order to improve the performance of KCl mud system	#4
#6	Effect of 0.04 wt% Nano Silica in salt treated DUOVIS and PAC polymer system	Nano Silica, PAC, Duovis, KCl	To study and screen out high concentration of KCl in DUO-Vis system	
#7	Effect of various Nano Silica in salt treated DUOVIS and PAC polymer system	Nano Silica, PAC, Duovis, KCl	The screened out KCl used in various nano silica conc.	
#8	Effect of various Nano Silica in 4gm KCl +0.75 Na2CO3 salt treated system	Nano Silica, CMC, Duovis, KCl, Na_2CO_3	To study the effect of nano in the given brine treated polymer system	
#9	Effect 0.75g Na_2CO_3 Ex-Situ in various Nano Silica in 4gm KCl salt treated system	Nano Silica, CMC, Duovis, KCl, Na_2CO_3	To study the effect of ex-situ salt in various nano	
#10	Effect 0.75 Na2CO3 Ex-situ in Drispac system	Nano Silica, CMC, Drispac, KCl, Na_2CO_3	Study the effect of Drispac in various nano	

Table 4.1 Summary of experimental test design program.

4.4 Test matrix #1: Base case-Effect of salts

The objective of test matrix #1 (Base case) was to study the effect of salts in bentonite drilling fluids and screen out the one which provides undesired result. At first, seven drilling fluids were formulated using seven different types of salts. After 48hours, two of the drilling fluids showed disintegration of bentonite system resulting two phase systems (Water and Bentonite settling out). The salts were $CaSO_4$ and $MgSO_4$. Due to poor results, these two salt systems were screened out and the rests were considered for further evaluations. The base case fluid systems are going to be used as a reference with which the other fluids with different additives to compared with.

4.4.1 Description of fluid systems

The salts used for the analysis are: Na_2CO_3, $NaHCO_3$, NaCl, Na_2SO_4, and KCl. A bentonite mud system was prepared by adding 500 ml H_2O with 25g Bentonite. The mud system was considered as a reference. On the reference mud system 2.0 g salt were added. The mud systems were mixed with a Hamilton beach mixer. The fluid was then allowed to stay for 48 hours in order for the bentonite to swell. The process of mixing and aging are applied for all drilling formulations. Table 4.2 shows the test matrix and the fluids were mixed in the order:

$$500ml\ H_2O + 2g\ Salt + 25g\ Bentonite$$

Table 4.2: Drilling fluid formulation of test matrix #1.

Base case: **Drilling fluids**						
Additives	Ref fluid	Fluid 2 (Na_2CO_3)	Fluid 3 ($NaHCO_3$)	Fluid 4 (NaCl)	Fluid 5 (Na_2SO_4)	Fluid 6 (KCl)
Water [ml]	500	500	500	500	500	500
Bentonite [g]	25	25	25	25	25	25
Salt [g]	0	2	2	2	2	2

4.4.2 Results and analysis

Figure 4.4 shows the effect of salt types on viscometer responses. As shown, the three salts systems (Na_2CO_3, Na_2SO_4 and KCl) increase the viscometer data significantly for all shear rates. The impact of these particular salts on the lower shear responses is higher than the reference, salt free system. On the other hand, two salts (NaCl and $NaHCO_3$) show also an impact on the reference, but less than the other three salts.

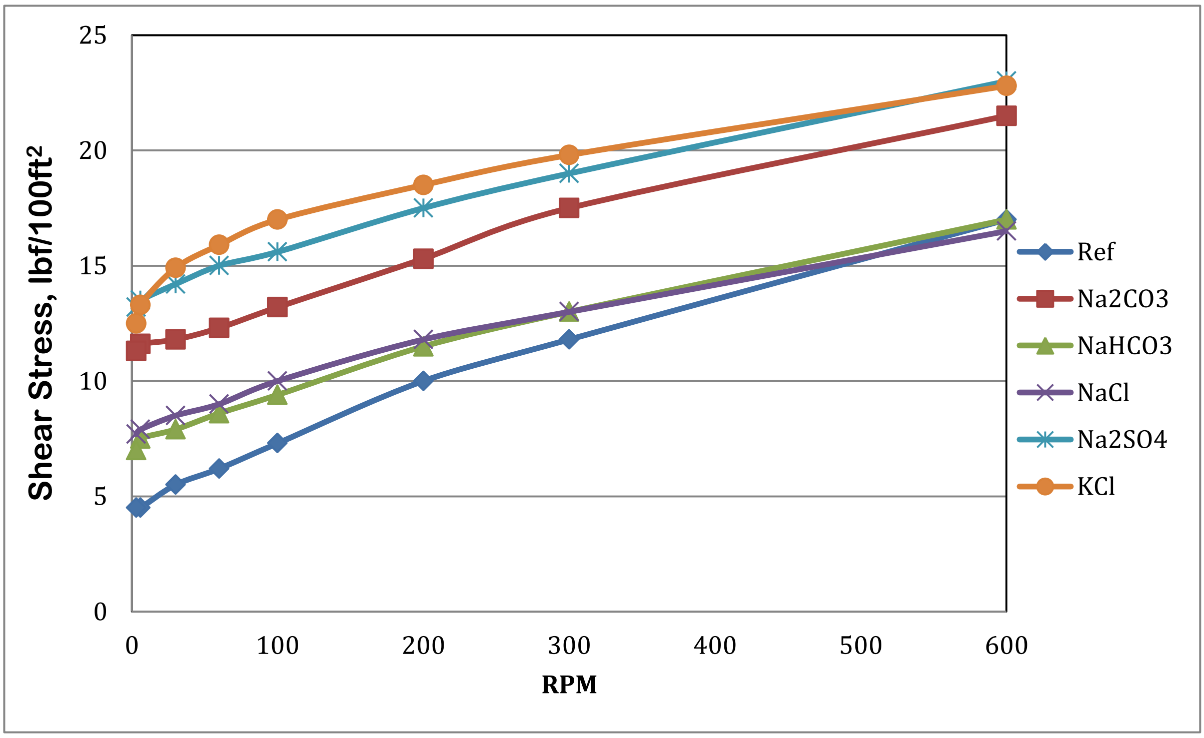

Figure 4.4: Viscometer data of test matrix #1 drilling fluids.

From the measured viscometer data, the Bingham and Power law parameters are calculated and shown in Figure 4.5 and Figure 4.6 respectively.

As displayed on figure 4.5, all the salt types reduced the plastic viscosity (PV) as compared with the salt free fluid system (reference). On the other hand, the yield stress (YS) values are increased, which is explained as a higher electrostatic force among the particles. The fluids exhibit a higher 300 and 600 RPM viscometer response. As provided in the theory part, the YS is calculated as ($YS = 2\theta_{300} - \theta_{600}$). The low shear yield stress (LSYS) is calculated from the lower shear rate readings as ($LSYS = 2\theta_3 - \theta_6$).

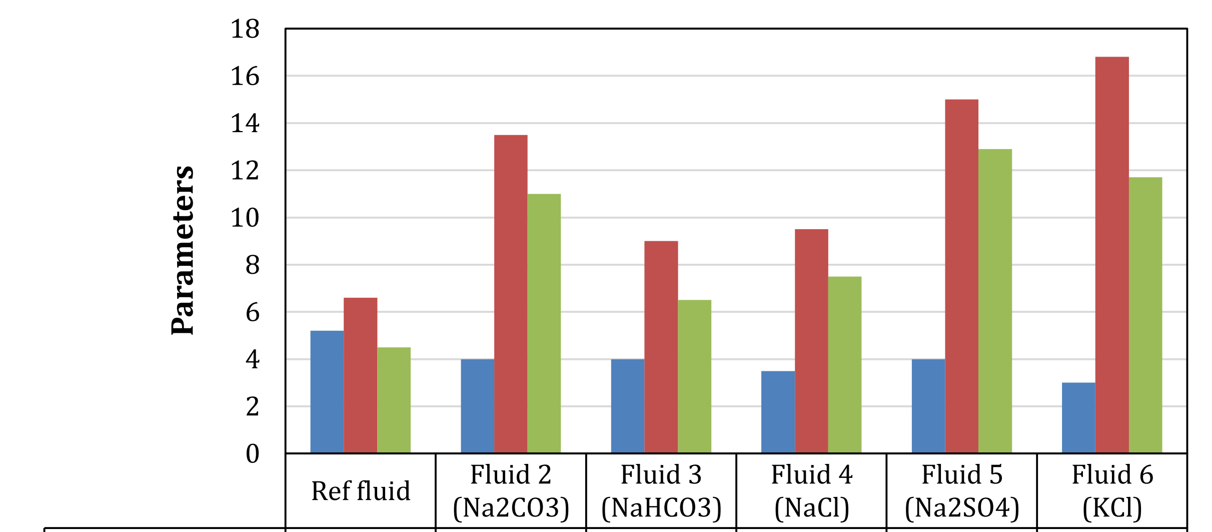

	Ref fluid	Fluid 2 (Na2CO3)	Fluid 3 (NaHCO3)	Fluid 4 (NaCl)	Fluid 5 (Na2SO4)	Fluid 6 (KCl)
PV [cP]	5.2	4	4	3.5	4	3
YS [lbf/100ft2]	6.6	13.5	9	9.5	15	16.8
LSYS[lbf/100ft2]	4.5	11	6.5	7.5	12.9	11.7

Figure 4.5: Test matrix #1-Bingham plastic (PV), Yield stress (YS) and low shear yield stress (LSYS) parameters of base case drilling fluids.

Figure 4.6 shows the consistency index (k) and flow behavior index (n) of fluids. From the figure, one can observe two clear effects, namely:

- Every mud containing salt shows a higher consistency-index (k) than the reference fluid.

- Every mud containing salt shows a lower exponent law index (n) than the reference fluid.

For high shear rates, k-value increases in the presence of 2g salt as compared with the salt free reference system.

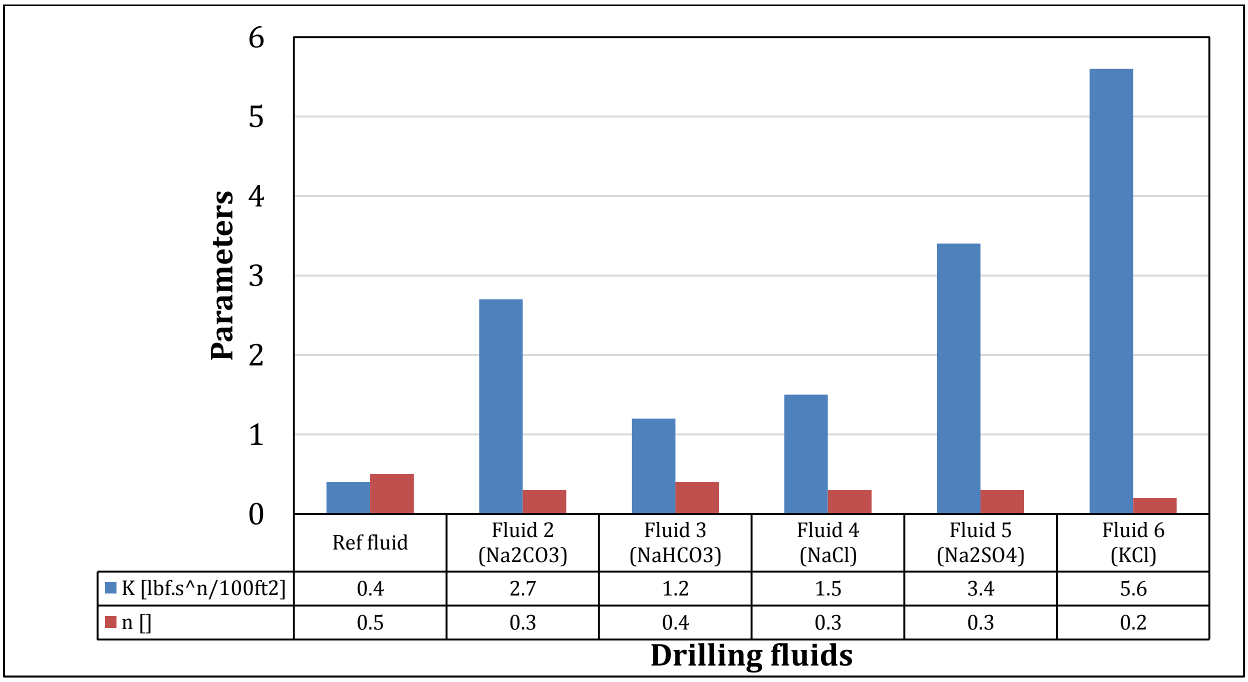

Figure 4.6: Power law parameters of base case drilling fluids.

Table 4.3 shows the static filter loss measured in 7.5min. As shown on the table, Na_2CO_3 and $NaHCO_3$ salts reduced the filtrate loss by -13.14% and -4% respectively. Salts such as NaCl, Na_2SO_4 and KCl increase the filtrate loss by +34.3%, +21.14% and +60%, respectively. One clear observation is that those salts, which causes an increase filtrate loss creates bubbles in the drilling fluid system. Table 4.4 shows the pH value of the drilling fluid. All the mud systems are alkaline.

Measurement	**Ref fluid**	**Fluid 2 (Na_2CO_3)**	**Fluid 3 ($NaHCO_3$)**	**Fluid 4 (NaCl)**	**Fluid 5 (Na_2SO_4)**	**Fluid 6 (KCl)**
Filtrate	8,75	7,6	8,4	11,75	10,6	14
% Change		-13,14	-4	34,28	21,14	60

Table 4.3: 7.5min filtrate loss values of the drilling fluid.

Measurement	**Ref fluid**	**Fluid 2 (Na_2CO_3)**	**Fluid 3 ($NaHCO_3$)**	**Fluid 4 (NaCl)**	**Fluid 5 (Na_2SO_4)**	**Fluid 6 (KCl)**
pH	9,90	10,65	8,90	9,40	9,45	9,15

Table 4.4: pH values of the drilling fluids.

4.5 Test matrix #2-Effect of 0.38% wt Salts types in 0.095% wt PAC treated drilling fluid

As illustrated in section §4.4, except Na_2CO_3 and $NaHCO_3$, the addition of 0.38% wt other salt types did not show a significant effect on filtrate loss. But, most of the salts have shown a significant effect on the viscosity parameters.

The objective of this part of experimental design was to investigate the effect of 0.095% wt PAC polymer on the filtrate and viscosity of the fluid systems presented in section § 4.4.

4.5.1 Description of fluid systems

Drilling fluids formulated by mixing the reference salt free mud system with 2g salts. Table 4.5 shows the test matrix.

<u>Formulation</u>

$$Reference\ (fluid\ 1)\ = 500ml\ H_2O + 0.5g\ PAC + 25g\ Bentonite$$

$$Salt\ treated\ systems\ fluid\ (2-6) = Reference\ Fluid\ 1 + 2g\ salt$$

Drilling fluids						
Additives	Ref fluid 1	Fluid 2 (Na_2CO_3)	Fluid 3 ($NaHCO_3$)	Fluid 4 (NaCl)	Fluid 5 (Na_2SO_4)	Fluid 6 (KCl)
Water [ml]	500	500	500	500	500	500
Bentonite [g]	25	25	25	25	25	25
Salt [g]	0	2	2	2	2	2
PAC [g]	0.5	0.5	0.5	0.5	0.5	0.5

Table 4.5: Test matrix #2 drilling fluid formulation.

4.5.2 Results and analysis

Figure 4.7 shows the viscometer data of the drilling fluids. As shown on the figure, fluid 6 (KCl) records a thinning effect in PAC system. This illustrates that KCl breaks the PAC polymer treated bentonite drilling fluid, which has a negative effect on the rheology of the fluid.

Comparing with the PAC free system presented in section § 4.4, the reference fluid, fluid 2 (Na_2CO_3), fluid 3 ($NaHCO_3$) and fluid 4 (NaCl) exhibit higher 600 and 300-rpm readings. On the other hand, fluid system 5 (Na_2SO_4) and 6 (KCl) show a lower reading. These values reflect in viscosity and gel strength parameters.

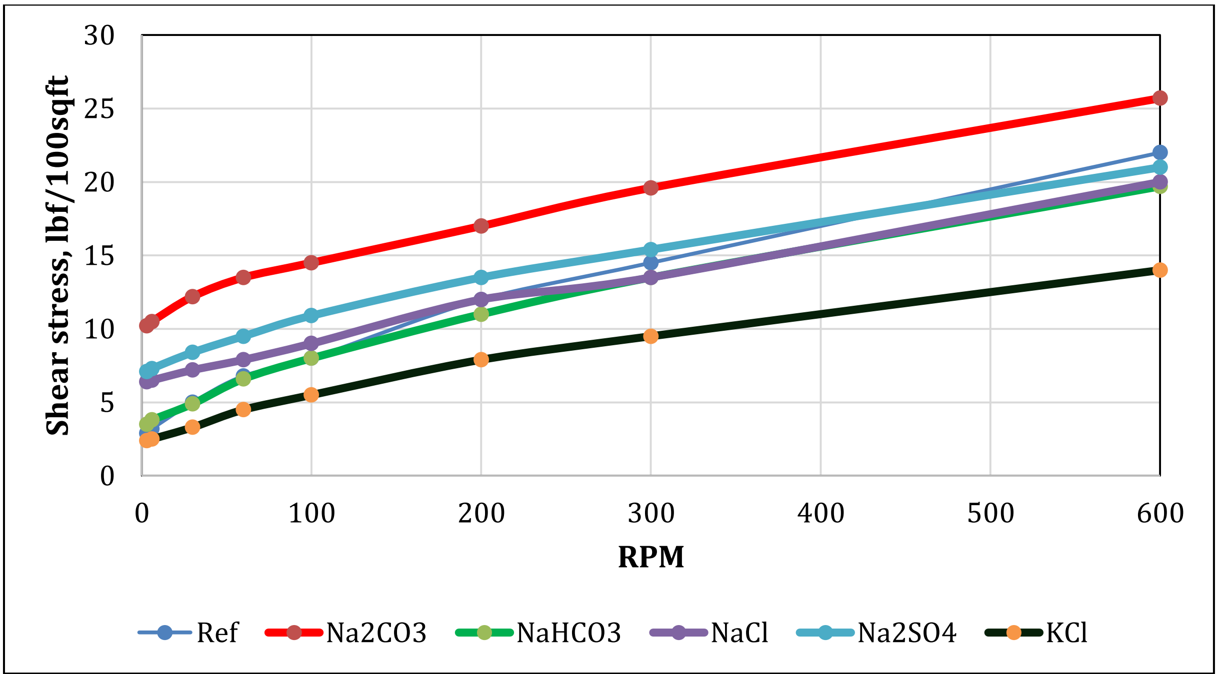

Figure 4.7: Viscometer data of test matrix #2 drilling fluids.

Figure 4.8 displays the computed Bingham plastic viscosity (PV), yield stress (YS) and low shear yield stress (LSYS) of Figure 4.7 drilling fluid systems.

In the following, the effect of PAC system compares with PAC free system (section §4.4, base case). As shown in Figure 4.8, the addition of PAC increased the plastic viscosity of all fluid systems. Comparing with PAC free system, the performance of PAC in Fluid 4 (NaCl) increased the plastic viscosity by 85.7% and the remaining drilling fluid systems increased by about 40-55 %.

Regarding yield stress, fluid 3, 4, 5 and 6 have a lower value than PAC free systems. Fluid 6 shows the most noticeable reduction by 70.2%.

PAC has also affected the low shear yield stress (LSYS). Fluid 6 (KCl) records a LSYS value lower than in section §4.4 by 9.4 lbf/100ft^2. In terms of percentage, the LSYS is reduced by 80.3%, which is the negative effect of PAC in KCL system. Reference fluid, fluid 3 and fluid 5 also showed a huge reduction of LSYS from base case (section § 4.4) by -42.2%, -50.8% and -46.5% respectively. Fluid 2 and fluid 4 showed a minor change (-10% and -16%) comparing with the other mud systems.

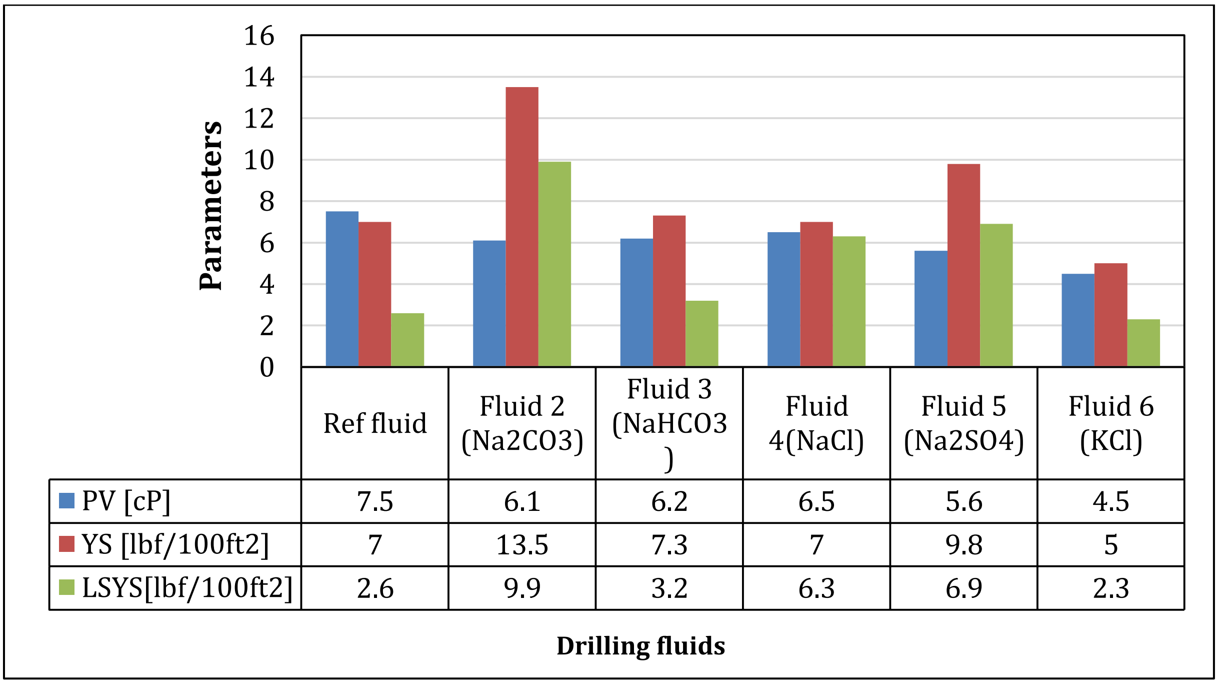

	Ref fluid	Fluid 2 (Na2CO3)	Fluid 3 (NaHCO3)	Fluid 4(NaCl)	Fluid 5 (Na2SO4)	Fluid 6 (KCl)
PV [cP]	7.5	6.1	6.2	6.5	5.6	4.5
YS [lbf/100ft2]	7	13.5	7.3	7	9.8	5
LSYS[lbf/100ft2]	2.6	9.9	3.2	6.3	6.9	2.3

Figure 4.8: Bingham plastic, yield strength and lower shear yield strength of test matrix #2.

From Figure 4.9 shows the consistency index (k-value) and flow index (n-value) of the drilling fluids. If we compare these results with the base case(section §4.4), the addition of 0.5g PAC reduces the k-values and increase the n-values. Table 4.6 shows the percentile change comparisons these changes.

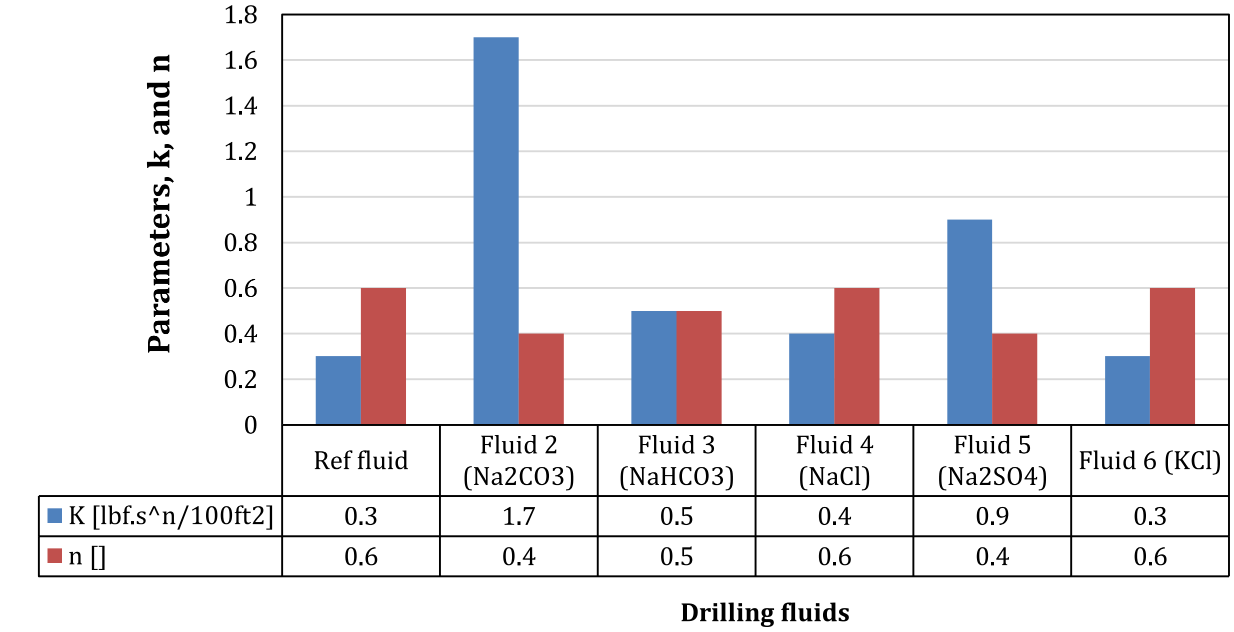

Figure 4.9: Power law parameters k-and n-values of test matrix #2.

	Ref	Fluid 2	Fluid 3	Fluid 4	Fluid 5	Fluid 6
%Change k	-22,9 %	-37,6 %	-61,3 %	-74,1 %	-72,2 %	**-94,8 %**
%Change n	14,2 %	31,6 %	40,9 %	64,9 %	62,3 %	**174,9 %**

Table 4.6: Percentile change of k- and n-values (comparisons between test matrix #2 and test matrix #1 systems).

As we can see from Table 4.6, fluid 6 is the most affected by the PAC and KCl. The mixture of KCl and PAC seems to break down the gel structure and resulting lower viscometer readings than the other salt treated fluid systems.

Regarding the other mud systems, the k- and n-values of the reference fluid shows a 23% reduction and a 14,2% increasing respectively. Fluid 4 and fluid 5 have shown very similar changes in percentage. A similar effect was also seen in Fluid 6, but the effect is most significant.

API-filter pressure measurement

Table 4.7 shows the measured filtrate loss and its percentile change comparisons with the reference fluid. As shown $NaHCO_3$ and NaCl fluid reduces the filtrate by -7% and -2 %, respectively. The filtrate volume for instance in KCl system increased by 40%. The increase in filtrate loss and the reduction of plastic viscosity in KCl, Na_2SO_4 and Na_2CO_3 system is an indication of aggregated assemblage of clay particles in the drilling fluids.

Measurement	Ref fluid	Fluid 2 (Na_2CO_3)	Fluid 3 ($NaHCO_3$)	Fluid 4 (NaCl)	Fluid 5 (Na_2SO_4)	Fluid 6 (KCl)
7.5min Filtrate, ml	5	6	4,65	4,9	6,6	7
% Change		20	-7	-2	32	40

Table 4.7: 7.5 min API filtrate loss of test matrix #2.

Comparing the filtrate loss of the mud systems without PAC (i.e test matrix #1), all the test matrix #2 mud systems show lower filtrate loss (See,Table 4.8). The huge filtrate loss improvement was due to the presence of PAC.

	Ref	**Fluid 2**	**Fluid 3**	**Fluid 4**	**Fluid 5**	**Fluid 6**
Difference	-3,75	-1,6	-3,75	-6,85	-4	-7
%Change	-42,9	-21,1	-44,6	-58,3	-37,7	-50

Table 4.8: Filtrate difference and % change comparisons between test matrix #2 and test matrix #1 systems.

4.6 Test matrix #3-Effect of 0.38%wt salts types in 0.038%wt Nano Silica treated drilling fluid

As shown from test matrix #2, the effect of the given PAC concentration has shown positive effect only in the two salt ($NaHCO_3$, NaCl) systems. It is documented that nano silica has shown positive results in improving the performance of cement [27].

The objective of this part of study was to evaluate the effect of 0.038% wt Nano silica on fluids systems presented in section §4.4.

4.6.1 Description of fluid systems

2g Nano silica treated based drilling fluids formulated by mixing bentonite with and without salt. Table 4.9 shows the test matrix. Reference mud was formulated by mixing 500g H_2O with 0.2g Nano. This fluid was then mixed with 25g Bentonite until the fluid system shows a homogenous soup like mixture. As shown on the Table, fluid systems 2-6 were obtained by mixing the reference mud with 2g different salt systems. The order of mixing of additives is as shown in the table.

<u>Formulation</u>

$$Reference\ (fluid\ 1)\ = 500ml\ H_2O + 0.2\ Nano\ Silica + 25g\ Bentonite$$

$$Salt\ treated\ systems\ fluid\ (2-6) = Reference\ (Fluid\ 1) + 2g\ Salts$$

Additives	Drilling fluids					
	Reference Fluid 1	Fluid 2 (Na_2CO_3)	Fluid 3 ($NaHCO_3$)	Fluid 4 (NaCl)	Fluid 5 (Na_2SO_4)	Fluid 6 (KCl)
Water [ml]	500	500	500	500	500	500
Nano [g]	0.2	0.2	0.2	0.2	0.2	0.2
Salt [g]	0	2	2	2	2	2
Bentonite[g]	25	25	25	25	25	25

Table 4.9: Test matrix #3-Bentonite and salt fluid system with nano.

Figure 4.10 shows the measured rheology data obtained from the drilling fluid systems formulated in Table 4.10.

Comparing with the results presented in section 4.4 (Test matrix #1/PAC free), the reference fluid, fluid 2 (Na_2CO_3), fluid 5(Na_2SO_4) and fluid 6 (KCl) all show a lower viscometer readings.

On other hand, the $NaHCO_3$ and the NaCl show higher viscometer readings.

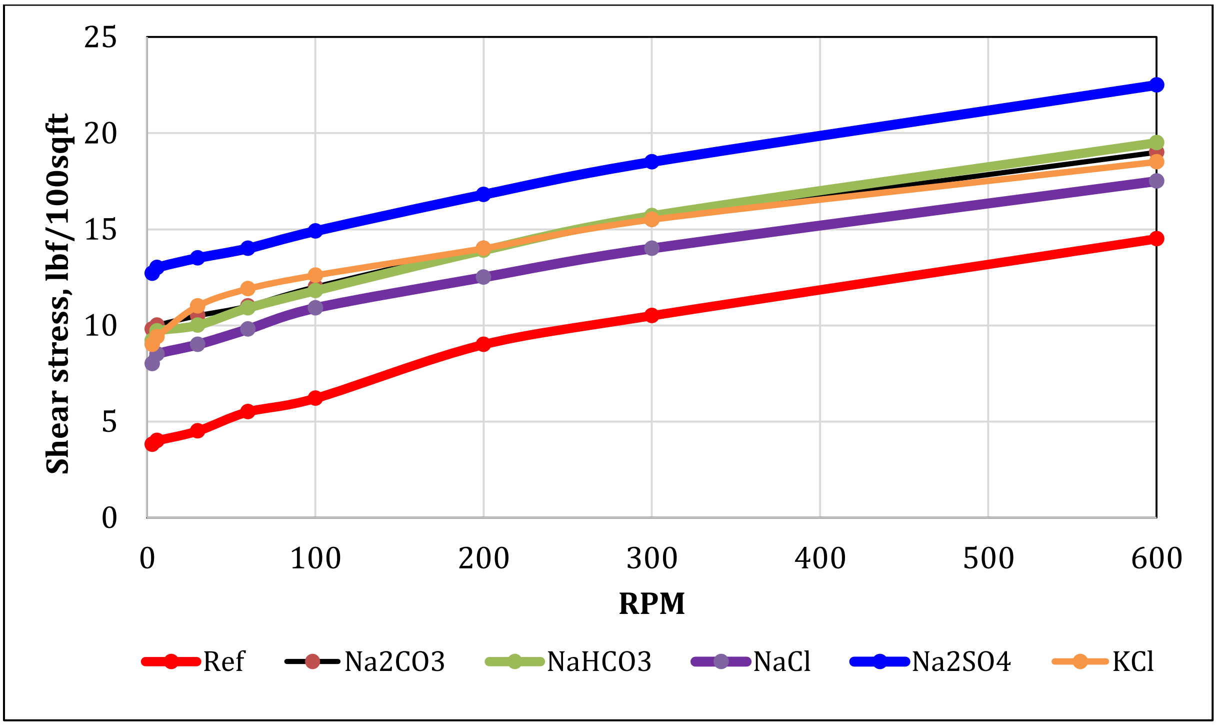

Figure 4.10: Viscometer data of test matrix #3 drilling fluids.

4.6.2 Results analysis

From the measured rheology data, the viscosity and the yield stress parameters were calculated and presented in Figure 4.11. As illustrated, effect of nano in various fluid systems is not very significant. For instance, we can observe a reduction of about 0.5 cP in Na_2CO_3 system and 1cP in KCl system. Comparing the drilling fluid that contains (Na_2SO_4) with the reference drilling fluid, the yield stress increases from 6.55 lbf/100sqft to 14.5lbf/100sqft just due to the salt additive. Comparing with nano free reference system presented in section § 4.4 (Test matrix #1), the addition of 0.2g Nano reduces the plastic viscosity by 1.2cP, which is by 24%.

0.2g Nano additive didn't show any impact on the yield strength (YS) of the reference fluid. Due to the additives, the YS of fluid 6 and fluid 3 are reduced by 25.6% and increasing by 32.2%, respectively.

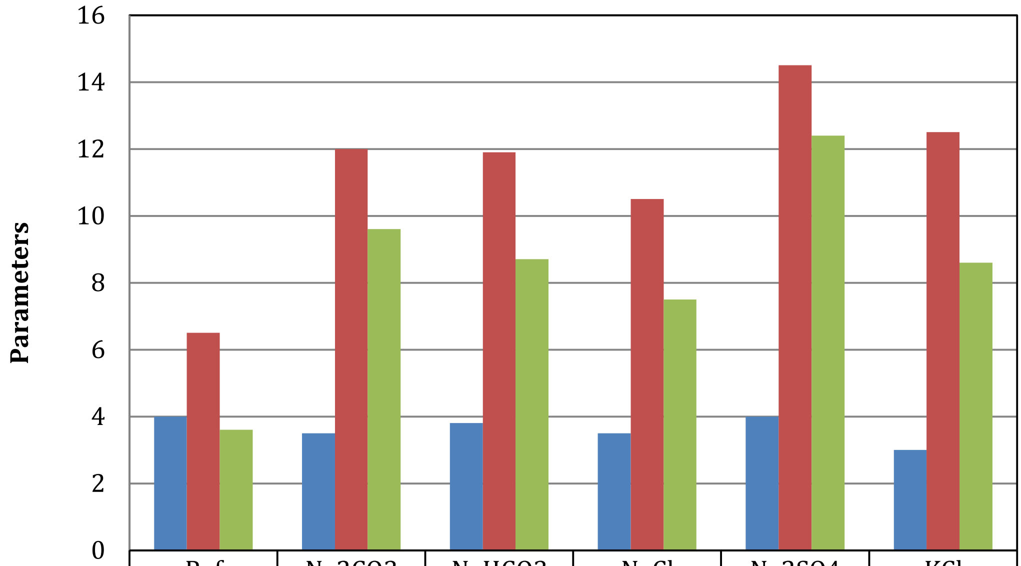

	Ref	Na2CO3	NaHCO3	NaCl	Na2SO4	KCl
PV (cP)	4	3.5	3.8	3.5	4	3
YS (lbf/100sqft)	6.5	12	11.9	10.5	14.5	12.5
LSYS(lbf/100sqft)	3.6	9.6	8.7	7.5	12.4	8.6

Figure 4.11: Test matrix #3-Plastic viscosity and Yield strengths of Nano silica treated bentonite and salt mud systems.

Figure 4.12 shows the consistency index (k-value) and flow index (n-value) of the drilling fluids. Comparing with the nano free system, the addition of nano silica reduces the consistency index of KCl system (Fluid 6) by -43.3 %. Similarly, fluid-2 and fluid 5 also have shown a reduction by - 9.6% and - 6.7% lower respectively.

On the other hand, that addition of nano silica increase the k-values of the reference fluid, fluid 3 and fluid 4 by 30%, 92% and 23.5%, respectively. Table 4.11 shows the comparison between the drilling fluid with and without nano-silica additives.

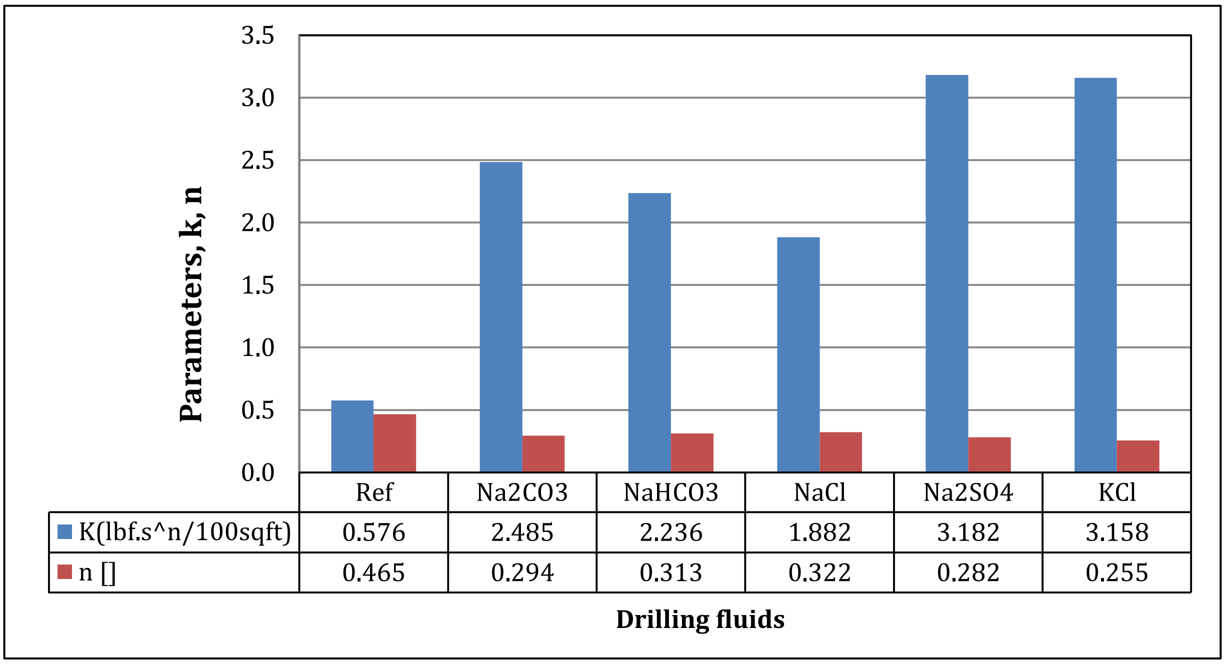

Figure 4.12: Power law k and n- parameters of test matrix #3 drilling fluids.

Power law parameters comparison of Nano free (Section §4.4) and & Nano treated (Section §4.6) drilling fluids in salts systems

In the comparison table 4.10, the % change of flow index (n-value) is also provided. As shown, the additive nano increase the n-value of fluid 5 and fluid 6 by 2.5% and 25.6 % respectively. On the other hand, the rest fluid systems show a reduction effect. This illustrates that the performance of nano silica is different in different salt systems.

	Ref	Fluid 2	Fluid 3	Fluid 4	Fluid 5	Fluid 6
%change k	30,0%	-9,6%	91,9%	23,5%	-6,7%	-43,3%
%change n	-11,6%	-1,0%	-19,1%	-6,4%	2,5%	25,6%

Table 4.10: k- and n-values percentile change of section § 4.5 mud systems compared to section §4.4 mud systems.

API filtrate measurement

Table 4.11 shows the API filtrate losses results obtained from test matrix #3 drilling fluid system. As shown, the addition of nano in salt treated system in general increase the filtrate for instance by 87% in Fluid 6 (KCl) and by 13% in Fluids 2 (Na_2CO_3) and Fluid 3 ($NaHCO_3$).

Measurement	Ref	Na_2CO_3	$NaHCO_3$	NaCl	Na_2SO_4	KCl
7.5min Filtrate, ml	7,5	8,5	8,5	11,75	10	14
% Change	-	13	13	57	33	87

Table 4.11: 7.5min API filtrate loss of of test matrix #3 drilling fluids.

API filtrate comparison of Nano free (Section §4.4) and & Nano treated (Section §4.6) drilling fluids in salts systems

Table 4.12 displays the comparison between drilling fluid systems formulated in section §4.6 (nano treated) and nano untreated (section§4.5)
As can be seen from the table, Nano additives reduce the filtrate of the reference fluid, fluid 4 (NaCl) and Fluid 5 (Na_2SO_4) systems. On the other hand Nano increase the filtrate of fluid 2 (Na_2CO_3) and Fluid (3) ($NaHCO_3$) by 11.8% and 1.2 % respectively. We can also observe that nano did not influence fluid 6 (KCl).

	Ref fluid	Fluid 2	Fluid 3	Fluid 4	Fluid 5	Fluid 6
Difference	-1 ml	0,9 ml	0,1 ml	-0,75 ml	-0,6 ml	0 ml
%change	-11,4%	11,8%	1,2%	-6,4%	-5,7%	0%

Table 4.12: Difference in filtrate loss between section §4.4 and section §4.6 mud systems.

4.7 Test matrix #4 Effect of salts types in 0.038%wt Nano Silica and 0.095%wt PAC system

From the previous studies, it is shown that the effect of Nano in salt treated system worsen the filtrate loss control performance. To study the effect of polymer PAC in fluid system presented in section § 4.6, this part of test matrix was designed.

4.7.1 Description of fluid systems

Table 4.13 shows the test matrix formulated to study the effect of 0.38% wt different salt treated with 0.038%wt Nano Silica and 0.095%wt PAC system.

Reference mud was formulated by mixing 500g H_2O with 0.2g nano and 0.5g PAC polymer. This fluid was then mixed with 25g Bentonite until the fluid system shows a homogenous soup like mixture. As shown on the Table, fluid systems 2-6 were obtained by mixing the reference mud with 2g different salt systems. The mixing sequences is in the order of #1-5.

<u>Formulation</u>

$$Reference\ (fluid\ 1)\ = 500ml\ H_2O + 0.2\ Nano\ Silica + 0.5g\ PAC + 25g\ Bentonite$$

$$Salt\ treated\ systems\ [fluid\ (2-6)] = Reference\ fluid\ 1 + 2g\ Salts$$

#	Additives	Drilling fluids					
		Ref fluid	Fluid 2 (Na_2CO_3)	Fluid 3 ($NaHCO_3$)	Fluid 4 (NaCl)	Fluid 5 (Na_2SO_4)	Fluid 6 (KCl)
1	Water (H_2O) [ml]	500	500	500	500	500	500
2	Nano [gm]	0.2	0.2	0.2	0.2	0.2	0.2
3-2	(Na_2CO_3) (gm)	-	2	-	-	-	-
3-3	($NaHCO_3$) (gm)			2			
3-4	(NaCl) (gm)	-	-	-	2	-	-
3-5	(Na_2SO_4(gm)	-	-	-	-	2	-
3-6	KCl (gm)	-	-	-	-	-	2
4	PAC (gm)	0.5	0.5	0.5	0.5	0.5	0.5
5	Bentonite [gm]	25	25	25	25	25	25

Table 4.13: Drilling fluid formulation of test matrix # 4.

4.7.2 Results analysis

The measured rheology drilling fluids formulated in Table 4.15 are shows on Figure 4.13. As shown, the KCl system rheology data lower than the reference bentonite fluid system and the Na_2CO3 system records higher value.

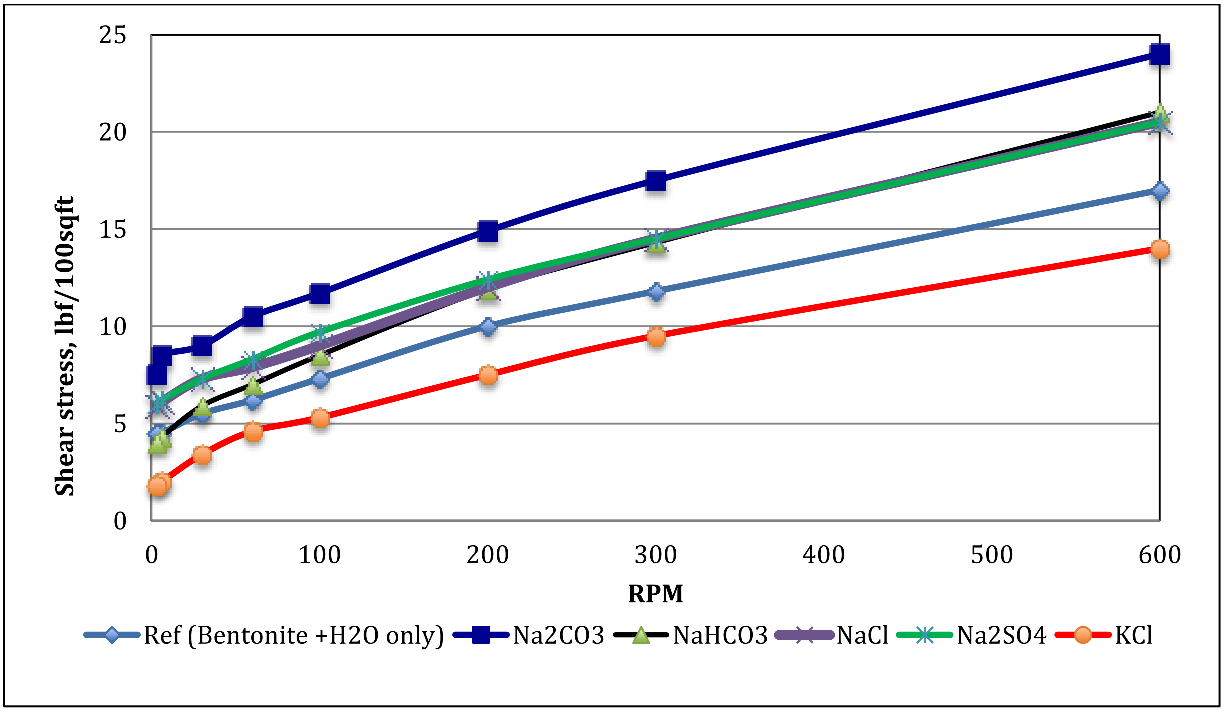

Figure 4.13: Viscometer data of test matrix #4 drilling fluids.

Figure 4.14 shows the computed drilling fluid parameters. The overall analysis result shows that Na_2CO_3 system shows the highest values, and the KCl system shows the least value. The results of the combined effect of PAC and nano silica are fairly close to the results obtained from the mud systems with only PAC.

The plastic viscosity (PV) of fluid 2, 3 and 5 show a little higher value in PAC/nano system than in only PAC system. PV is unchanged for KCl and fluid 4 shows lower value. Although there are some changes, it is clear that PAC has a more dominant effect on the PV than nano silica does.

The yield stress values of all mud systems are lower than in section §4.4 (salt only) and section § 4.6 (nano treated). The fluid systems with $NaHCO_3$ and NaCl salts, the yield stresses are higher than the similar mud systems presented in section §4.5(PAC only).

In the fluid systems with Na_2CO_3 and Na_2SO_4, the yield stresses are lower than similar fluids in section §4.5 (PAC only).

Comparing with section § 4.5 (PAC only), the yield strength of the KCl fluid in nano system shows no changes.

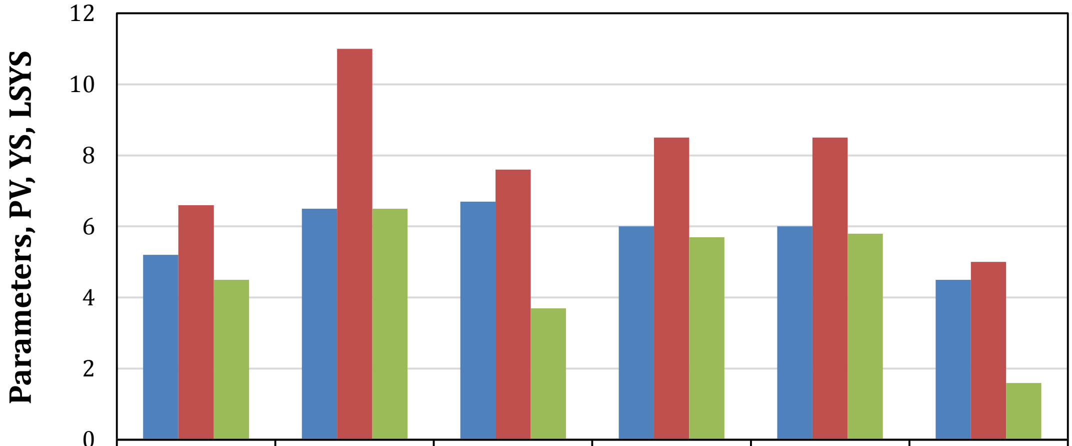

	Ref	Na2CO3	NaHCO3	NaCl	Na2SO4	KCl
PV (cP)	5.2	6.5	6.7	6	6	4.5
YS (lbf/100sqft)	6.6	11	7.6	8.5	8.5	5
LSYS(lbf/100sqft)	4.5	6.5	3.7	5.7	5.8	1.6

Drilling fluids

Figure 4.14: Bingham parameters and lower shear yield strength of test matrix #4.

Figure 4.15 shows the consistency index and flow index values of the fluid system. The n-values are almost in the range of 0.5-0.56. The k-value of the Na_2CO_3 system is also shows higher than the rest. This makes the performance of KCl, polymer and Nano better in Na_2CO_3 than in KCl. For the consistency index, only the system with Na_2CO_3 is above1 $lbf \cdot s^n/100ft^2$.

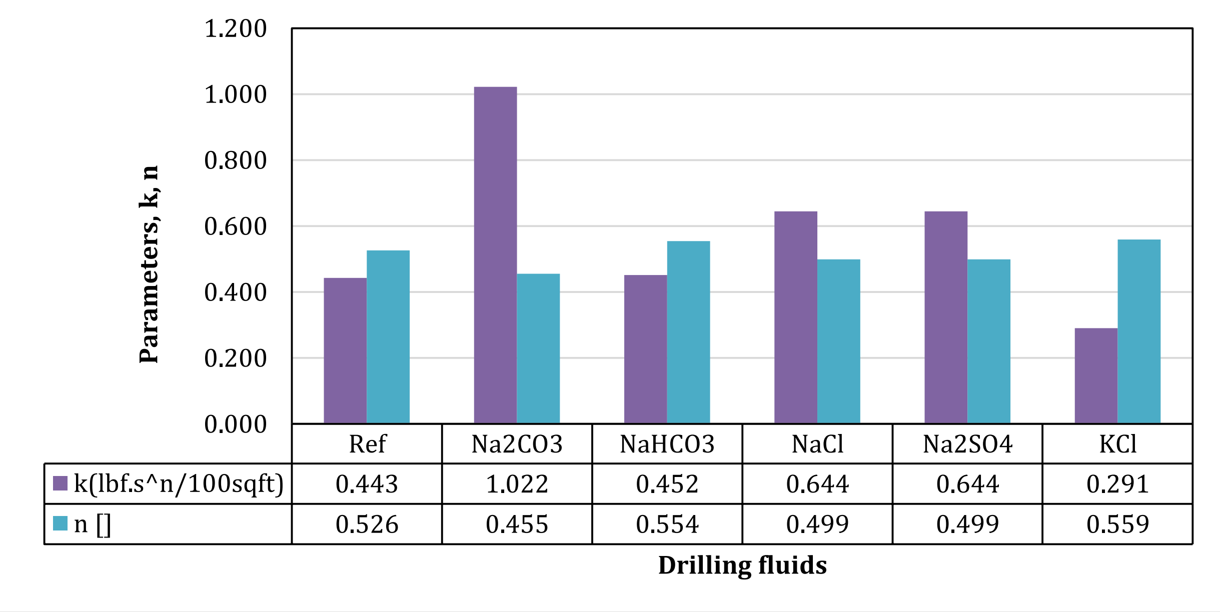

Figure 4.15: Power law parameters of test matrix #4 drilling fluids.

Comparing test matrix #4 systems with only PAC systems (test matrix #2), NaCl is the only system with positive effect on the consistency index. The other salts created lower n-values and no effect as shown for KCl system.

	Na_2CO_3	$NaHCO_3$	NaCl	Na_2SO_4	KCl
% change K	-40,4 %	0,1 %	63,6 %	-32,0 %	0,0 %
% change n	16,6 %	1,7 %	-11,9 %	11,6 %	0,0 %

Table 4.14: Percentile change in k- and n-values of test matrix #4 compared with test matrix #2.

7.5 min API filter press measurement

Table 4.15 shows the API filtrate loss for the different mud systems. Among these, fluid 4 shows the lowest filtrate loss.

Measurement	**Ref fluid**	**Fluid 2 (Na_2CO_3)**	**Fluid 3 ($NaHCO_3$)**	**Fluid 4 (NaCl)**	**Fluid 5 (Na_2SO_4)**	**Fluid 6 (KCl)**
Filtrate, ml	-	5,5 ml	5,5 ml	4,5 ml	5,5 ml	5,75

Table 4.15: 7.5 min filtrate loss of test matrix #4 drilling fluids.

Comparison of nano silica and PAC [Section § 4.7] & PAC salt [Section § 4.5] systems

Table 4.16 shows the difference in filtrate loss between 0.5g PAC and 2g salt mud systems with- and without 0.2g nano silica. Except fluid 3, all mud systems have a lower filtrate loss. This effect is due to the addition of 0.2g nano silica.

	Ref fluid	**Fluid 2 (Na_2CO_3)**	**Fluid 3 ($NaHCO_3$)**	**Fluid 4 (NaCl)**	**Fluid 5 (Na_2SO_4)**	**Fluid 6 (KCl)**
Difference	-	-0,5 ml	0,85 ml	-0,4	-1,1 ml	-1,25 ml
% change	-	-8,3%	18,3%	-8,2%	-16,7%	-17,6%

Table 4.16*:* Comparison of PAC polymer mud with and without nano silica.

4.8 Test matrix #5-Effect of salts mixtures in 0.038%wt Nano Silica and 0.095%wt PAC system

From the previous studies, it is shown that the effect of Nano in salt treated system worsen the filtrate loss control performance. This might have created a dispersed and deflocculated system. To study the effect salt mixtures in polymer PAC and nano system, three fluid systems are formulated and the results will be compared with the single salt systems KCl and NaCl.

4.8.1 Description of fluid systems

Table 4.17 shows test matrix of a single and combined salt systems. The single systems are Fluid 1 and Fluid 2. These are considered as reference systems. The salt mixture systems are fluid 4, fluid 5 and fluid 6, which are going to be compared with the single salt systems. The common additives among the considered drilling fluids are H_2O, Bentonite, Nano and PAC.

#	Additives	References Single salts		Combined salt mixtures		
		Fluid-1 (KCl)	Fluid 2 (NaCl)	Fluid 3 (NaCl+ KCl)	Fluid 4 (Na_2CO_3 +KCl)	Fluid 5 (Na_2SO_4)+ KCl)
1	Water [ml]	500	500	500	500	500
2	Nano [gm]	0.2	0.2	0.2	0.2	0.2
3	(Na_2CO_3) (gm)	-	-	-	1	-
3	(NaCl) (gm)	-	2	1	-	-
3	(Na_2SO_4(gm)	-	-	-	-	1
3	KCl (gm)	2	-	1	1	1
4	PAC (gm)	0.5	0.5	0.5	0.5	0.5
5	Bentonite [gm]	25	25	25	25	25

Table 4.17: Drilling fluid formulation of test matrix #5.

4.8.2 Results analysis

The measured viscometer reading of the drilling fluids are displayed in Figure 4.16. As shown on the figure, the single KCl system response is lower than the other fluid systems.

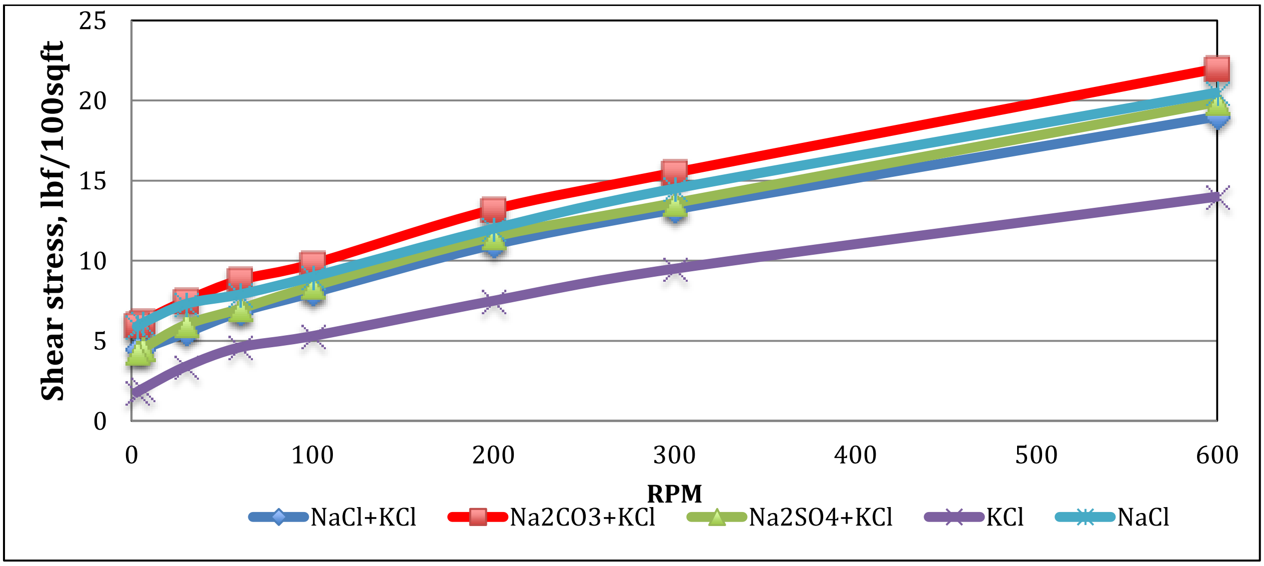

Figure 4.16 Viscometer data of test matrix #5 drilling fluids.

Figure 4.17 shows the computed drilling fluid properties obtained from Figure 4.16. The horizontal lines on the figure are drawn on the reference KCl system. Based on the color code it is very easy to compare the effect of salts in the fluid system. As shown, the single effect of NaCl shows a higher performance than the single effect of KCL. The viscosity and yield strength of the KCl system has been improved when blended with NaCl.

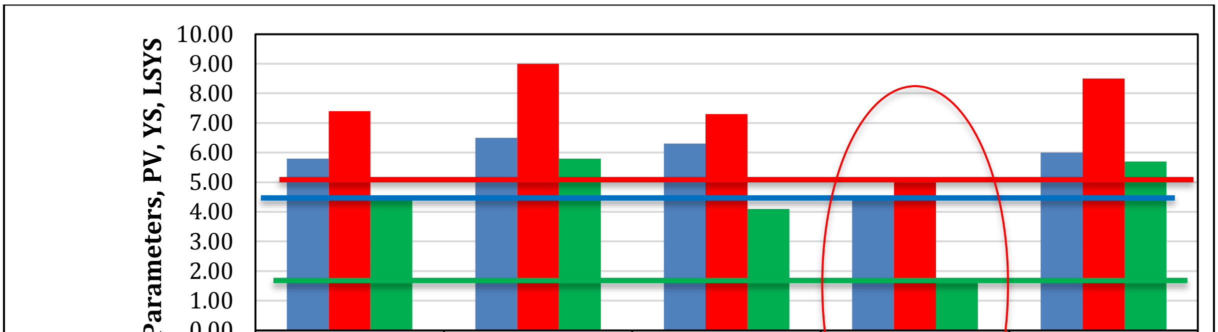

	NaCl+KCl	Na2CO3+KCl	Na2SO4+KCl	KCl	NaCl
PV (cP)	5.80	6.50	6.30	4.50	6.00
YS (lbf/100sqft)	7.40	9.00	7.30	5.00	8.50
LSYS(lbf/100sqft)	4.50	5.80	4.10	1.60	5.70

Figure 4.17: Bingham parameters and lower shear yield strength test #5

Comparing with the single effect, the combined effect of presence of 1g KCl in 1g Na_2CO_3 and 1g Na_2CO_3 reduces the plastic viscosity and the yield strengths. On the other hand the addition of NaCl on KCl as shown on Figure 4.18 improved the parameters as compared with the single effect of KCl. One reason could be due to the fact that the KCl has thinning effects in the Nano and PAC systems. Figure 4.18 shows the computed power law parameters. As shown, the k-value of the single KCl system is improved when mixed with NaCl and Na_2CO_3. The n-values are nearly similar.

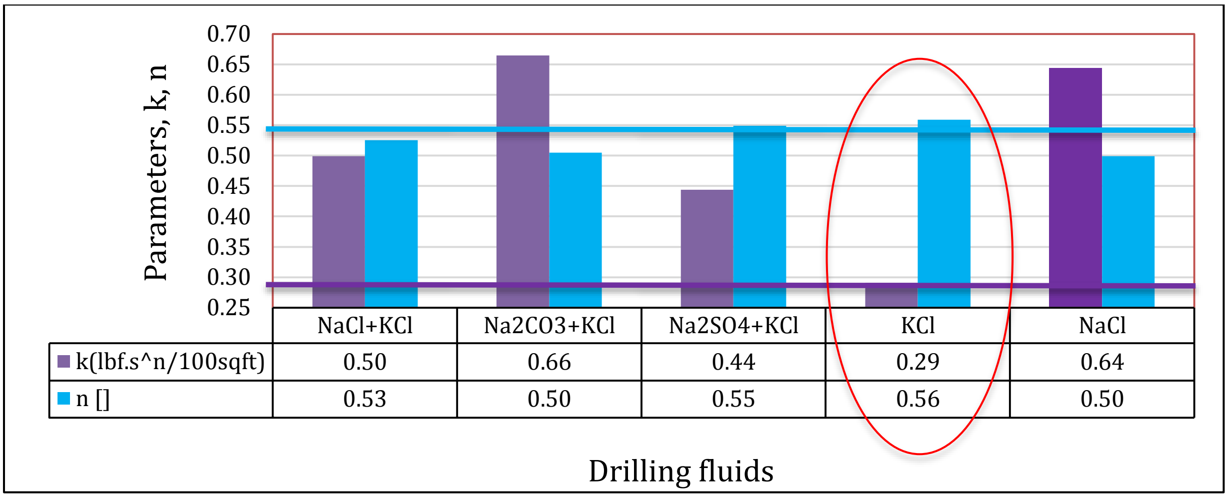

Figure 4.18: Power law parameters of test matrix #5 drilling fluids.

7.5 min API filter press measurement

Table 4.18 shows the measured filtrate loss of the three salt combined systems and the two single salt references systems. The table also contains a view of the percentage filtrate loss changed as compared with the KCl reference system. As we can see, all systems exhibit a better filtrate loss performance than the KCl reference system, but not as good as the NaCl reference system. Of the combined salt systems, the NaCl and KCl mix shows the lowest filtrate loss.

	Single , Ref		**Combined salt effects**		
Measurement	**KCl**	**NaCl**	**NaCl + KCl**	**Na_2CO_3 + KCl**	**Na_2SO_4 + KCl**
Filtrate loss	5,75 ml	4,5 ml	4,75 ml	5,25 ml	5 ml
% Change	-	-22 %	-17 %	-9 %	-13 %

Table 4.18: 7.5 min API filtrate loss of test matrix #5 and % increase from KCl.

pH measurements

Table 4.19 displays the pH values of the drilling fluid.

Measurement	**NaCl + KCl**	**Na_2CO_3 + KCl**	**Na_2SO_4 + KCl**
pH	8,65	9,85	8,85

Table 4.19: pH values of test #5 drilling fluids.

4.9 Test matrix #6- Effect of 0.04% Nano Silica in salt treated DUOVIS and PAC polymer system

In the previous sections, it is shown that the presence of more KCl in PAC system creates thinning effect. This behavior also was observed in the Nano additive system. Since most of the drilling formation contains shale, which is reactive, the common practice is to add more KCl to control shale swelling. In order to formulate a system, which allows taking more KCl, at first we tested three DUOVIS (0.12%, 0.18%, & 0.22%) wt until we get good rheology and filtrate lose.

4.9.1 Description of fluid systems

Table 4.20 shows the formulation of 0.038% Wt Nano silica. The water to bentonite ratio of fluid 1, 2 and 3 is 20, which is the same as the previous section test matrices. The concentrations of DUO-VIS are also different in the three fluid systems.

Additives	**Drilling fluids**		
	Fluid 1 +3 KCL	**Fluid 2 +4 KCL**	**Fluid 3 +5 KCL**
Water (H_2O) [ml]	463	456	458
Bentonite [gm]	23.14	22.8	22.9
KCl Salt [gm]	3	4	5
Nano [gm]	0.2	0.2	0.2
PAC [gm]	0.35	0.35	0.35
DUOVIS [gm]	0.65	0.95	1.15

Table 4.20: Drilling fluid formulation of test matrix #6.

4.9.2 Results analysis

Figure 4.19 shows the measured rheology drilling fluids formulated in Table 4.21.As displayed in the figure, we can observe that the behavior of fluid 2 and 3 are nearly similar, but the Fluid 1 shows a little bit higher specially the lower shear. The rheology parameters computed are plotted on Figure 4.20. As shown, as salt content and DUOVIS increase the plastic viscosity shows nearly same, but a reduction behavior is observed on yield strength and lower shear yield stress.

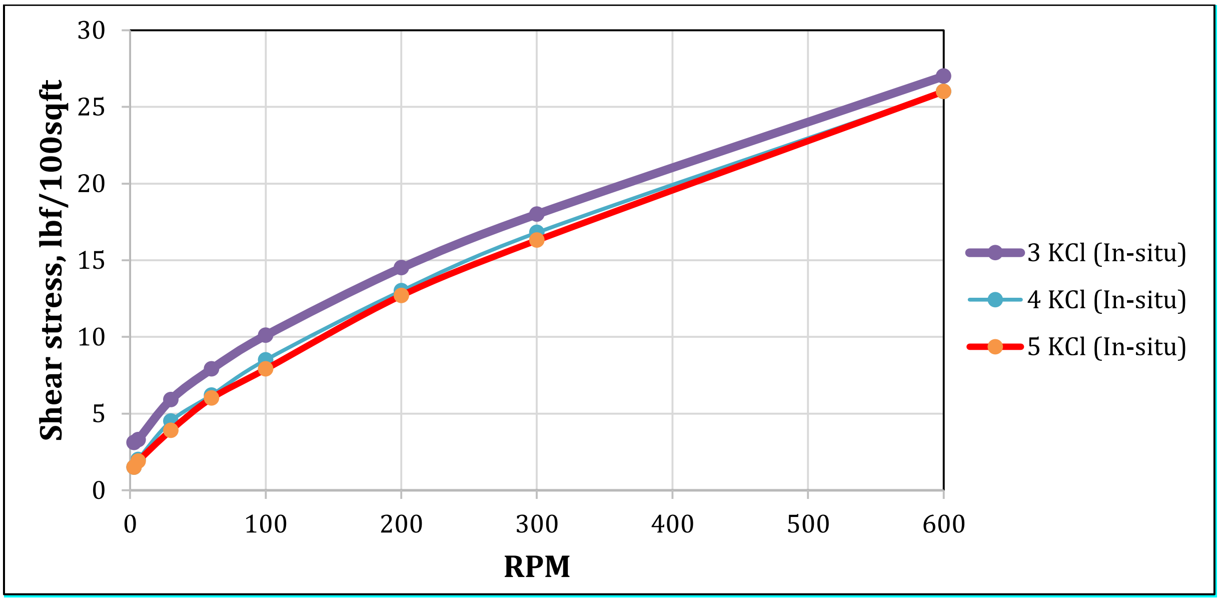

Figure 4.19: Viscometer responses of test matrix #6 drilling fluids.

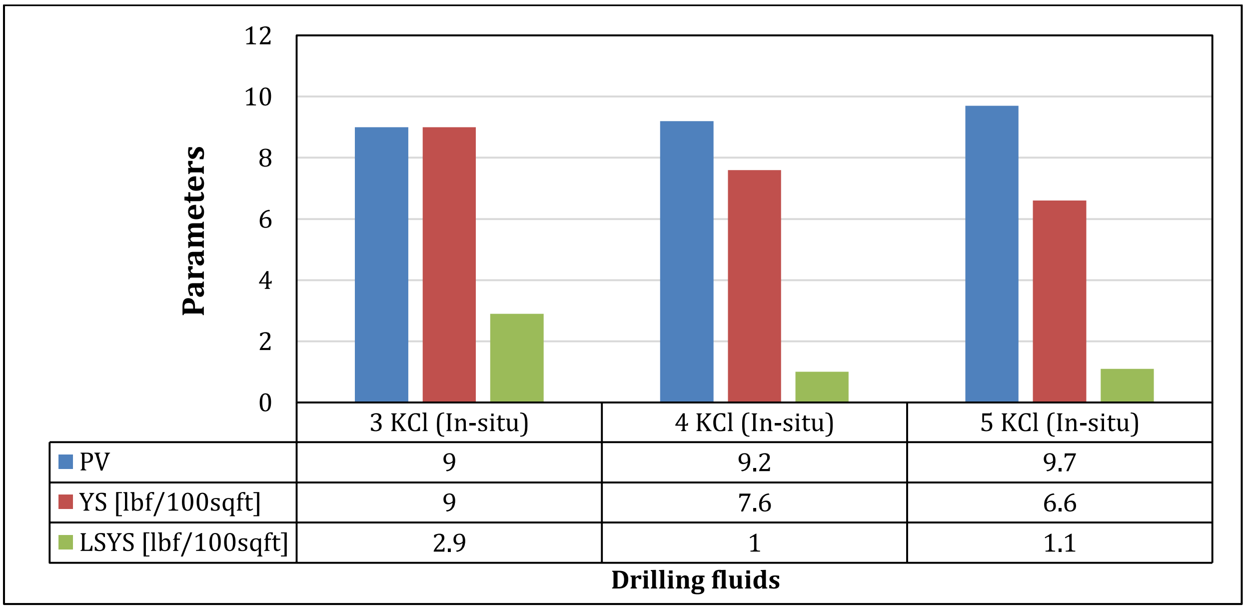

	3 KCl (In-situ)	4 KCl (In-situ)	5 KCl (In-situ)
PV	9	9.2	9.7
YS [lbf/100sqft]	9	7.6	6.6
LSYS [lbf/100sqft]	2.9	1	1.1

Figure 4.20: Bingham parameters and low shear yield stress of Test matrix #6 drilling fluid.

Figure 4.21 is the computed flow (n) and consistency index (k). In terms of trends, one can also observed a minor increase in k-value and decreases in n-value.

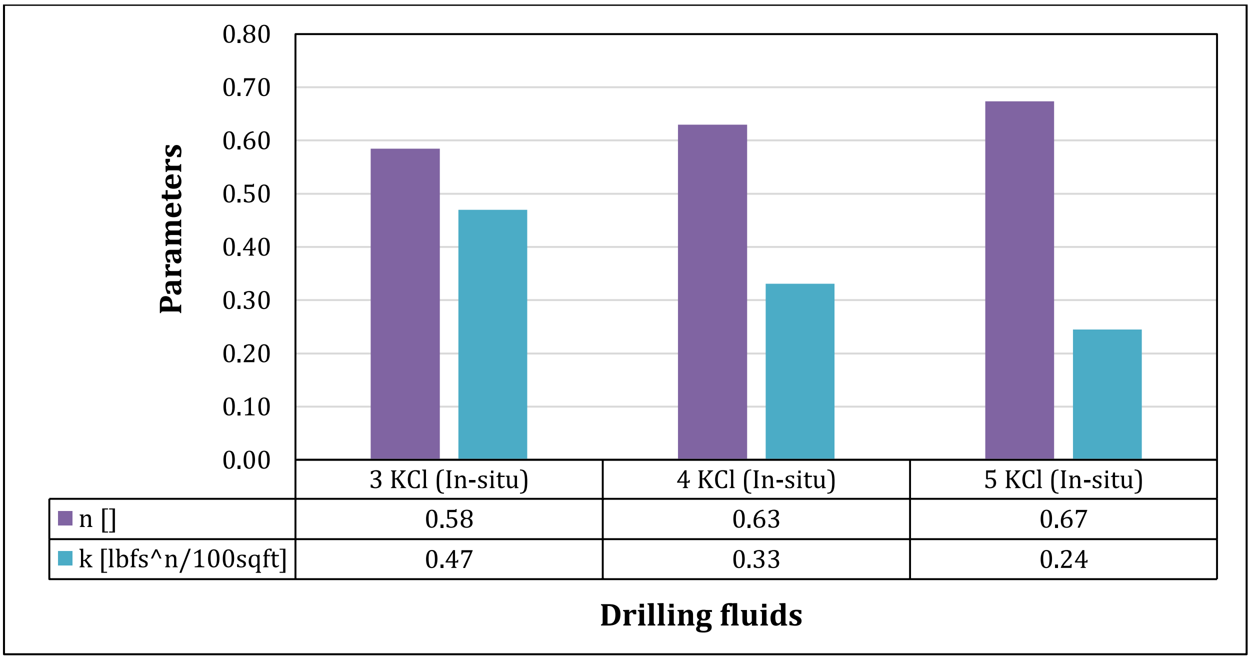

Figure 4.21: Power law model parameters of test matrix # 6 drilling fluids.

API filtrate loss measurement

As shown in Table 4.21, filtrate loss in the fluid 2 and 3 are the same. Fluid #1 shows 0.2ml less than the other two. However, we selected fluid 2 systems for further test matrix design. The main reason was that fluid 2 allows 4g KCL, which contains 0.95g Duovis polymer.

Measurement	3 KCl (In-situ)	4 KCl (In-situ)	5 KCl (In-situ)
Filtrate (ml)	3.9	4.1	4.1

Table 4.21: 7.5min API filtrate losses of test matrix #6 drilling fluids.

pH- measurement

Table 4.22 shows the pH values of the drilling fluids. All the fluids are of nearly the same alkalinity.

Measurement	3 KCl	4 KCl	5 KCl
pH	8.75	8.75	8.7

Table 4.22: pH values of test matrix #6 drilling fluids.

4.10 Test matrix #7 Effect of various Nano Silica in salt treated DUOVIS and PAC polymer system

The amount of KCl in previous sections (#1-#5) was very low and not sufficient to handle shale swelling problem. With the idea of increasing the amount of KCl, we can observe from test matrix #6 that the performance of 4g KCl and 5g KCl are nearly the same.

For this section and the coming other parts of the study, we have selected the 4g KCl and 0.95g DUO-Vis polymer system to analyze the effect of various nano-silica concentrations. The main objective is to formulate a realistic fluid system, which uses more KCl in drilling operation.

4.10.1 Description of fluid systems

Table 4.23 shows nano treated formulation. The fluid systems are treated with 2.81ppb (8.0 kg/m^3) KCl. The concentration of nano varied from 0 to 0.06 % wt. The sum of PAC and DUOVIS is 1.3g (0.91 ppb).

Additives	**Fluid systems**				
	Fluid 1 +4 KCL	Fluid 1 +4 KCL	Fluid 1 +4 KCL	Fluid 1 +4 KCL	Fluid 1 +4 KCL
Water [ml]	500	500	500	500	500
KCl [gm]	4	4	4	4	4
Nano [gm]	0.1	0.15	0.2	0.25	0.3
PAC (gm)	0.35	0.35	0.35	0.35	0.35
DUOVIS (gm)	0.95	0.95	0.95	0.95	0.95
Bentonite [gm]	25	25	25	25	25

Table 4.23: Drilling fluid formulation of test matrix #7.

4.10.2 Results analysis

Figure 4.22 shows the viscometer reading of the drilling fluids formulated in Table 4.24. From the figure, we can observe that the Fann reading of nano treated fluids looks similar.

Figure 4.23 shows the computed viscosity and yield strengths of the fluids. As shown on the figure, the 0.1g nano treated system records a higher value relative to the others, but not significantly.

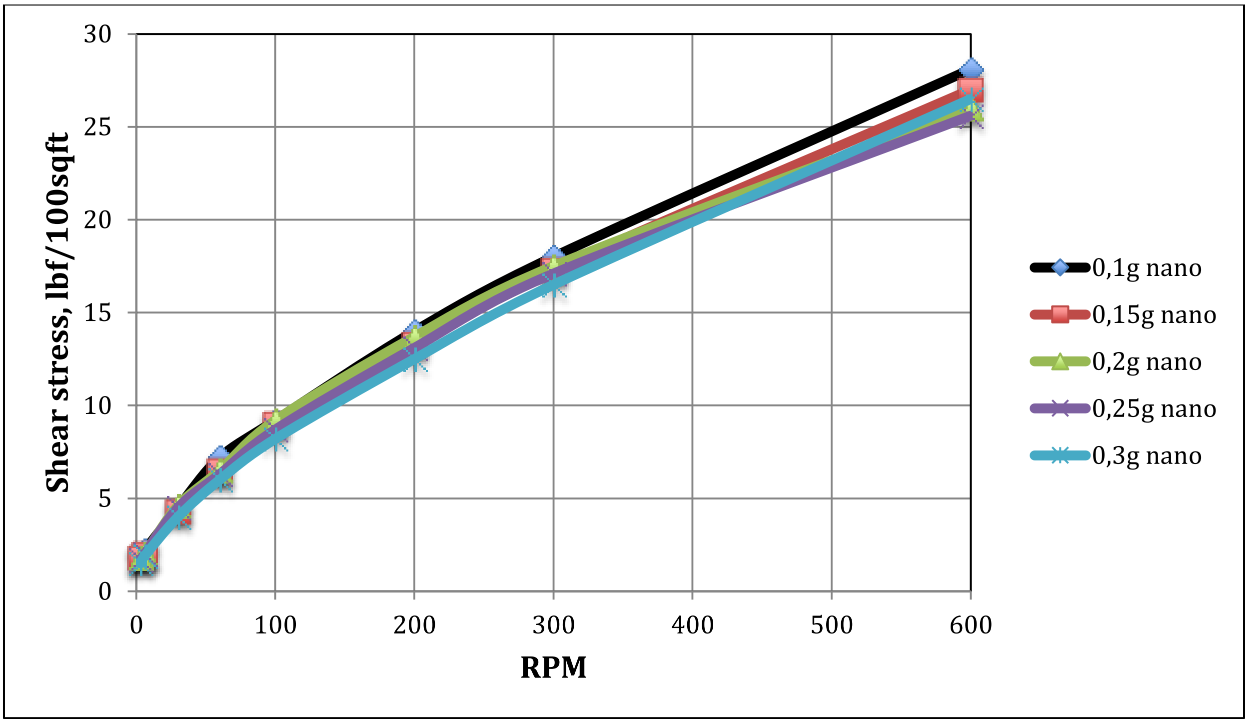

Figure 4.22: Viscometer data of test matrix #7.

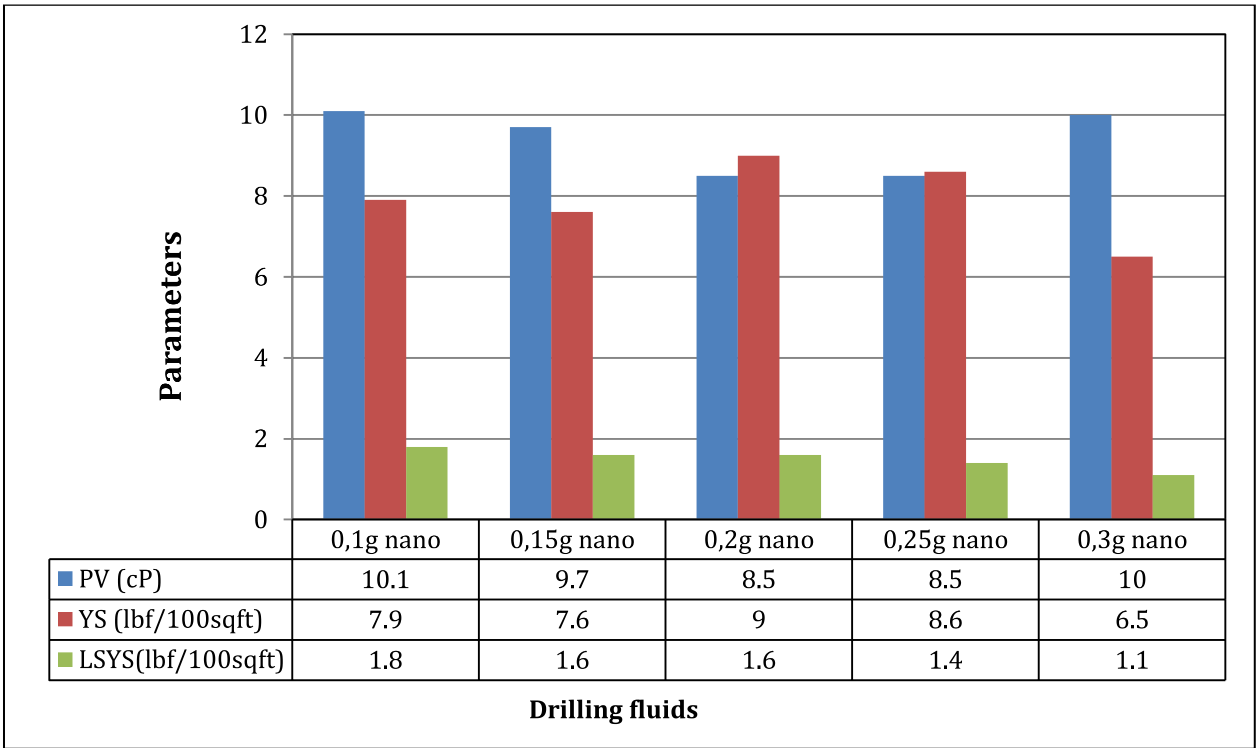

	0,1g nano	0,15g nano	0,2g nano	0,25g nano	0,3g nano
PV (cP)	10.1	9.7	8.5	8.5	10
YS (lbf/100sqft)	7.9	7.6	9	8.6	6.5
LSYS(lbf/100sqft)	1.8	1.6	1.6	1.4	1.1

Figure 4.23: Bingham parameters and low shear yield strength of test matrix #7.

Figure 4.23 also shows the computed power law model parameters. As shown on the figure, the k-values of the 0.1g and 0.15g nano show relatively higher than the other fluid systems. The n-values of the 0.1g, 0.15g and 0.3g nano systems are higher than the other two nano systems.

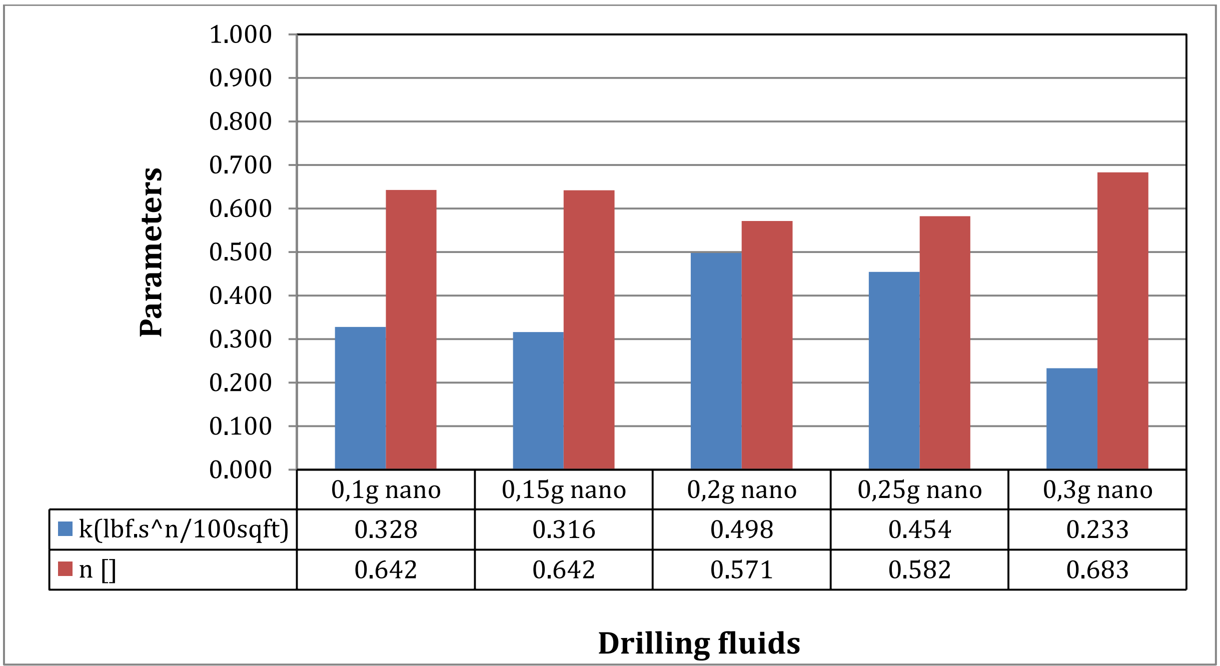

Figure 4.24: Power law parameters of test matrix #7.

API filtrate loss measurement

Table 4.24 shows the measured API filtrate values. Drilling fluids, which contain 0.1g and 0.25g nano, show lower filtrate loss.

Measurement	0,1g nano	0,15g nano	0,2g nano	0,25g nano	0,3g nano
Filtrate loss [ml]	3,5	4,5	4,25	3,5	5

Table 4.24: 7.5min API filtrate measured values of test matrix #7.

pH- measurement

As shown in Table 4.25, the measured pH values of the fluid systems, all shows almost the same alkalinity. This shows that the rheology parameters and filtrate values are not the affected by degree of pH.

Measurement	0,1g nano	0,15g nano	0,2g nano	0,25g nano	0,3g nano
pH	8,75	8,8	8,75	8,75	8,65

Table 4.25: pH measured values of test matrix #7 drilling fluids.

4.11 Test matrix #8 Effect of various Nano Silica in 4g KCl +0.75g Na_2CO_3 salt treated system

As mention in test matrix #7, the objective was to formulate a system which can receive a lot of KCl in order to inhibit shale swelling. For the test results, it was shown that three of the fluid systems almost behave the same. From test matrix #5, it is shown that the addition of Na_2CO_3 salt in KCl system improves the performance of rheology and fluid loss. Therefore, in test matrix #8, we added 0.75g Na_2CO_3 in-situ in test matrix #7.

The term in-situ is to describe the mixing of Na_2CO_3 was along with KCl in water before bentonite has been mixed.

4.11.1 Description of fluid systems

Table 4.26 shows the test matrix #8 formulation. The fluid systems were treated with 2.81ppb (8.0 kg/m^3) KCl. The concentration of nano varied from 0 % to 0.06 % wt. The sum of CMC and DUOVIS is 1.3g, (0.91 ppb).

<u>Formulation</u>

Text matrix # 8 = Test matrix #7 + 0.75g Na_2CO_3 in-situ.

PAC was also replaced with CMC

The order of mixing is according to the list of additives shown on the table.

#	Additives	Drlling fluids					
		Ref	Fluid 1 +0.1 Nano	Fluid 2 +0.15 Nano	Fluid 3 +0.2 Nano	Fluid 4 +0.25 Nano	Fluid 5 +0.3 Nano
1	Water [ml]	500	500	500	500	500	500
2	KCl [gm]	4	4	4	4	4	4
	Na_2CO_3[gm]	0,75	0,75	0,75	0,75	0,75	0,75
3	Nano [gm]	-	0.1	0.15	0.2	0.25	0.3
4	CMC [gm]	0.35	0.35	0.35	0.35	0.35	0.35
	DUOVIS [gm]	0.95	0.95	0.95	0.95	0.95	0.95
5	Bentonite [gm]	25	25	25	25	25	25

Table 4.26: Drilling fluid formulation of test matrix #8.

4.11.2 Results analysis

Figure 4.25 shows the fann 35 measured data of test matrix #8. From the figure, we can observe the higher viscometer response of the 0.1g nano system. As nano concentration increases (above 0.1), the response of the fluid systems become lower than the reference (nano free) system.

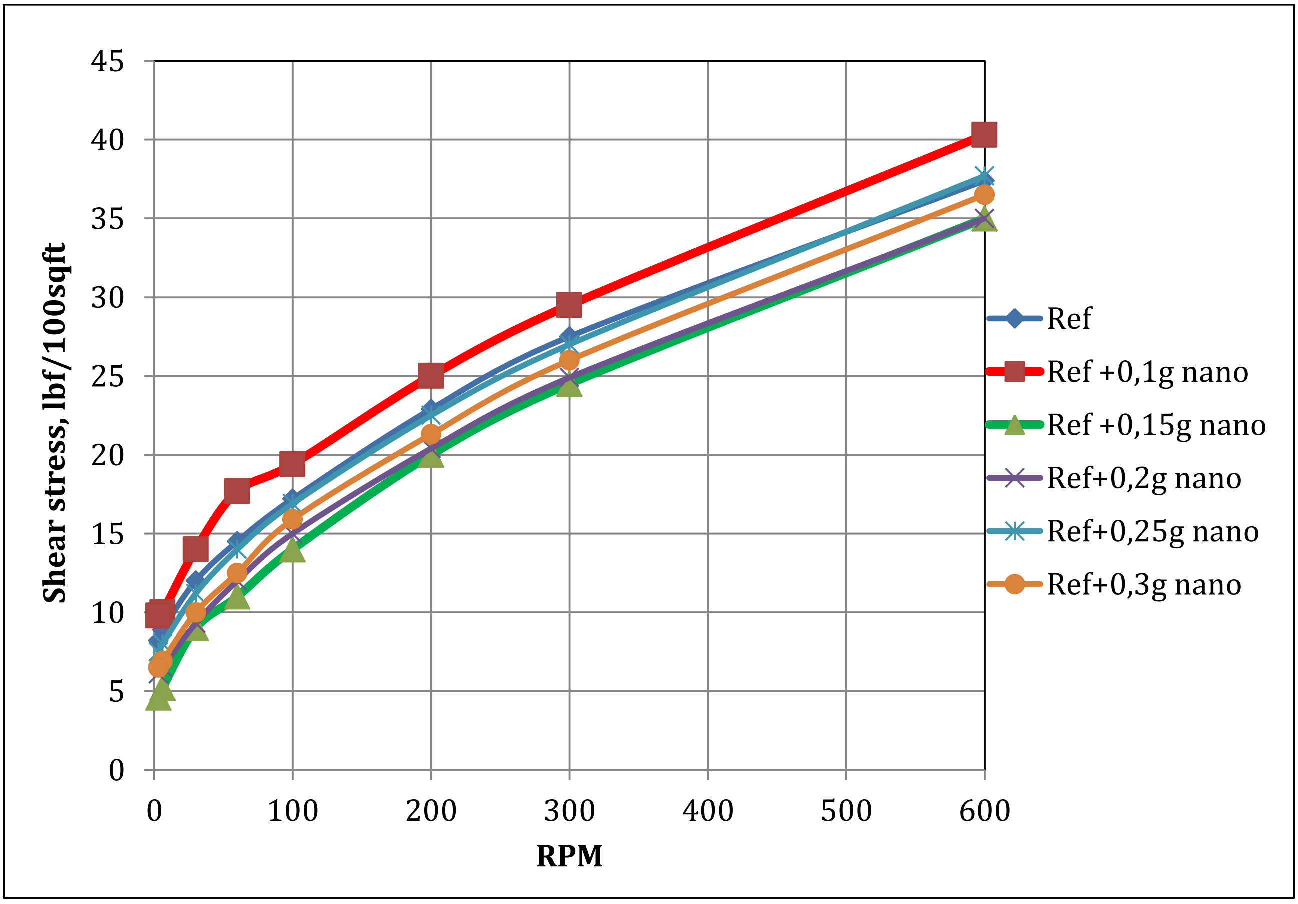

Figure 4.25: Viscometer data of test matrix #8.

Fluid 1 and reference fluids were modified by miixing with 0.3gm Na_2CO_3 ex-situ and obtained two other fluid systems namely:

- **Fluid 6** = Ref + 0.3Na_2CO_3 Ex-Situ
- **Fluid 7** = Fluid 1+ 0.3Na_2CO_3 Ex-Situ

These two modified fluids are compared with the reference and fluid 1 (+0.1g Nano). The results are shown in Figure 4.26. As displayed in the figure, fluid 7 exhibited a higher viscometer response. Fluid 6 and Fluid 1 (i.e 0.1g nano silica treated) show almost similar responses and higher than nano untreated reference drilling fluid system. This illustrates the impact of ex-situ salt additive effect on the rheology of drilling fluid.

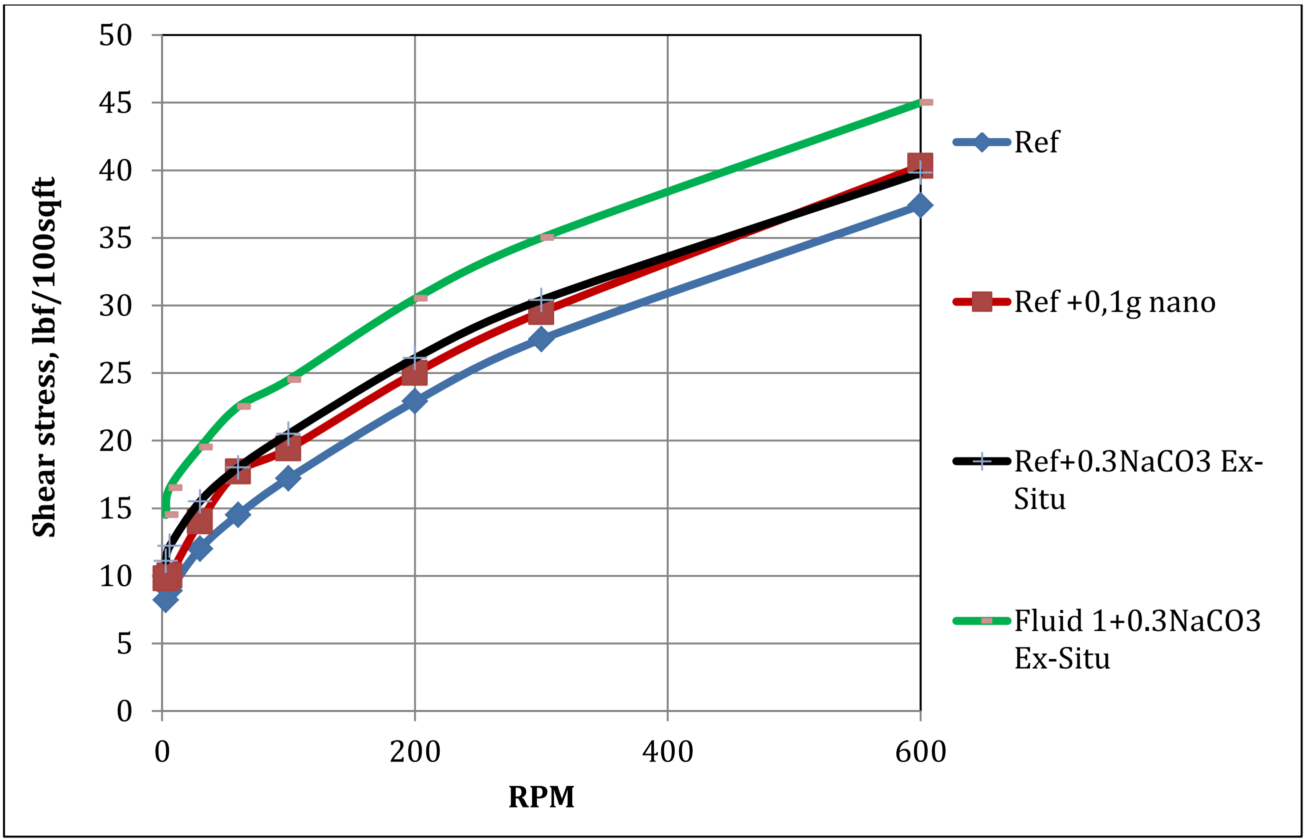

Figure 4.26: Comparisons of ref, ref+0.1g Nano, Fluid 6 and Fluid 7.

Table 4.27 shows the computed viscosity and yield strengths of the fluids. In addition, the measured 7.5min API filtrate loss and the pH values are provided.

Parameters	Ref	Fluid 1	Fluid 2	Fluid 3	Fluid 4	Fluid 5	Fluid 6	Fluid 7
		Ref +0,1g nano	Ref +0,15g nano	Ref+0,2g nano	Ref+0,25g nano	Ref+0,3g nano	Ref+0.3Na_2CO_3 Ex-Situ	Fluid 1+0.3Na_2CO_3 Ex-Situ
PV (cP)	9.9	10.8	10.5	10.1	10.7	10.5	9.4	10
YS (lbf/100sqft)	17.6	18.7	14	14.8	16.3	15.5	21	25
LSYS(lbf/100sqft)	7.5	9.6	4	5.7	7	6.1	10	12.5
k(lbf.s^n/100sqft)	1.732	1.785	0.992	1.166	1.342	1.231	2.696	3.653
n []	0.443	0.450	0.514	0.491	0.481	0.489	0.388	0.362
7.5min Filtrate[ml]	3,9	4	4	4,25	4,15	4,5	4,5	4
pH	10	9,95	9,95	9,85	9,85	9,80	10	9,95

Table 4.27: Calculated Bingham and power law parameters and measured pH and API filtrate of test matrix #8.

4.12 Test matrix #9 Effect 0.75 Na2CO3 Ex-Situ in various Nano Silica in 4KCl salt treated system

In test matrix #8, 0.75g Na_2CO_3 was added in-situ before mixing with bentonite. The order of in-situ 0.75g Na_2CO_3 mixing was (water + 4KCl +0.75g Na_2CO_3+Nano+Polymers+Bentonite). The test result showed no significant difference between the fluid systems (See, Figure 4.22).

Test results on the effect of 0.75g Na_2CO_3 ex-situ salt additives showed a different result. Based on these results, in this section we designed an ex-situ text matrix #9. In test matrix #9, we added 0.75g Na_2CO3 after bentonite had been mixed. The order of 0.75 gm Na_2CO_3 ex-situ formulations was (water + 4g KCl +Nano+ Polymers + Bentonite+ 0.75gm Na_2CO_3).

4.12.1 Description of fluid systems

Table 4.28 shows the drilling formulation. The fluid systems are treated with 2.81ppb (8.0 kg/m^3) KCl. The concentration of nano varied from 0 to 0.03 % wt. The sum of CMC and DUOVIS is 1.3g, (0.91 ppb).

#	Additives	Drilling fluids			
		Fluid 1 Ref+075 Ex-situ Na_2CO3	**Fluid 2** + 0.06 Nano+ 075 Ex-situ Na_2CO3	**Fluid 3** + 0.1 Nano+ 075 Ex-situ Na_2CO3	**Fluid 4** +0+ 0.15 Nano+ 075 Ex-situ Na_2CO3
1	Water [ml]	500	500	500	500
2	KCl Salt [g]	4	4	4	4
3	Nano [g]	-	0.06	0.1	0.15
4	DUOVIS (g)	0.95	0.95	0.95	0.95
	CMC [g]	0.35	0.35	0.35	0.35
5	Bentonite [g]	25	25	25	25
6	Na_2CO_3[g]	0.75	0.75	0.75	0.75

Table 4.28: Drilling fluid formulation of test matrix # 9.

4.12.2 Results analysis

Figure 4.27 shows the measured rheology drilling fluids formulated. From the figure, we can observe that the viscometer responses of drilling fluids which are treated with less than or equal to 0.1g nano exhibits relatively higher value and similar behaviors. For this particular formulation, when the nano concentration increases to 0.15g, the system behaves like a nano free fluid. This indicates that for the given salt system, probably there exists an optimum nano concentration, which gives good rheology properties.

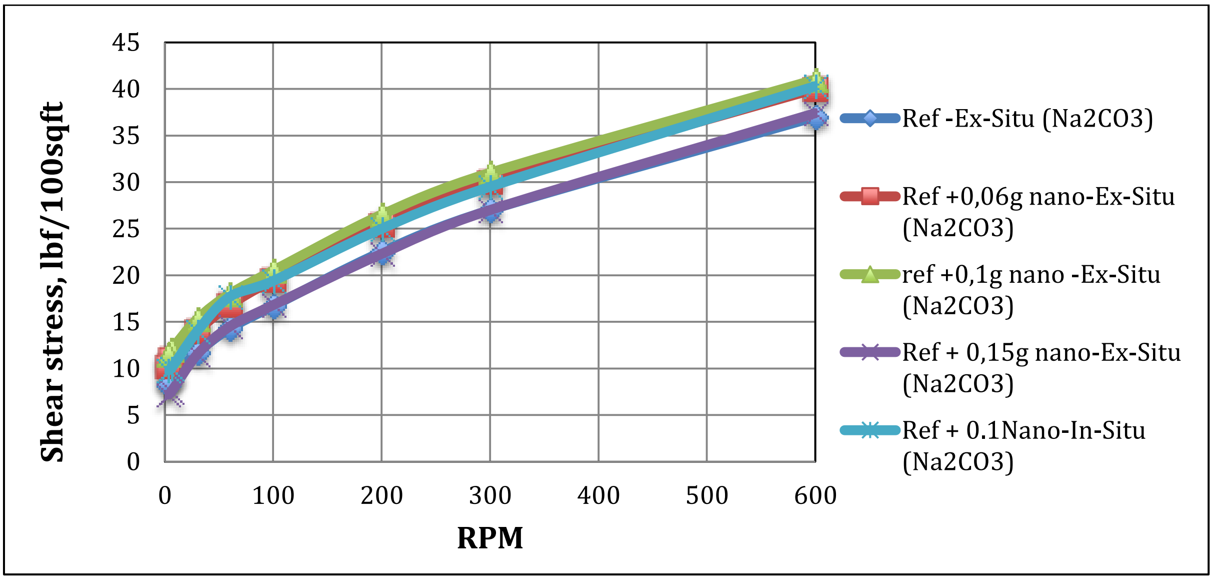

Figure 4.27: Viscometer data of test matrix #9.

Table 4.29 shows the comparison of test matrix # 8 & # 9 fluids in terms of their computed Bingham, power law parameters, the measured filtrate loss and pH. As shown, the ex-situ salt additive systems of test matrix #9 are relatively higher values than the in-situ test matrix #8.

Parameters	Test matrix #9				Test matrix #8	
	Ref -Ex-Situ (Na2CO3)	Ref +0,06g nano-Ex-Situ (Na_2CO_3)	Ref +0,1g nano -Ex-Situ (Na_2CO_3)	Ref + 0,15g nano-Ex-Situ (Na_2CO_3)	Ref + 0.1Nano-In-Situ (Na_2CO_3)	Ref-In-Situ (Na_2CO_3)
PV (cP)	10	10	10	10.4	10.8	9.9
YS (lbf/100sqft)	17	20	21	16.6	18.7	17.6
LSYS(lbf/100sqft)	7.4	9.4	11	6.9	9.6	7.5
k($lbf.s^n$/100sqft)	1.588	2.258	2.509	1.442	1.785	1.732
n []	0.454	0.415	0.403	0.470	0.450	0.443
pH	10.1	10.1	10.05	10.05	10	9.95
7.5 min. Filtrate loss [ml]	4	4.1	4.5	4.5	4	3.9

Table 4.29: Parameters extracted and measured values of test matrix 8 & 9.

Comparison between ex-situ and in-situ

For better visualization, the figures below display the effect of in-situ and ex-situ salt additive. As shown, in nano free systems (Figure 4.28), the viscometer responses of both systems are almost the same.

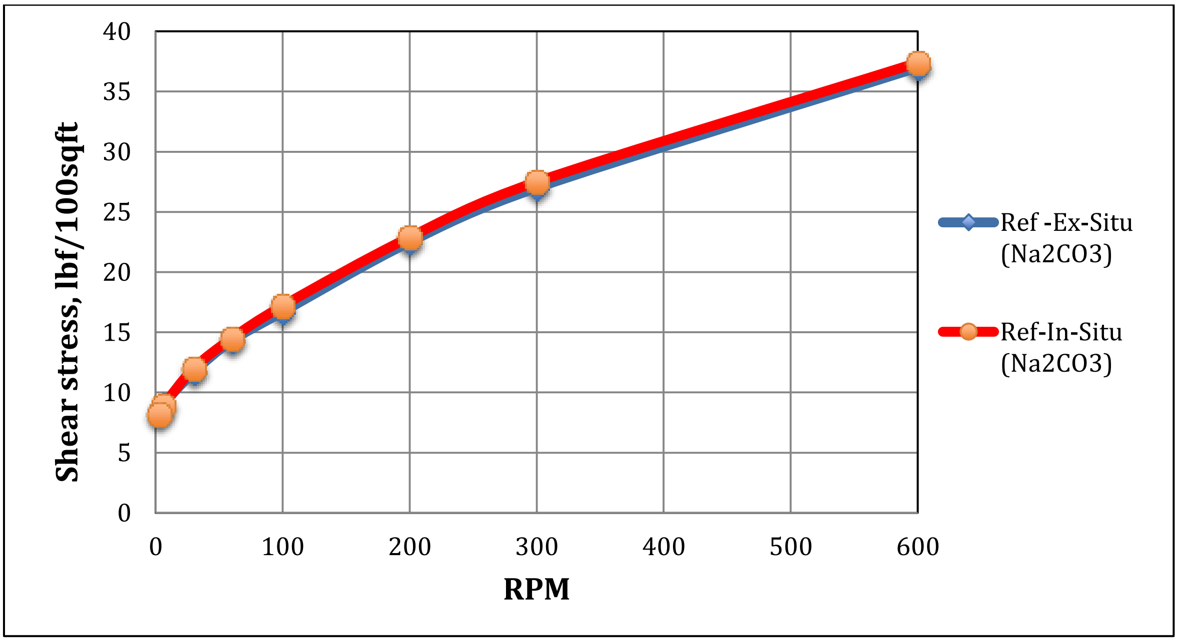

4.28: Comparisons of in-situ and ex-situ Na_2CO_3 additives in nano free systems.

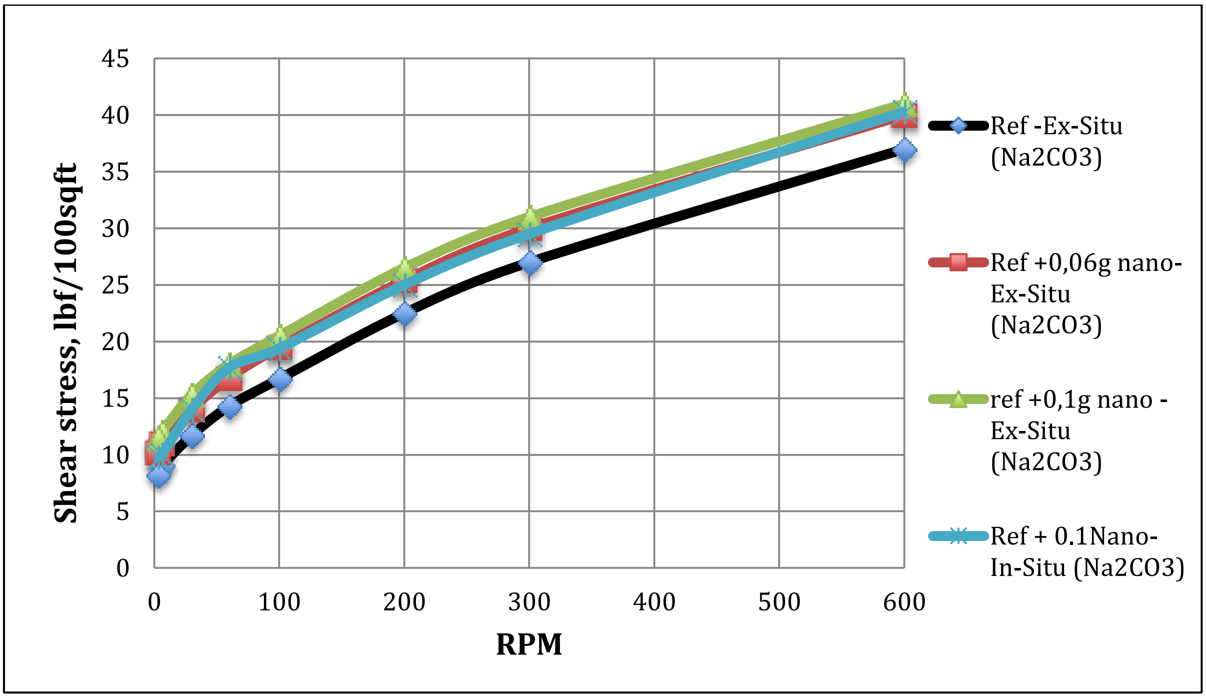

4.29: Comparisons of in ex-situ Na_2CO_3 additives in Nano free and in Nano treated systems.

4.13 Test matrix #10 Effect 0.75 Na_2CO_3 Ex-Situ in various Nano Silica in 4KCl salt CMC & Drispac treated system

In test matrix #10, the drilling formulation is the same as test matrix #9. The difference is that in test matrix #10, we used Drispac polymer from 1989 and lower nano concentrations.

During formulation, we added 0.75 g Na_2CO_3 after bentonite has been mixed, which we may call it as an ex-situ salt additive. The order of mixing was (Water + 4g KCl + Nano + Polymers [CMC + Drispac] + Bentonite + 0.75g Na_2CO_3 ex-situ).

4.13.1 Description of fluid systems

Table 4.30 shows the ingredients of the drilling fluids. The fluid systems are treated with 2.81ppb (8.0 kg/m^3) KCl. The concentration of nano varied from 0 to 0.015 % wt. The sum of CMC and Drispac is 1.3g, (0.91 ppb).

#	**Additives**	**Drilling fluids**			
		Fluid 1 +0.02 Nano	Fluid 2 +0.04 Nano	Fluid 3 +0.06 Nano	Fluid 4 +0.08 Nano
1	Water [ml]	500	500	500	500
2	KCl Salt [gm]	4	4	4	4
3	Nano [gm]	0.02	0.04	0.06	0.08
4	Drispac (gm)	0.95	0.95	0.95	0.95
	CMC [gm]	0.35	0.35	0.35	0.35
5	Bentonite [gm]	25	25	25	25
6	Na_2CO_3[gm]	075	075	075	075

Table 4.30: Drilling fluid formulation of test matrix # 10.

4.13.2 Results analysis

Figure 4.30 shows the fann 35 viscometer response of test matrix #10 drilling fluids. From the figure, we can learn that the viscometer responses of nano treated fluids look similar. Comparing the Drispac system (Test matrix #10) with Duo-vis system (Test matrix #9), we can clearly see that the

Drispac systems show relatively lower responses, which are thinner than the DUOVIS system.

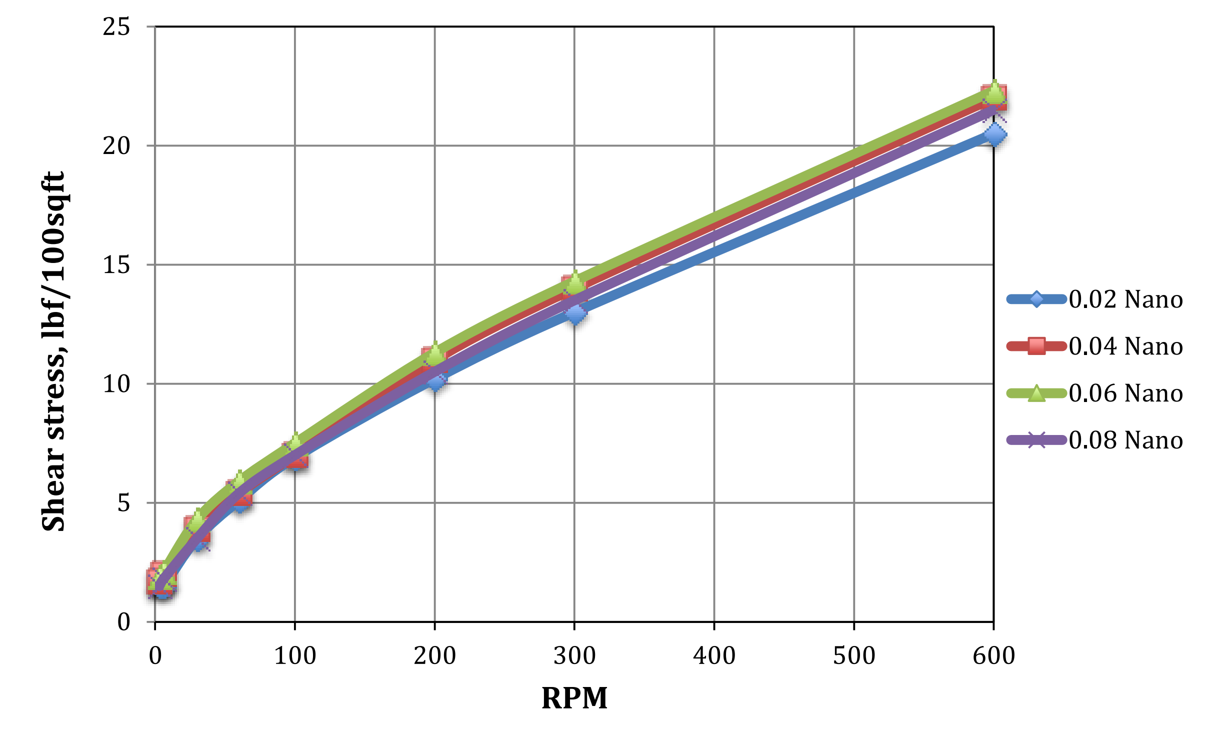

Figure 4.30: Viscometer data of test matrix #10.

Table 4.31 provides Bingham plastic and Power law parameters computed from Figure 4.30. In addition, the filtrate and pH values are also provided in the table. As shown, the fluid behaviors are nearly the same and the parameters are lower than DUO-VIS systems. However, in terms of filtrate loss the Drispac fluid systems show lower filtrate losses.

Parameters	Test matrix #10			
	Fluid 1 + 0.02 Nano	Fluid 2 + 0.04 Nano	Fluid 3 + 0.06 Nano	Fluid 4 + 0.08 Nano
PV (cP)	7.5	8	8	8
YS (lbf/100sqft)	5.5	6	6.3	5.5
LSYS(lbf/100sqft)	1.5	1.4	1.7	1.2
k($lbf.s^n$/100sqft)	0.216	0.240	0.263	0.206
n []	0.657	0.652	0.641	0.671
pH	10.1	10.1	10.05	10.05
7.5 min /Filtrate loss [ml]	3.5	3.5	3.75	4

Table 4.31: Bingham and power law parameters extracted and measured pH & filtrate loss values of test matrix # 10.

4.14 Viscoelastic behavior of test matrix #9

This section evaluates the effect of nano-additives on the viscoelasticity of drilling fluid. The drilling fluids to be compared are formulated in test matrix #9 (section § 4.12). The concentration of nano was varied from 0 to 0.03% wt (0.06g, 0.1g, and 0.15g). The amplitude and the frequency responses of these drilling fluids are tested. Anton Paar MCR 301 [51] rheometer was used to characterize the viscoelastic properties of the considered drilling fluids. The tests were performed at 20^{o}C in parallel plate.

4.14.1 Amplitude sweep test

The amplitude test was performed to determine the linear viscoelastic zone. From this test, one can analyze the drilling fluid internal structure stability, the gel strength and yield point and flow points where the storage modulus (G') is equal to the loss modulus.(G")

During testing, we kept the frequency constant and vary the strain from 0.0005 to 500%. Figure 4.31 displays the oscillatory amplitude test results obtained from the considered drilling fluids. All the drilling fluids show that the storage moduli are higher than the loss moduli. This indicates a stable gel structure. In all of the fluids systems, the yield point was obtained at 10% strain deformation, which is the limit for linear viscoelastic (LVE) regions of the fluids. This value was used for frequency test later. The flow points where the loss modulus equal to the storage modulus are determined by plotting the phase angel against the shear stress. These are clearly displayed in figure 4.32. The vertical points on the x-axes are flow points which corresponds to the phase angle is 45 deg. Figure 4.33 shows the flow points of the drilling fluids peaked from Figure 4.32. As shown, all the nano treated systems flow point is higher than the reference fluid. The 0.06g nano fluid is higher than all others. This information is based on a single run. Figure 4.34 shows the yield point of the drilling fluids. Unlike the flow point, the 0.15g nano fluid shows the lowest yield point and the 0.06g nano system still shows the highest yield point.

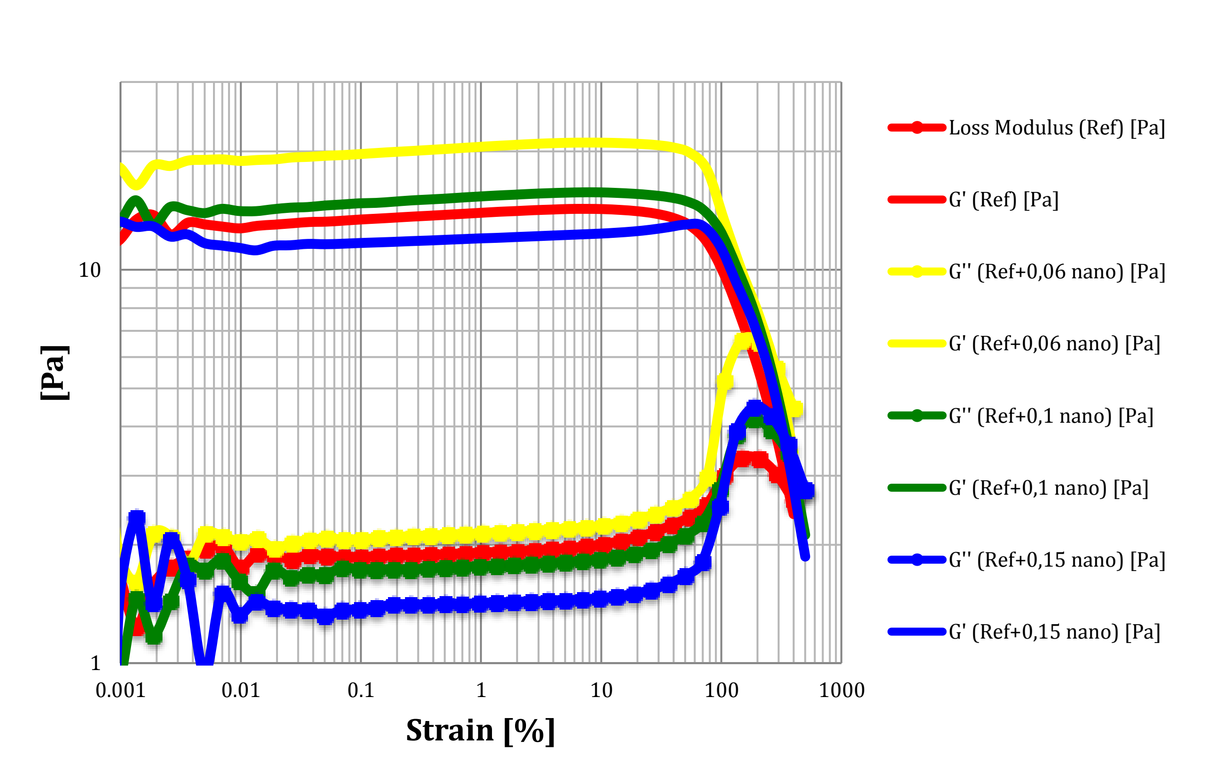

Figure 4.31: Amplitude sweep test of the drilling fluids (Test matrix #9.

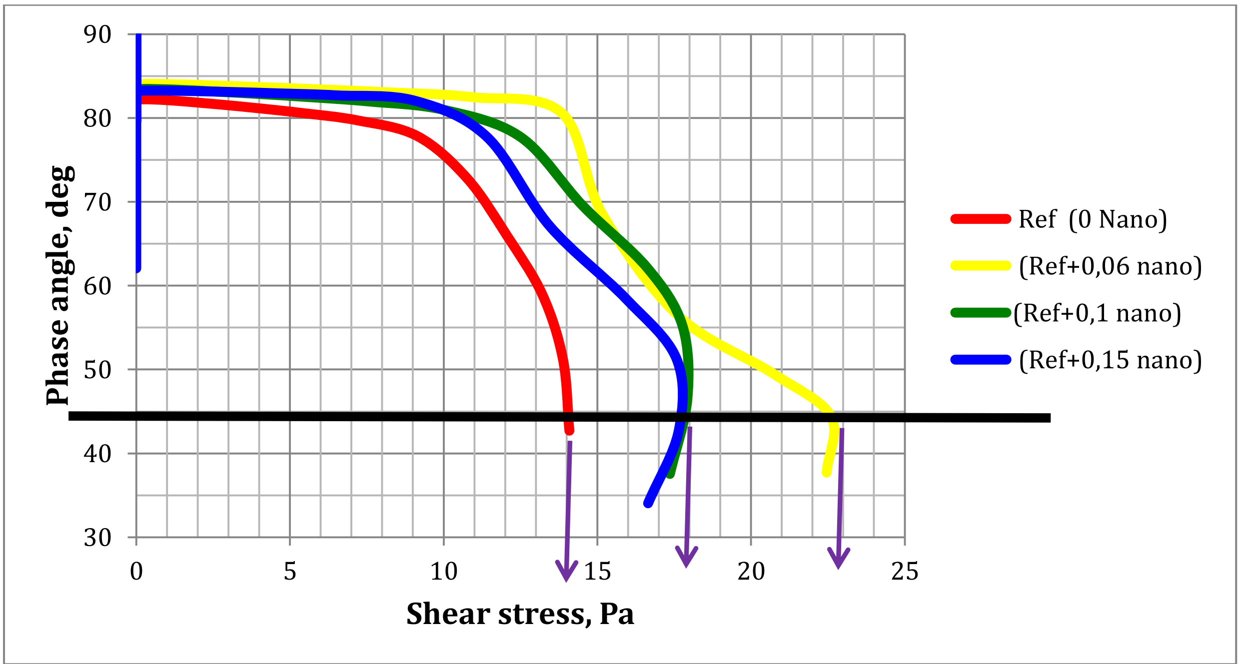

Figure 4.32: Phase angle vs shear stress.

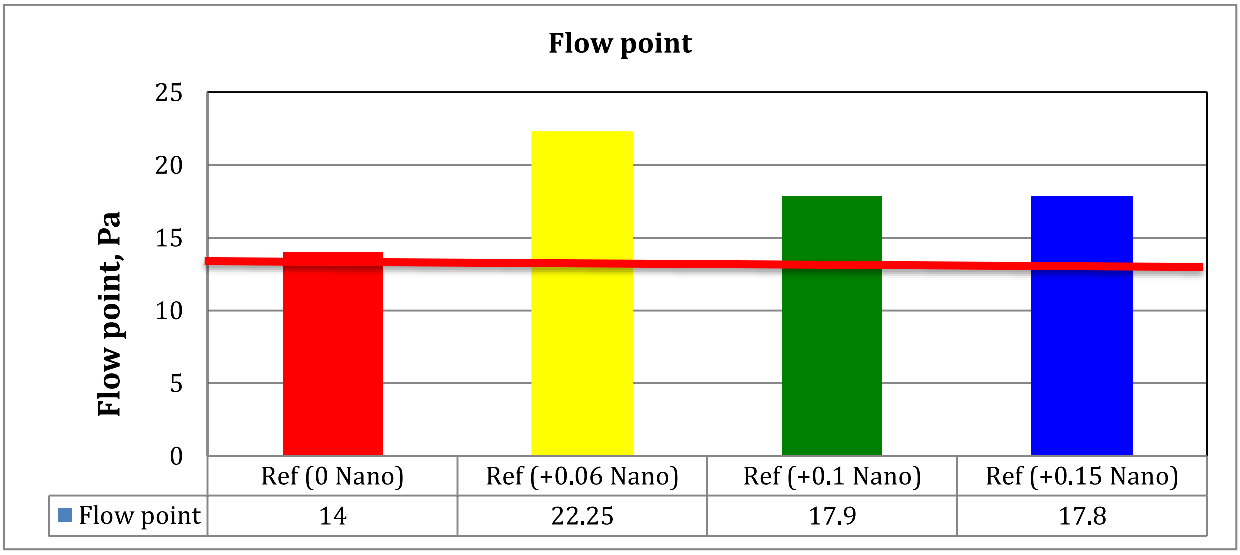

Figure 4.33: Flow point of the drilling fluids.

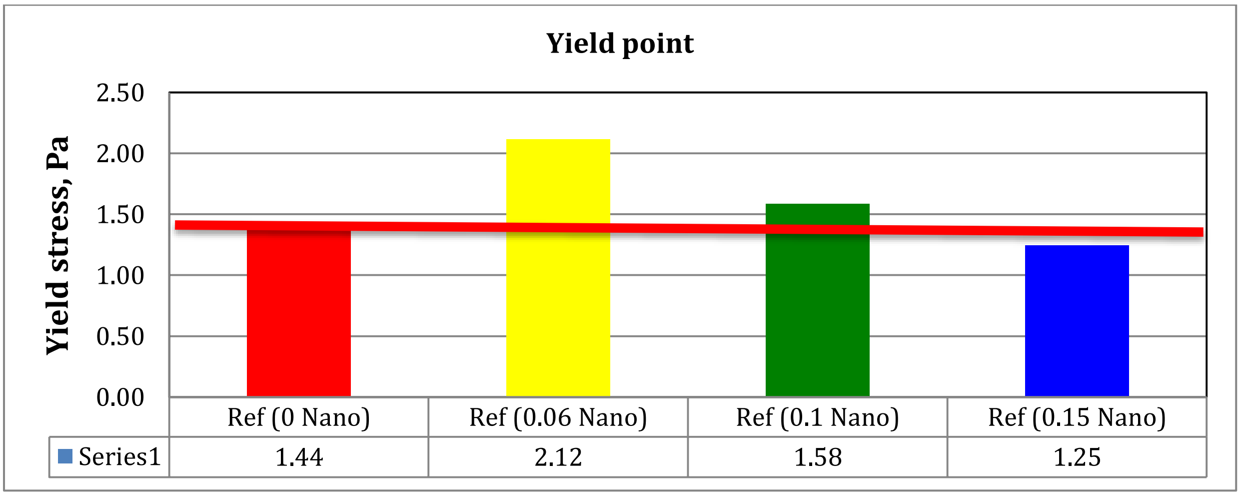

Figure 4.34: Yield point of the drilling fluids.

4.14.2 Frequency sweep test

Similarly, the oscillatory frequency sweep test also performed in the linear viscoelastic rage determined from the amplitude sweep test. In this test, the frequency was varied from 100 to 0,01. Figure 4.35 shows the frequency sweep test results of the drilling fluids (Test matrix #9). As shown, as nano concentration increases, the storage and loss moduli are decreasing. In all of the systems, the storage modulus is greater than the loss modulus. In addition, these moduli don't cross each other at the lower frequency. This is an indication that the fluid systems have a stable gel structure. Figure 4.36 shows the complex viscosity, which is computed from the storage and loss modules shown on Figure 4.32. As the concentration of nano increases, the viscosities are decreasing at a given angular frequency.

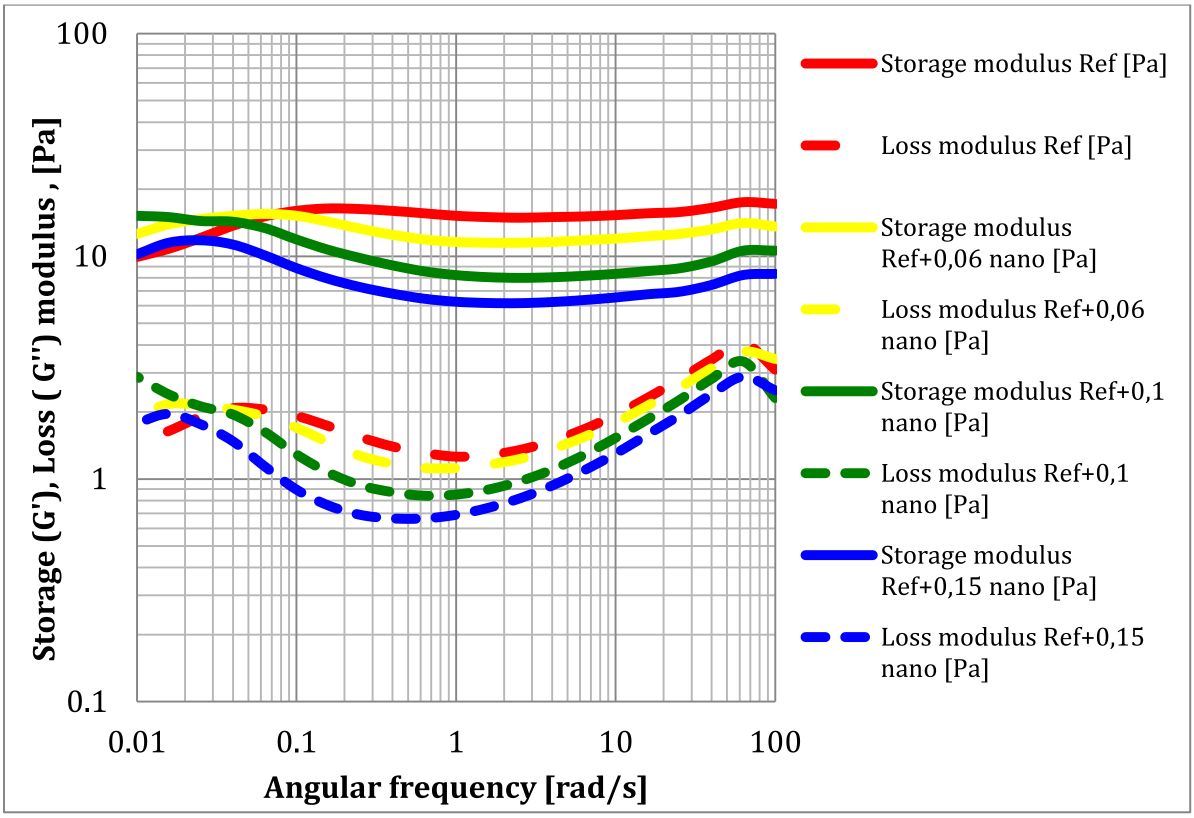

Figure 4.35: Frequency sweep test of the drilling fluids.

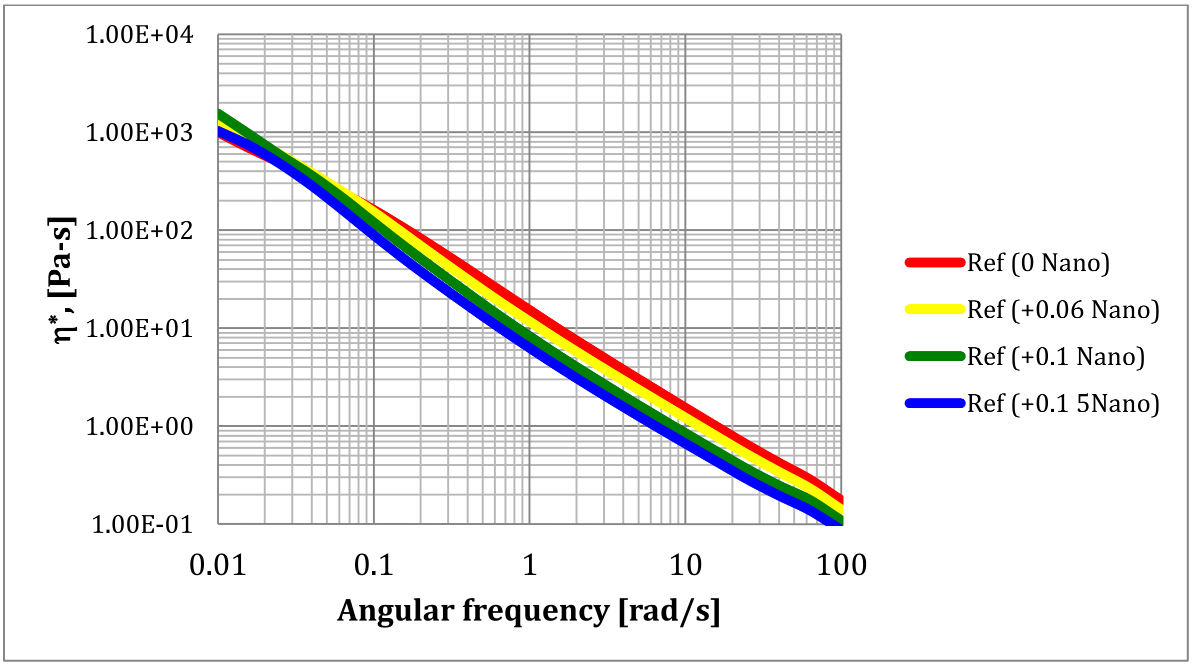

Figure 4.36: Complex viscosity of the drilling fluids. ($\eta^* = \sqrt{\left(\frac{G'}{\omega}\right)^2 + \left(\frac{G''}{\omega}\right)^2}$)

5 Performance simulation studies

5.1 Hydraulic simulation

As mentioned in the introduction part, drilling fluid is very important during drilling process. It is also pointed out that the higher the flow rate is good for hole-cleaning. However, as a flow rate increases, the circulation effective density also increases. To determine the flow rate, which is suitable for wellbore stability and hole-cleaning, it is important to perform simulation studies.

This section presents the hydraulics simulation studies to characterize the ECD and pump pressure required for the considered drilling fluids. As discussed in the theory part, among others hydraulics models, the unified model has shown good prediction. Therefore, this section uses the model summarized on Table 3.4.

5.1.1 Simulation arrangement

A vertical well of 12000ft length was used for the simulation. The well is constructed with 8.75 in casing as the last casing and the casing shoe is set at the 9000 ft depth. The inner diameter of casing is 8.5 in. The rest of the well is an open hole. A typical 5in OD and 4.8in ID drill string was used for drilling.

In this simulation, we didn't use BHA elements. We assume that the drill string is connected with a drill bit having 3 nozzles at the size of 28/32-in.

We also assume that the surface pressure loss due to surface equipment is not considered.

Figure 5.1 is the sketch of simulation well. Table 5.1 is the drilling fluids viscometer data used to inject into the well. The fluids have been designed characterized in section §4.11 (Table 4.27). The injection rates were varied from 1 gpm to 600gpm.

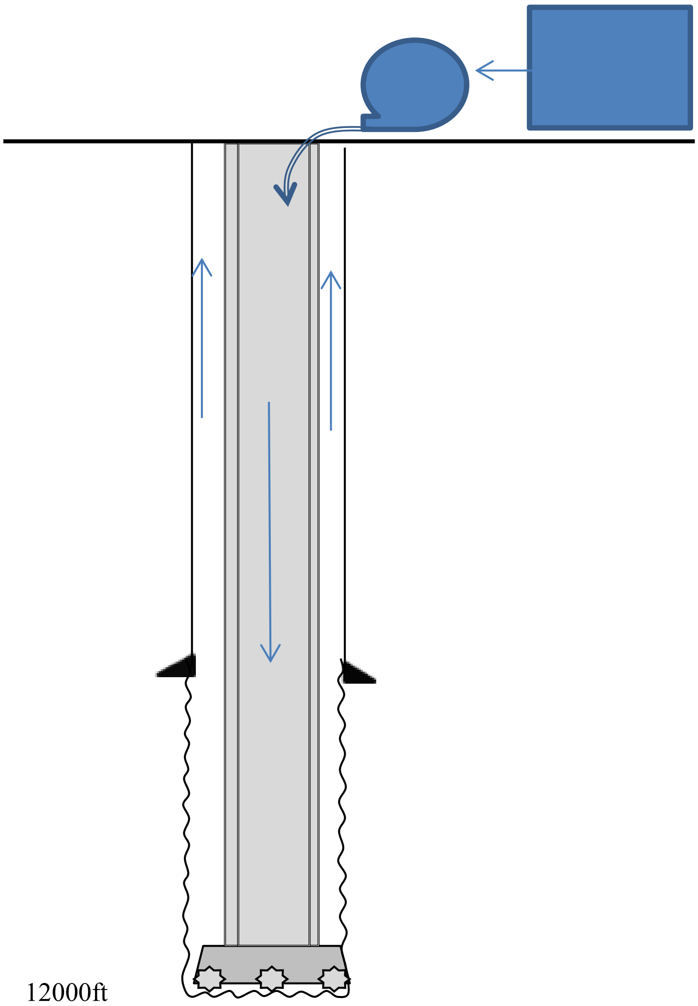

Figure 5.1: Illustration of simulation well

RPM	Ref	Fluid 1 (0,1g nano)	Fluid 2 (0,15g nano)	Fluid 3 (0,2g nano)	Fluid 4 0,25g nano	Fluid 5 (0,3g nano)	Fluid 6= Ref + $0.3Na_2CO_3$ Ex-Situ	Fluid 7= Fluid $1+0.3Na_2CO_3$ Ex-Situ
θ_{600}	37.4	40.3	35	35	37.7	36.5	39.8	45
θ_{300}	27.5	29.5	24.5	24.9	27	26	30.4	35
θ_{200}	22.9	25	20	20.4	22.5	21.3	26.1	30.5
θ_{100}	17.2	19.4	14	15	16.9	15.9	20.5	24.5
θ_6	8.9	10	5.2	6.5	8	6.9	12.2	16.5
θ_3	8.2	9.8	4.6	6.1	7.5	6.5	11.1	14.5

Table 5.1: Drilling fluids used in the simulation well.

5.1.2 Simulation result and discussion

Here two simulation results are presented, namely ECD and pump pressure.

Figure 5.2 shows the simulation results of ECD, which is calculated using Eq. 1. As the flow rate increase the friction loss in the annulus are also increasing. This as a result causes an increase in ECD. As shown, fluid #7 system exhibits a higher ECD than the reference. The main parameters, which plays an important role on ECD are the rheology parameters such the consistency index, the k-value and the lower shear yield stress values.

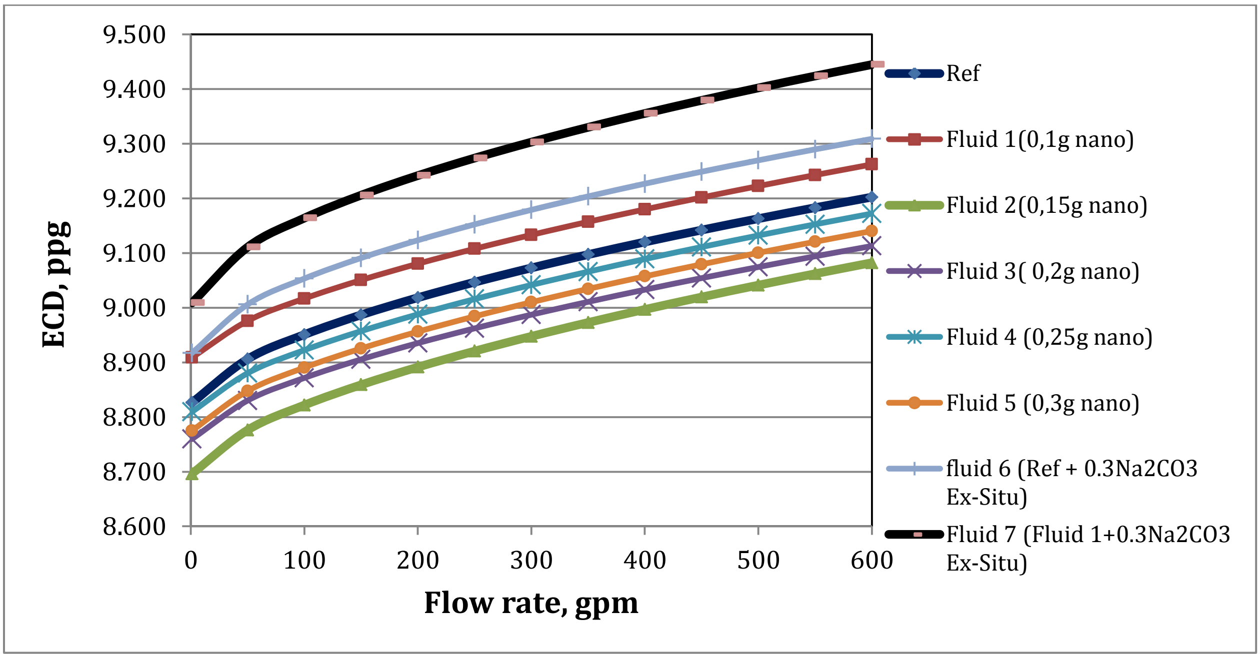

Figure 5.2: ECD of the drilling fluid systems.

As shown on the figure, the fluid system with 0.15g nano exhibits a lower ECD. Figure 5.3 shows the comparison of the change in ECD of the Fluid 2 (+0.15g Nano) system and the Fluid 7 (Fluid 1 +0.3g Na_2CO_3 ex-situ) system with the reference (Ref). The reference drilling fluid as shown on figure 5.2 is in the middle of the other two drilling fluids. That is why we just selected these three for comparison purposes. As shown in figure 5.3, comparing with the reference drilling fluid, Fluid 2 shows lower ECD by 0.65 % at higher flow rates. In terms of ppg, the ECD reduced by 0.06 ppg at higher flow rate.

Comparing with the reference fluid (Ref), Fluid 7 increased the ECD 2.57 % at the highest flow rate. In terms of ppg the ECD is increased by 0.24 ppg.

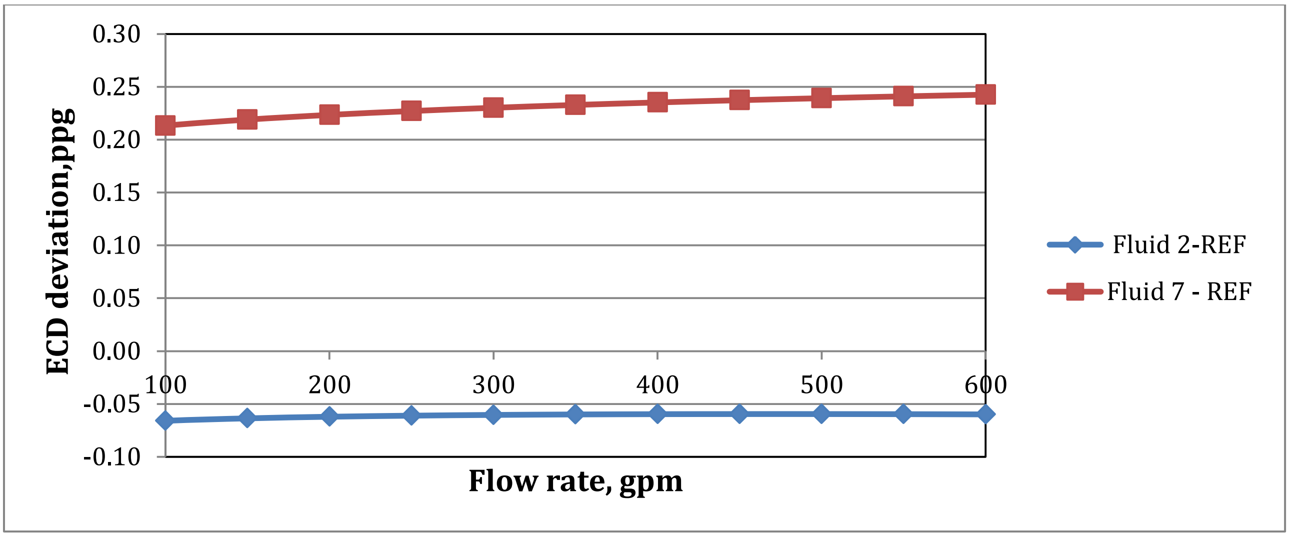

Figure 5.3: Percent ECD deviation of fluid 2 and Fluid 7 from Reference (Ref) fluid.

Figure 5.4 shows the simulated pump pressure required to circulate the drilling fluids all the way up to the surface. Similar to ECD plot, Fluid 7 shows a higher pump pressure and fluid 2 shows the lowest pressure.

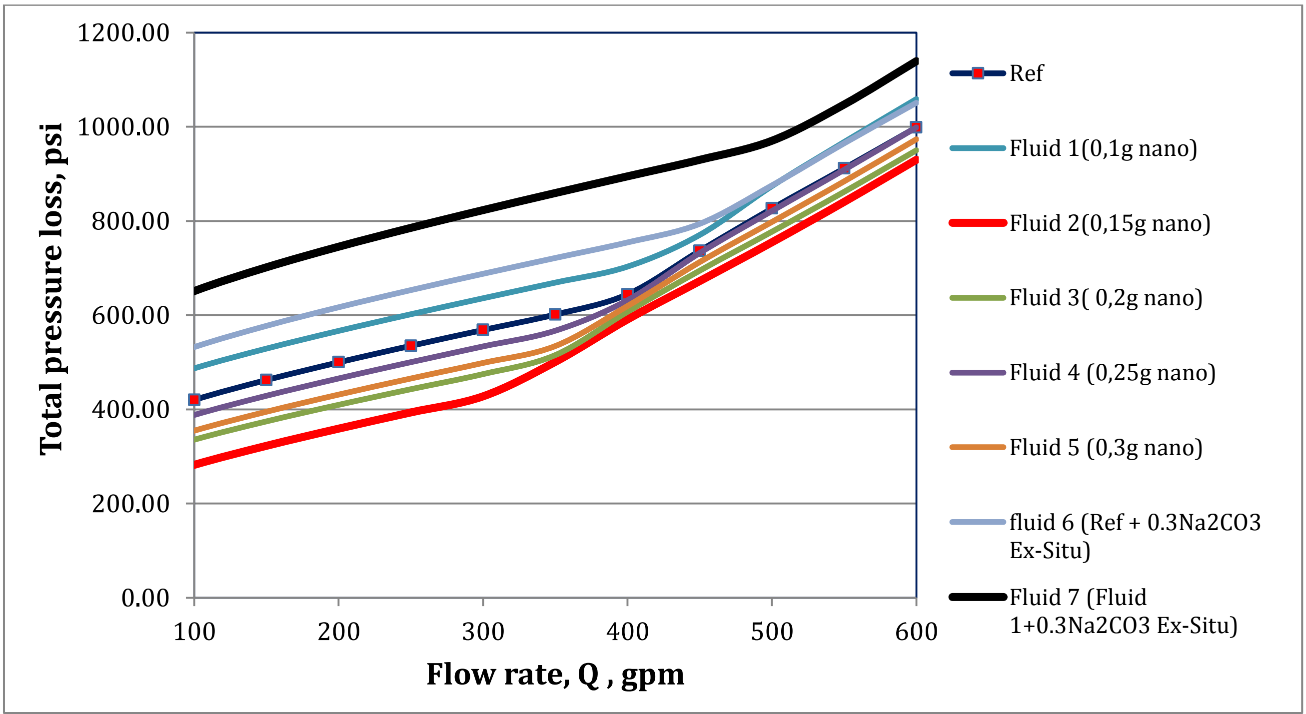

Figure 5.4: Total pressure loss of the fluid systems at room temperature.

For comparison purpose, three pump pressures obtained from the three drilling fluids were selected. As shown in Figure 5.5, the higher pressure difference between Fluid 7 and Ref (red curve) is about 250psi at 400gpm. The maximum pressure difference between fluid 2 and Ref (green curve) was 140psi reduction at 300gpm.

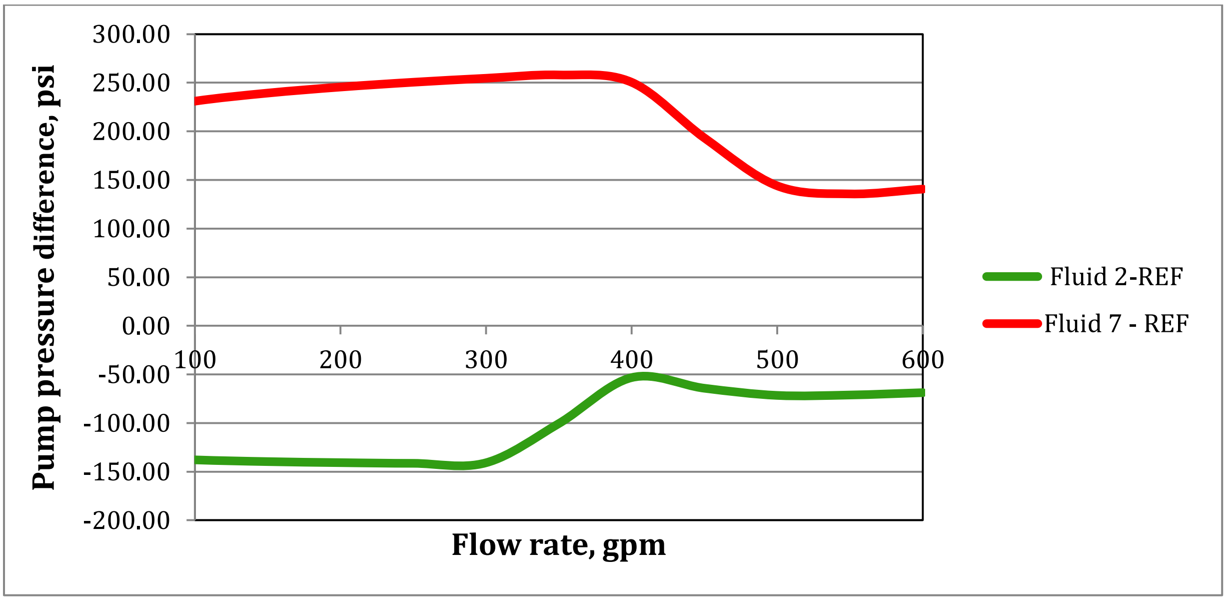

Figure 5.5: Pump pressure deviation of fluid 2 and Fluid 7 from Reference fluid.

5.2 Cuttings transport simulation

One of the functions of drilling fluid is to lift cuttings to surface. During design phase, it is important to evaluate the cutting lifting performance of a drilling fluid.

In this thesis, the cutting transport efficiency of the nano-treated fluid system formulated in section §4.11 are simulated in a deviated well.

It is known that the higher flow rates are good for the hole cleaning. However, the higher flow rates influence the ECD and erosional effects on wellbore and drill string. The higher flow rates also do have an impact on the state of stresses in the string. It is important to investigate the flow rate, which works best for the various operations without causing problems.

5.2.1 Simulation setup

The hole cleaning performance of the formulated drilling fluid has been simulated in 13123.3ft MD deviated well. The well consists of 13 3/8" casing and 12,615 " open hole.

During drilling a 5"OD and 4.86" ID drilling pipe was used. The BHA components are presented in Appendix A. The well is constructed in Landmark/Wellplan™ software. The well structure is shown on Figure 5.6.

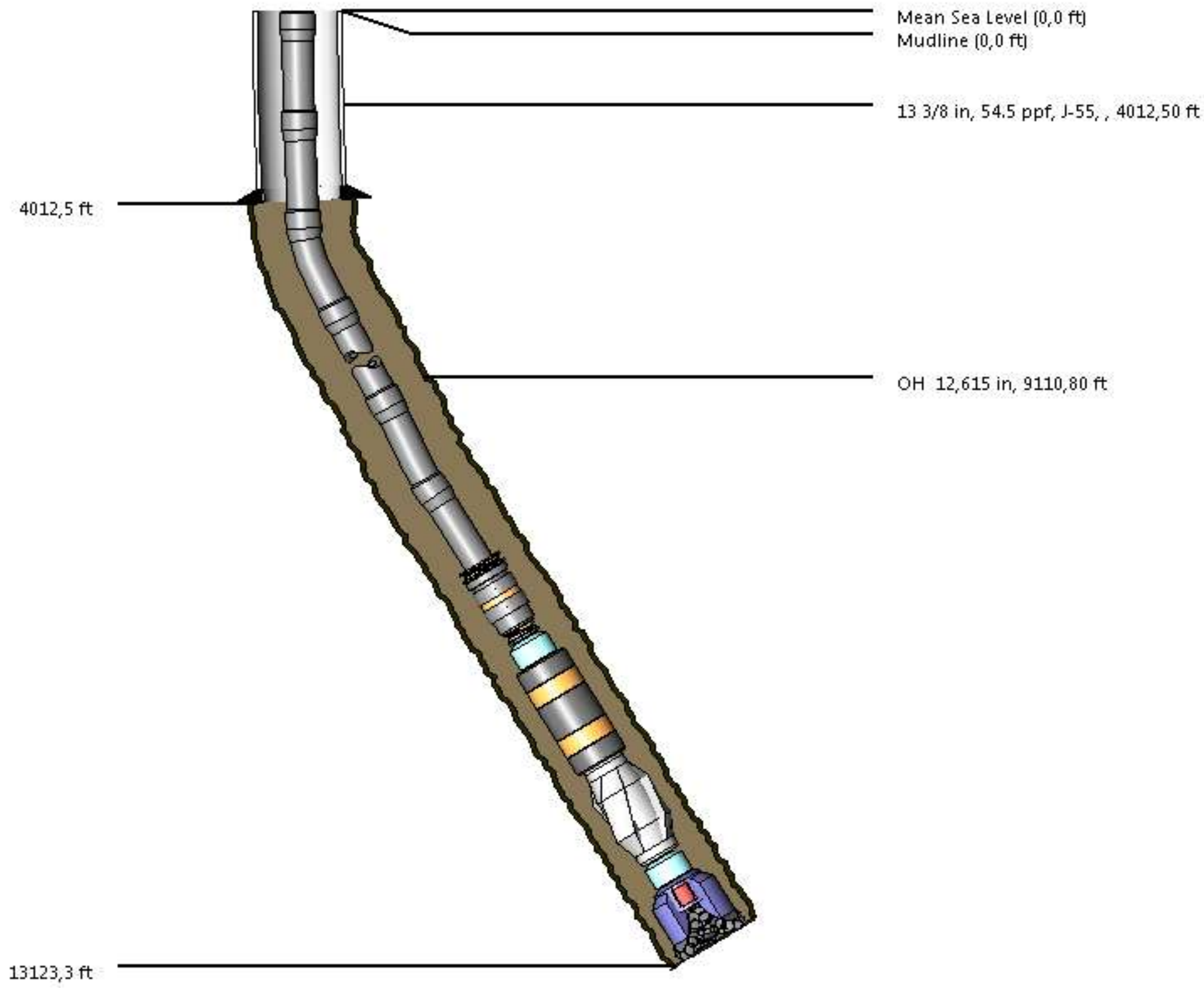

Figure 5.6: Deviated well used for cuttings transport simulation.

5.2.2 Drilling fluids

For the simulation, the viscometer data of the fluids are again provided here in Table 5.2. The fluids have been formulated and their properties characterized in section § 4.11.

RPM	Ref	Fluid 1 0,1gm nano	Fluid 2 0,15gm nano	Fluid 3 0,2gm nano	Fluid 4 0,25gm nano	Fluid 5 0,3gm nano	Fluid 6= Ref + $0.3Na2CO_3$ Ex-Situ	Fluid 7= Fluid 1+ $0.3Na_2CO_3$ Ex-Situ
θ_{600}	37.4	40.3	35	35	37.7	36.5	39.8	45
θ_{300}	27.5	29.5	24.5	24.9	27	26	30.4	35
θ_{200}	22.9	25	20	20.4	22.5	21.3	26.1	30.5
θ_{100}	17.2	19.4	14	15	16.9	15.9	20.5	24.5
θ_6	8.9	10	5.2	6.5	8	6.9	12.2	16.5
θ_3	8.2	9.8	4.6	6.1	7.5	6.5	11.1	14.5

Table 5.2: Nano treated and nano-free drilling fluids used for hole cleaning simulations.

5.2.3 Simulation result and discussion

Two simulation results are presented. The first one is to analyze performances of the fluid systems in terms of the minimum flow rate required to transport in a vertical to horizontal well. The second one is to simulate the behavior of bed height at 600gpm flow rate.

5.2.3.1 Bed height

Typical cutting transport parameters were used for the simulations. The rate of penetration is 60 ft/hr. so that it generates cuttings. The drill string is rotated at 90 RPM, which is good enough to lift bed cuttings in suspension. Figure 5.7 shows the simulation result. The figure on the left side is the well inclination. As shown, up to about 5000 ft. the well is near vertical and the simulation results show that nearly no cutting has been deposited. As the well inclination increase, the bed height is also increasing. Out of the considered drilling fluids, Fluid 7 shows good hole-cleaning performance. Comparing fluid 1 and fluid 7, the addition of 0.3g Na_2CO_3 ex-situ salt reduces the bed height by about 1.8in.

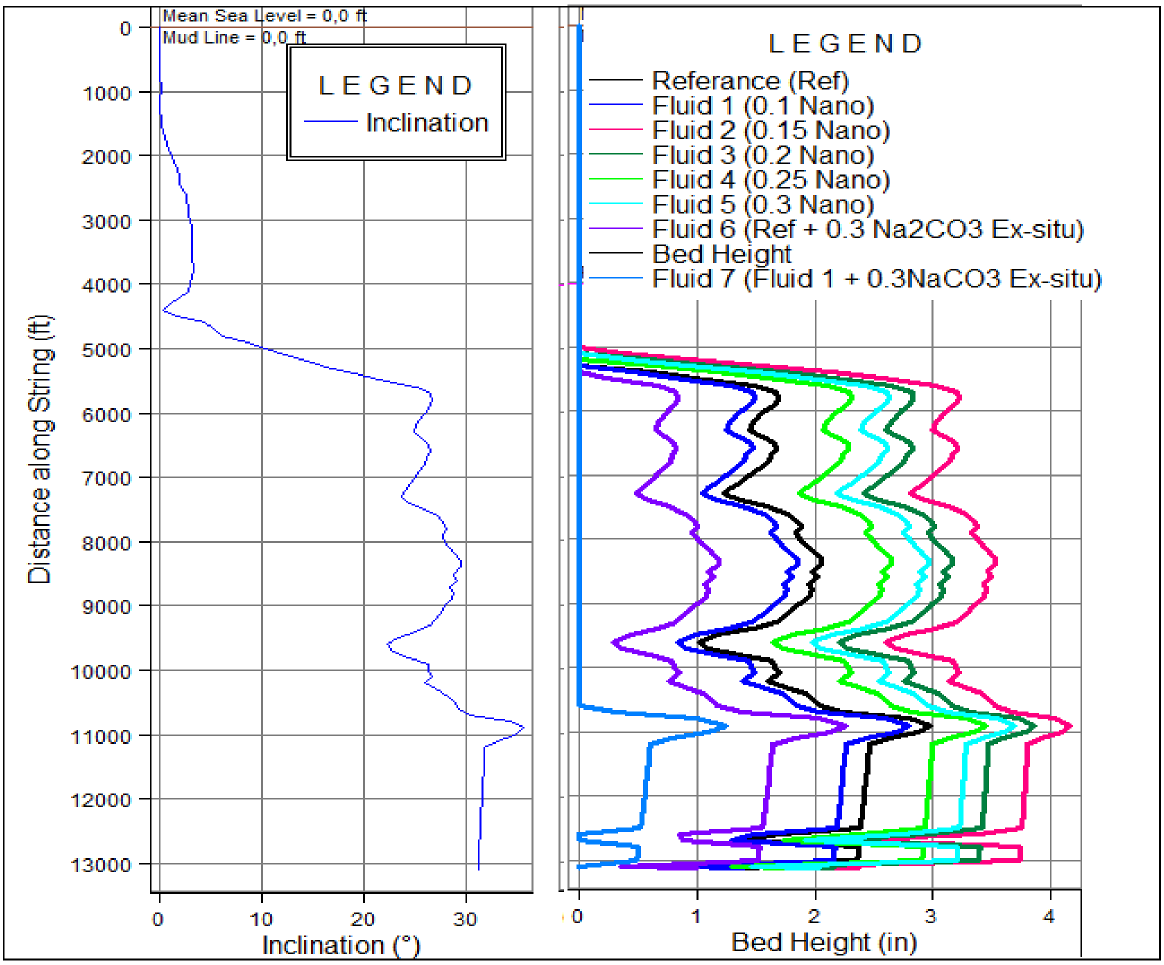

Figure 5.7: Bed height of cuttings in nano treated and nano free drilling fluids at 600gpm injection rate.

5.2.3.2 Minimum flow rate simulation

The second simulation was to determine the minimum flow rate required to transport cutting out of the well. If the flow velocity is below this critical velocity, cutting will be deposited. In this simulation, the well is assumed to be deviated from vertical (0 deg) to horizontal (90 deg). Unlike the previous simulation, the drill string does not contain BHA system. Table 5.3 is the simulation parameters

Cuttings diameter [in]	Cuttings density [sg]	ROP [ft/hr]	Rotary speed [RPM]	Bit diameter [in]	Annulus diameter [in]
0.125	2.500	60	90	8.5	8.5

Table 5.3: Cutting transport analysis parameters.

Figure 5.8 shows the critical minimum velocity simulation results. As shown in horizontal well, Fluid 7 requires about 460 pgm to completely transport and Fluid 1 requires 546gpm. This illustrates the impact of 0.3g (0.06%wt) - Na_2CO_3 salt on 0.1g nano-treated drilling fluid system. Table 3 shows the summary of the minimum flow rates in 90 deg. horizontal well.

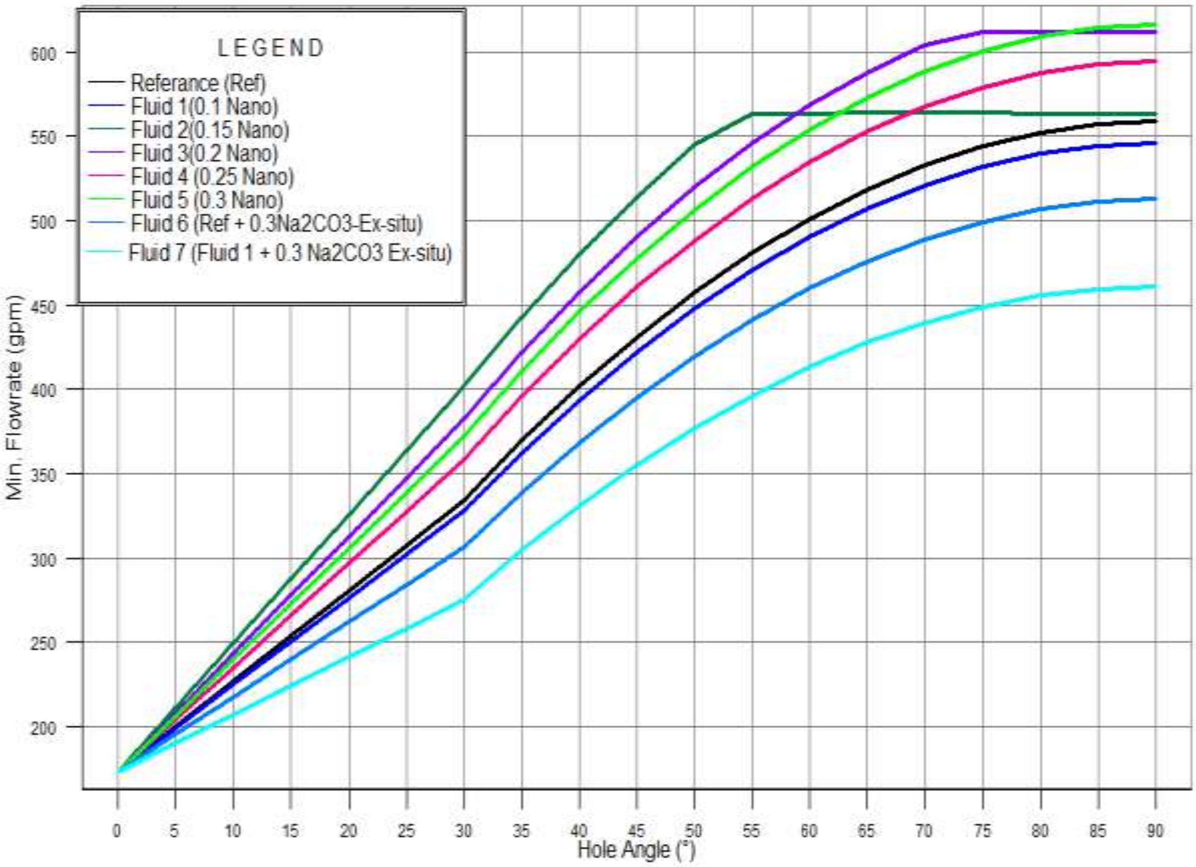

Figure 5.8: Minimum flow rate as a function of well deviation.

Flow rate at 90deg well	Reference (Ref)	Fluid 1 +0.1 Nano	Fluid 2 +0.15 Nano	Fluid 3 +0.2 Nano	Fluid 4 +0.25 Nano	Fluid 5 +0.3 Nano	Fluid 6= Ref + $0.3Na_2CO_3$ Ex-situ	Fluid 7= (Fluid 1 + 0.3 Na_2CO_3 Ex-situ
Q, gpm	558,53	546,02	563,71	612,23	594,37	615,98	512,71	460,73

Table 5.4: Summary of flow rate in horizontal well.

6 Summary and discussions

This section presents the summary and discussion of the overall results obtained from the experimental and performance simulation parts of the main thesis. The objective of the experimental part was to formulate a drilling fluid system containing nano silica, which produces a favorable rheology and filtrate properties. The viscoelastic properties of the selected nano based fluids were tested. Finally, the hydraulic performance and cutting transport of the selected nano based drilling fluid systems were assessed.

6.1 Drilling fluids formulation and rheology/filtrate/pH characterization

In this part of study, several test matrixes were designed. The fluids behaviors were characterized in terms of their rheology, filtrate loss and pH-values. The experimental designs and test results are presented in the main thesis report. In addition, in order to compress the thesis, some other test results are attached in Appendix C-S. These plots give a good overview of the behavior of drilling fluids with respect to the additives that dominate in positive or negative ways. All the drilling fluids have been prepared by using 500gm H_2O and 25g Bentonite (i.e 525g bentonite fluid). In the following, the effect of various additives in the bentonite fluid will be summarized. The additives are salts, nano silica, polymers (PAC, CMC, DUO-VIS and Drispac and XC)

6.1.1 Effect of salt

The first test matrix was designed to evaluate the performance of seven salts in bentonite drilling fluids. These salts were: Na_2CO_3, $NaHCO_3$, NaCl, Na_2SO_4, KCl, $CaSO_4$, and $MgSO_4$

Out of these salts systems, the addition of 2gm $CaSO_4$ and $MgSO_4$ salts created two phases by separating out bentonite and pure water. The main reason could be the concentration of salts was high enough and caused the system disintegrated. However, the addition of Na_2CO_3, Na_2SO_4, and KCl showed very good rheology properties of the bentonite fluids. Two salts, $NaHCO_3$ and NaCl, also improved the rheology of salt free system, but less than the previously mentioned salt systems.

6.1.2 Salt and PAC

The effect of salts in PAC polymer has also been evaluated. First, the effect of PAC in bentonite system was studied in the absence of salts with the objective of obtaining soup like system. From this study, we found out that 0.5g PAC was suitable.

Five salts were mixed with 0.5 g PAC in bentonite mud system. The results showed that the performance of PAC in KCl made drilling fluid very thin. This resulted in lower PV, YS and LSYS values. The other salts reacted better with PAC, raising the 600 and 300 readings. However, the dial readings at the lower shear rates were lower than the PAC free system. Regarding the filtrate loss, all fluids systems improved filtrate loss as compared with PAC free systems. Comparing with PAC free system, the addition PAC in NaCl and KCl salt reduced the filtrate rate by over 50%.

6.1.3 Effect of Salt and nano silica

Here we treated the reference 25/500 bentonite/water with five salts and 0,2g nano silica. The objective was to evaluate the performance of nano-silica in various salts. In the reference fluid, Na_2CO_3, and $NaHCO_3$ treated fluid systems, the addition of 0.2g nano didn’t show any significant impact on the plastic viscosity (PV).

On the other hand, nano silica showed both negative and positive minor effects on the yield stress (YS). The higher impact on the YS was observed in KCl treated fluid, which reduced the YS by 25,6%. Similar effect was also observed on the LSYS value.

For this particular nano concentration (0.2g Nano in 525drilling fluid), nano silica alone seems to have little effect on the filtrate loss. The results varied from salt type to salt type. In addition, the concentration of salt also played an important role when mixing with nano particles. However, it is important to remember that increasing or reducing the concentration of nano in the given concentration of salt may provide different positive or negative result.

6.1.4 Effect of Salt, PAC and nano silica

Here we treated 2g of salts, 0,2g nano silica and 0.5g PAC in 525g bentonite fluid. The objective of this design was to study the combined effects the mentioned additives.

The result showed that the plastic viscosity of the fluids increased and the YS and LSYS decreased. A significant effect was observed in fluid system treated with KCl. The YS and LSYS values of KCl system were reduced by 70% and 86%, respectively.

PAC and nano silica also showed a significant effect on the consistency index (k) and exponent law index (n) as well. The k- values were reduced by over 50% for every system and KCl-fluid system showed the highest reduction from 5,568 to 0,291 lbf.s^n/100sqft. The n-values the fluids increased by at least 40%.

The dramatic reduction in YS, LSYS, k and n has been observed in KCl/PAC fluid system, which is evaluated in test matrix #2.

Considering the filtrate losses, all mud system reduced filtrate rate in PAC and nano silica, even better than the PAC drilling fluids except the $NaHCO_3$ treated fluid. $NaHCO_3$ salt system actually creates bubble, which could probably be the main reason for a little bit higher filtrate loss in nano/ PAC than PAC only system. Please see section § 6.1.7 below.

6.1.5 Effect of salt mixture (two salts), nano silica and PAC

During the salt effect studies, it was found out that the performance of KCl in PAC was not good in terms of rheology and filtrate properties of fluid. KCl and PAC are the commonly used additives in drilling fluids. It is also observed that some other salts showed good performance in PAC polymer. With the objective of improving the performance of KCl in PAC, we formulated salt mixture test in nano silica and PAC system.

For this study, NaCl, Na_2CO_3 and Na_2SO_4 were tested separately and mixed with KCl as well. The test results showed that the three salt mix systems improved the rheology comparing to the single KCl, PAC and nano silica mud system. All the Bingham and power law model parameters improved due to the salts added with KCl.

For instance, the viscometer responses of fluid treated with (Na_2CO_3 and KCl) was the highest compared with the other systems. In terms of API filtrate loss, every salt mixture systems showed better result than the single salt KCl system. But, the results are not as good as the single NaCl system. The NaCl/KCl mix showed the lowest filtrate loss. Please note that this analysis is based on the considered additives and concentrations. When changing the concentration, one might get a different result.

6.1.6 Effect of KCl concentration, polymers and nano silica

KCl is an important salt used for swelling control, and is often used in higher concentrations than 0.38 wt% of the mud. It was observed the negative performance of nano in KCl and PAC system. To formulate a system which allows 4g KCl (i.e 2.81 ppg) in 525g bentonite drilling fluid when treated with 0.35g PAC and 0.95g DUO-Vis. In addition, 4g KCl, 0.35g CMC and 0.95g DUOVIS mixed in 525g bentonite drilling fluid. In the later system the addition of 0.3g Na_2CO_3 ex-situ in 0.1g nano treated drilling fluid showed an improved result. Similarly, the addition of 0.3g Na_2CO_3 ex-situ in nano free system also improved the result, but lower than the 0.1g nano system. This illustrates the performance of nano in different polymers and the addition of Na_2CO_3 in improving the performance of nano blended in 2.81 ppb KCl salt.

6.1.7 Comparisons of filtrate losses

Figure 6.1 shows the comparisons of filtrate losses obtained from four different test matrixes. The reference drilling fluid (Ref) is the base case presented in section §4.4. The second fluid types (Ref + 0.5g PAC) presented in section § 4.5. The third fluid types (Ref + 0.2g Nano) presented in section §4.6. The fourth fluid types (Ref + 0.5g PAC + 0.2g Nano) presented in section §4.7. As shown in the figure, the performance of reference and the third fluid (nano additive) show higher filtrate loss and the loss volumes are almost comparable. The third fluid type (PAC) system reduced the filtrate loss very much. The performance of the 0.2g nano greatly improved when blended with 0.5g PAC. This shows that the behaviors of drilling fluid depend on the concentrations and type of additives. Several other test results have shown this.

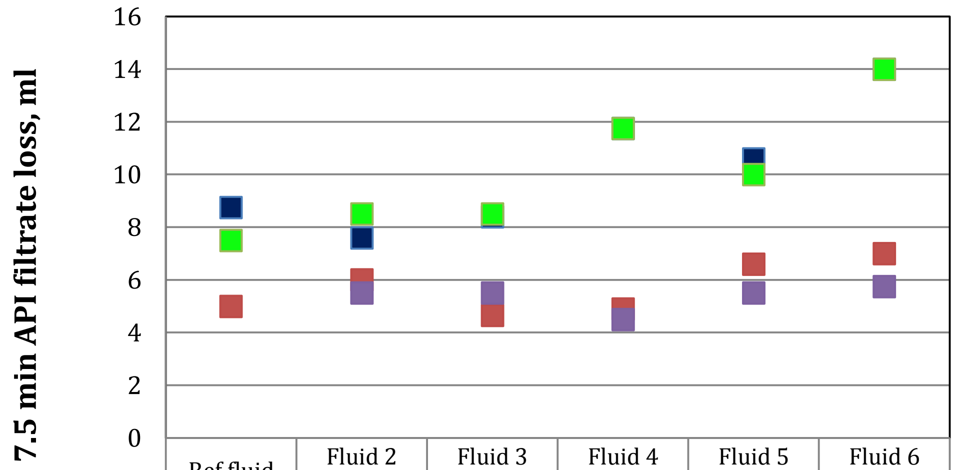

	Ref fluid	Fluid 2 (Na2CO3)	Fluid 3 (NaHCO3)	Fluid 4 (NaCl)	Fluid 5 (Na2SO4)	Fluid 6 (KCl)
Ref	8.75	7.6	8.4	11.75	10.6	14
Ref+ 0.5gm PAC	5	6	4.65	4.9	6.6	7
Ref+ 0.2gm Nano	7.5	8.5	8.5	11.75	10	14
Ref + 0.5gm PAC+ 0.2gm Nano		5.5	5.5	4.5	5.5	5.75

Figure 6.1 Comparisons of filtrate losses.

6.2 Viscoelasticity behavior of formulated nano based drilling fluids

During at rest (i.e connection period), good drilling fluids should create gel structure quickly in order to hold particles in suspension. The internal gel structure and stability of the nano-fluid were studied using Anton-Paar [51]. Four drilling fluids were evaluated. These are nano free and nano treated (0.06g, 0.1g and 0.15g), which were mixed in-situ with 525g bentonite fluid. The fluids have been formulated in section § 4.12.

Two types of viscoelasticity measurements were performed, namely amplitude and frequency sweep.

From the amplitude test, the LVE ranges of the fluids were found out to be at 10% strain. From this test, we determined the flow point and yield stress. One clear observation is that as the nano concentration increase, the storage moduli and loss moduli are decreasing. In all of the fluids, it is shown that in the elastic dominated zone, the storage moduli are greater than the loss moduli. This is an indication that the fluid systems are stable gel structure.

The flow points and the yield stresses are not showing in a uniform variation as the concentration of nano increases. However, the 0.06g nano fluid system showed the highest flow point and yield strength. The flow point of the nano-free (Ref) system was the lowest. The yield stress of the 0.15g nano system is lower than the nano free system (see the following table)

In the main report, the yield points obtained from the oscillatory amplitude test (Figure 4.34) is compared with the Bingham yield stress (Table 4.29). The differences between these are quite high as shown in Table 6.1. .

Methods	Ref (0 Nano)	Ref (0.06 Nano)	Ref (0.1 Nano)	Ref (0.15 Nano)
Anton Paar, YS [Pa]	1.44	2.12	1.58	1.25
Bingham, YS [Pa]	8.14	9.58	10.05	7.95
Difference, [Pa]	6.70	7.46	8.47	6.70

Table 6.1 Comparison of Anton Paar and Bingham yield stresses.

The results obtained from the oscillatory frequency test also showed that as the nano concentration increases, the G' and G" and the complex viscosity parameters are reducing. The G' and G" curves are not crossing each other at the lower frequency, which is an indication of a stable gel structure in the drilling fluids.

6.3 Performance simulation studies of nano based drilling fluids

This section summarizes the hole cleaning efficiency and the hydraulics of nano based drilling fluids.

6.3.1 Hydraulics

It is always important to analyse the performance of a formulated drilling fluid. In this thesis, the selected nano based drilling fluids were analysed in terms of their ECD and Pump pressure in a vertical well. For this, we used the unified model. Comparing with the reference (nano free) system, some of nano treated drilling fluids showed lower ECD/pump pressure than the reference and some of them showed higher than the reference system. The main drilling fluid controlling parameters for ECD/pump pressure are the rheology and density.

6.3. 2 Cutting transport

The drilling fluid analysed for hydraulics are also used to simulate their cutting transport efficiency. Simulation study was carried out in a deviated well. The performances of the drilling fluids were assessed in terms of the minimum velocity to transport cutting and bed height deposition at 600gpm.

The simulation results showed that the fluid systems with higher YS & LSYS lift cutting with a lower flow rate than the reference nano-free system. Please note that there are also other drilling fluids parameters that govern the hole cleaning efficiency.

7 Conclusion

The objective of this thesis was to formulate nano silica treated water based mud systems, which improve the rheology and filtrate loss of a conventional water based mud system. Several conventional and nano silica based systems were designed and tested. *The mud systems were evaluated in various concentrations/types of polymer, salts and nano silica.* These additives were blended in 25g bentonite and 500g H_20.

One of the desires of the design was to use high concentration of KCl in order to handle swelling problem. However test results have shown that KCl causes a thinning effect when mixed with PAC/Drispac polymers and/or nano silica. In order to allow a system take more KCl, a mixture of Duovis and CMC was used. In addition, it was found out that among many others salts, Na_2CO_3 improves viscometer readings.

After several attempts, the composition of the best nano-silica based is:

500g H_2O + 0.1g Nano silica + 4g KCl +0.75g Na_2CO_3 + 0.95g DUOVIS + 0.35g CMC + 25g Bentonite+ 0.3g Na_2CO_3 (ex-situ)

From the experimental and the simulation studies, the main observations are summarized as follows. Please note that the summary is based on the considered additives concentration and types. When changing these, we may get different results. The lessons learnt were:

- KCl in PAC polymer system decreases Fann viscometer dial readings. As a result a lower PV, YS and LSYS and higher the filtrate loss was obtained.
- The addition of 0,75g and 1,05g Na_2CO_3 in KCl and polymer systems (PAC, DUOVIS and CMC) improves the viscometer data of the conventional and nano silica based fluids. 2g Na_2CO_3 also raises Fann dial data of PAC and nano silica blended system.

- The addition of 0.1g nano silica in DOVIS/CMC mud system is the optimal amount. Comparing with other concentration of nano (i.e higher or lower), the 0.1g increases the viscometer data. The result is higher YS and LSYS than the reference fluid.

- Also, drilling fluid with 0.1g nano in test matrix #9 (used for viscoelastic test) experiences a great increase in consistency index (k) by 58% compared to the nano free reference.

- In the absence of polymer (PAC), the performance of nano silica with KCl salt has shown poor result on filtrate loss (14ml). The performance of PAC in KCl has shown reduction of filtrate by half (7ml). When treating the PAC + KCl with 0.2g Nano silica, the filtrate loss has further reduced to 5.75 ml. Comparing matrix #2 (PAC + KCl) with Test matrix #4 (PAC + Nano +KCl), the 0.2g (0.038%wt) nano silica additive system reduced filtrate loss by 18%. When changing the systems, one may get different results. This illustrates how nano works better when mixed with PAC. However, one needs to optimize the right concentration through experimental work based on the desired rheology parameters.

- From viscoelasticity oscillatory test results, it is observed that all nano and nano free systems (section § 4.12.) yielded at 10% strain. As nano concentration increases from zero to 0.15g, the storage (G') and loss (G") moduli are decreasing. In other words, the ratios of G'/G" show decreasing, but higher than one. This is an indication that all the fluids systems are stable. In addition, the complex viscosity also shows decreasing. All nano treated fluids have shown higher flow point than the nano-free reference fluid system. Except the 0.15g Nano additives, the two nano (0.06g & 0.1g) additive fluids have shown higher yield stress. The highest yield stress was obtained for a fluid treated with 0.06g nano, which is 0.68Pa higher than the nano free. The yield strength of the 0.15g nano fluid has shown 0,19 Pa lower than the nano-free system. The results show that there exists an optimum nano concentration, which works best when it comes to stability and strength. This can be investigated through experiments.

- In the hydraulic simulation only the fluid containing 0,1g nano silica (Fluid 1) had a higher ECD/Pump pressure than the reference fluid. Also the modified fluid 7 (Fluid 1+ 0,3g Na_2CO_3) had higher ECD than the modified reference. The higher results were due to the fact that the reference fluids modified with nano and Na_2CO_3 had shown higher viscosity parameters. One needs to perform an optimization study in order to get best rheology parameters which works for a desired ECD /pump pressure.

- On the other hand, the cuttings transport simulation fluid 1 and fluid 7 was the only fluids better than its references. Fluid 7 was the best mud system, with the lowest bed height composition and lowest minimum flow rate.

Finally, this thesis comes to the conclusion that the performance nano has shown positive and negative results. The negative results can be improved by treating with polymers, which creates a positive synergy. A positive effect nano is the result of using the right concentration in a given salt and polymers. In addition, the performance of KCl in nano treated system could be improved with treated with other salts such as NaCl and Na_2CO_3.

References

1 Mukul M. Sharma, R. Zhang, M.E. Chenevert, L. Ji, Q. Guo, J. Friedheim, **2012 //A New Family of Nanoparticle Based Drilling Fluids// SPE 160045** This paper was prepared for presentation at the SPE Annual Technical Conference and Exhibition held in San Antonio, Texas, USA, 8-10 October 2012.

2 Katherine Price Hoelscher, Guido De Stefano, Meghan Riley, Steve Young, M-I SWACO 2012//**Application of Nanotechnology in Drilling Fluids//** SPE 157031, SPE International Oilfield Nanotechnology Conference, 12-14 June 2012, Noordwijk, The Netherlands

3 Gongrang Li, Jinghui Zhang, Huaizhen Zhao, Yegui Hou. Shengli Drilling Technology Institute, Sinopec, 2012// **Nanotechnology to Improve Sealing Ability of Drilling Fluids for Shale with Micro-cracks During Drilling// SPE** 156997-MS SPE International Oilfield Nanotechnology Conference , 12-14 June 2012, Noordwijk, The Netherlands

4 Rahul C. Patil, Abhimanyu Deshpande 2012 //**Use of Nanomaterials in Cementing Applications**// SPE-155607 SPE International Oilfield Nanotechnology Conference and Exhibition, 12-14 June, Noordwijk, The Netherlands 2012

5 Mezan Y. Kanj, Jim J. Funk, and Zuhair Al-Yousif: 2009// **Nanofluid Coreflood Experiments in the ARAB-D**// SPE 126161 paper presented at the 2009 SPE Saudi Arabia Section Technical Symposium and Exhibition held in Alkhobar, Saudi Arabia, 09-11 May 2009

6 Elena Rodriguez, Matthew R. Roberts, Haiyang Yu, Chun Huh and Steven L. Bryant: 2009//**Enhanced Migration of Surface-Treated Nanoparticles in Sedimentary Rocks**// SPE 124418 paper presented at the 2009 SPE

Annual Technical Conference and Exhibition held in New Orleans, Louisiana, USA, 4-7 October 2009.

7 Skjeggestad, O. (1989) **Boreslamteknologi: teori og praksis**, Bergen: Alma Mater forlag.

8 H. H. Rodriguez, J. B. Ramirez, D. C. Velazquez, A. N. Conejo, J. A. Martinez, "**Annular flow analysis by tracers in drilling operations**,2004.

9 Statoil. 2010, **Activity Program**, Drilling

10 Bourgoyne, A.T. Jr., Millheim, K.K., Chenevert, M.E., and Young J, F.S., "**Applied Drilling Engineering**", SPE Textbook Series Vol. 2, 1991. Richardson, Texas (ISBN: 978-1-55563-001-0)

11 MI-SWACO "**Drilling Fluids Engineering Manual**". 1998.

12 Caenn, R. et al. (2011) **Compostion and properties of drilling and completion fluids**. USA: Elsevier Inc.

13 Håvard Stangeland, 2015 //**Experimental loss circulation and performance simulation studies of 60/40, 70/30, 80/20 and 90/10OBMs**// MSc thesis, UiS 2015

14 Gernr, A. 2012// **Loss circulation experimental study in Oil based mud and analyzing experimental data/**/ MSc thesis, UiS

15 Mitchell, R. F., Miska, S. Z. & Aadnoy, B.S., "**Fundamentals of drilling engineering**", Society of Petroleum Engineers (2011) (ISBN: 978-1-55563-207-6)

16 Zheng Xiuhua, Ma Xiaochun **Drilling Fluids School of Engineering and Technology China University of Geosciences** (Beijing) 29 Xueyuan Road

Beijing, 100083 P.R.China

17 *H.C.H Darley George R. Gray* //**Composition and properties of drilling and completion fluids**// *Fifth edition*
18 *Roland F. Krueger//* **Evaluation of drilling fluid filter loss additives under dynamic condition** //, SPE-431-PA Journal of Petroleum Technology **Volume** 15 **Issue** 01 januar 1963

19 *J.T.Dewan and M.E. Chenevert,Petrophysics//* **A model for filtration of water based mud during drilling determination of mudcake parameters** *Vol.42 NO 3 (May- June 2001)*

19. *L.P. Roodhart,//* **Fracturing Fluids: Fluid-Loss Measurements under Dynamic Conditions,** *SPE, 11900* Society of Petroleum Engineers Journal **Volume** 25 **Issue** 05 October 1985

20: Mesfin Belayneh, 2004 / **Wellbore stability experimental and analytical study**// PhD thesis, UiS

21 DAVID MAURICIO MOSQUERA NARVÁEZ **// study of the use of products sodium polyacrylate and paper industry from the diaper in oil drilling processes**// MSc thesis, **BOGOTÁ D.C., COLOMBIA 2012**

22 ANAMARIJA KUTLIĆ, GORDAN BEDEKOVIĆ, IVAN SOBOTA**//bentonite processing oplemenjivanje bentonita//** Rud.-geol.-naft. zb., Vol. 24, 2012

23 Skule strand //"**Øvinger I Bore og Brønnvæsker**" (compendium in the undergraduate drilling fluid course).University of Stavanger.
24 http://www.irooildrilling.com/Viscosifier/CMC.htm

25.http://www.cpchem.com/bl/drilling/en-us/tdslibrary/Drispac%20Polymer.pdf

26: Andreas Egholm, 2015// **Effect of Synthetic salt water on Nano silica treated cement slurry**// BSc thesis UiS, 2015

27 U.S. Tare et al //**Mitigating Wellbore stability problems white drilling water based muds in Deepwater environments**, 6-9 May 2002-OTC 14267

28 www.wikipedia.org

29 Azar.J.J., Samuel.G.R., "**Drilling Engineering**". PennWell Corporation. Tulsa, Oklahoma, 2007

30.Khodja, M., Khodja-Saber, M., Canselier, J.P., Cohaut, N., Bergaya, F., "**Drilling Fluid Technology: Performances and Environmental Considerations**." InTech. ISBN: 978-953-307-211-1, 2010.

31 Belayneh, M. (2013) **PET 525 Advanced drilling lecture note**, [Lecture].

31 Preston L Moore// **drilling practices manual, second edition** //1986 ISBN 0-87818-292-4

32 : Strand, S. (1998) Øvinger i bore- og brønnvæsker, Høyskolen i Stavanger, Stavanger.

33 Binh, B. Saasen, A. Maxey, J. et al. (2012) "**Viscoelastic Properties of Oil-Based Drilling Fluids**" Annual Transactions of the Nordic Rheology Society. Vol 20.

34 API RP 13-B1, **Recommend Practice for Field Testing Water-Based Drilling Fluids, third edition**. 2003. Washington, DC: API.

35 Hemphill T, Campos W and Pilehvari A: "**Yield-Power Law Model More Accurately Predicts Mud Rheology**," *Oil & Gas Journal* 91, no. 34 (August 23, 1993): 45–50.

36 Versan, M. and Tolga, A. (2005) “E**ffect of Polymers on the Rheological properties of KCl/Polymer Type Drilling Flui**d” Energy Sources, 27(5), pp. 405-415.

37 Zamora .M and Power D 2002 **Making a case for AADE hydraulics and the Unified model**, AADE 2002 technology conference Drilling and completion fluids and waste management, Houston, Texas

38 Thomas G. Mezger // **The Rheology Handbook, 4th Edition4th Edition**// ISBN-13: 978-3866308428 ISBN-10: 3866308426

39.http://www.wee-solve.de/English/Rheologie/Methoden/Frequenztest.htm

40 “**Recommended Practice on the Rheology and Hydraulics of Oil-Well Drilling Fluids**, API RP 13D”, Fourth Edition. American Petroleum Institute, (June 1995).

41 Tommy M. Warren, SPE, Amoco Production Co. 1989. **Evaluation of Jet-Bit Pressure Losses**. SPE17916

42 Jeyhun Sadigov, 2013// **Comparisons of rheology and hydraulics prediction of mud systems in concentric and eccentric well geometry**// MSc thesis, UiS

43 Ochoa, M.V. (2006) **Analysis of Drilling Fluid Rheology and Tool Joint Effect to Reduce Errors in Hydraulics Calculations**. PhD Thesis. Texas: A&M University.

44 Nazari, T. Hareland, G. and Azar J.J. (2010) “**A Review of Cuttings Transport in Directional Well Drilling: Systematic Approach**”, SPE 132372, SPE Western Regional Meeting, Anaheim, California, U.S.A, 27-29 May.

45 BAKER HUGHES **Drilling Fluids Reference** Manual REVISION 2006

46 **WellPlan (Landmark)**™ Software, Halliburton.

47 Ahmed S. Mohammed and C. Vipulanandan, P.E. and D. Richardson // **Range of Rheological Properties for Bentonite Drilling Muds//** CIGMAT-2013 Conference & Exhibition

48 EPRUI **Nanoparticles and Microspheres** Co. Ltd. (2015) Available at: http://www.nanoparticles-microspheres.com (Accessed: 15.03.15).

49 Gucuyener, I.H., Middle East Technical U.// **A Rheological Model for Drilling Fluids and Cement Slurries// SPE** 11487-MS Middle East Oil Technical Conference and Exhibition, 14-17 March 1983, Bahrain

50 Zamora, M., Roy, S. and Slater, K.: "**Comparing a Basic Set of Drilling Fluid Pressure-Loss Relationships to Flow-Loop and Field Data**," paper AADE-05-NTCE-27 presented at the AADE 2005 National Technical Conference and Exhibition, Houston, 5-7 April

51 http://www.anton-paar.com/corp-en/

Appendix

Appendix A: Well construction input parameters

Hole cleaning simulation well input parameters.

Drill String data (Drill pipe + BHA)

String Editor

String Initialization

String Name: Assembly

String (MD): 13123.3 ft   Specify: Top to Bottom   Import String

Library: Export   Import

	Section Type	Length (ft)	Measured Depth (ft)	OD (in)	ID (in)	Weight (ppf)	Item Description
1	Drill Pipe	12564,30	12564,3	5,000	4,000	28,26	Drill Pipe 5 in, 25.60 ppf, E, 5 1/2 FH, P
2	Heavy Weight	120,00	12684,3	6,625	4,500	70,50	Heavy Weight Drill Pipe Grant Prideco, 6 5/8 in, 70.50 ppf
3	Jar	33,00	12717,3	6,500	2,750	91,79	Hydraulic Jar Dailey Hyd., 6 1/2 in
4	Heavy Weight	305,00	13022,3	5,000	3,000	49,70	Heavy Weight Drill Pipe Grant Prideco, 5 in, 49.70 ppf
5	Sub	5,00	13027,3	6,000	2,400	79,51	Bit Sub 6, 6x2 1/2 in
6	MWD	85,00	13112,3	8,000	2,500	154,36	MWD Tool 8 , 8x2 1/2 in
7	Stabilizer	5,00	13117,3	6,250	2,000	93,72	Integral Blade Stabilizer 8 1/2" FG, 6 1/4 x2 in
8	Sub	5,00	13122,3	6,000	2,400	79,51	Bit Sub 6, 6x2 1/2 in
9	Bit	1,00	13123,3	10,625		166,00	Tri-Cone Bit, 0.589 in²

Hole data (Casing + Open hole)

Hole Section Editor

Hole Name: Hole Section   Import Hole Section

Hole Section Depth (MD): 13123,3 ft   Additional Columns

	Section Type	Measured Depth (ft)	Length (ft)	ID (in)	Drift (in)	Effective Hole Diameter (in)	Friction Factor	Linear Capacity (bbl/ft)	Item Description
1	Casing	4012,5	4012,50	12,615	12,459	12,615	0,28	0,1547	13 3/8 in, 54.5 ppf, J-55,
2	Open Hole	13123,3	9110,80	12,615		12,615	0,28	0,1546	

Well inclination

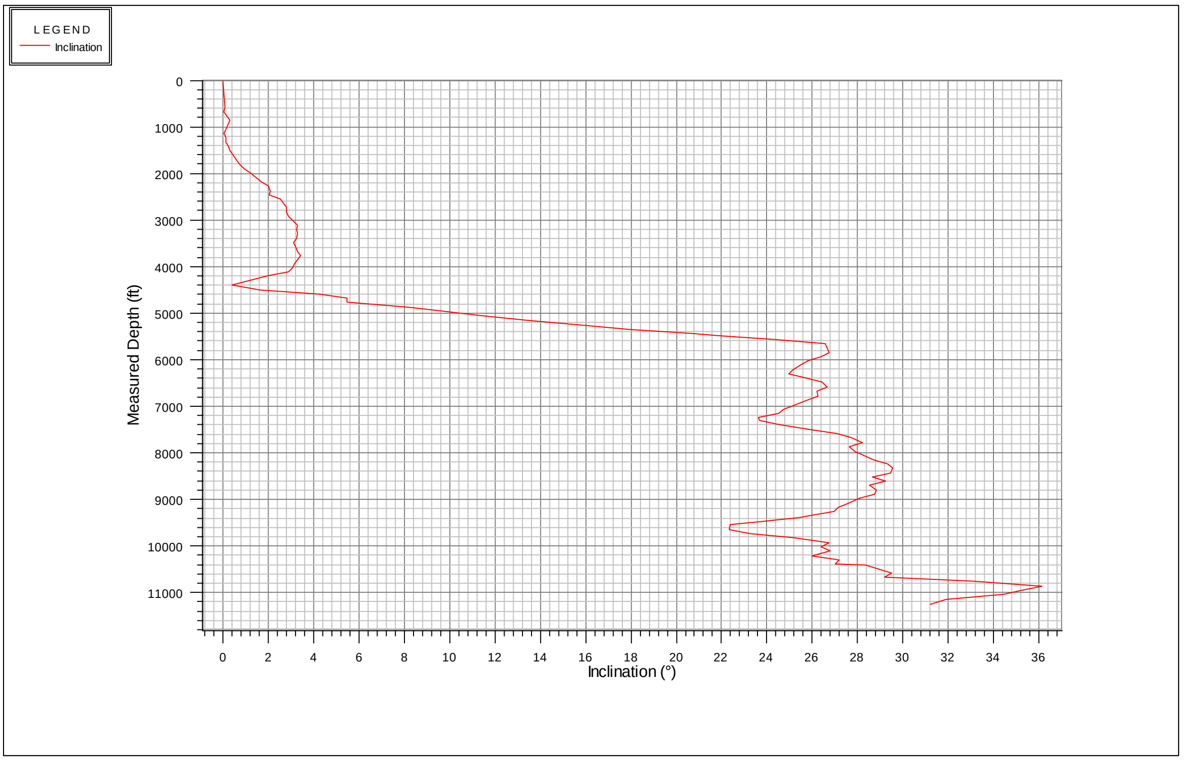

Azimuth

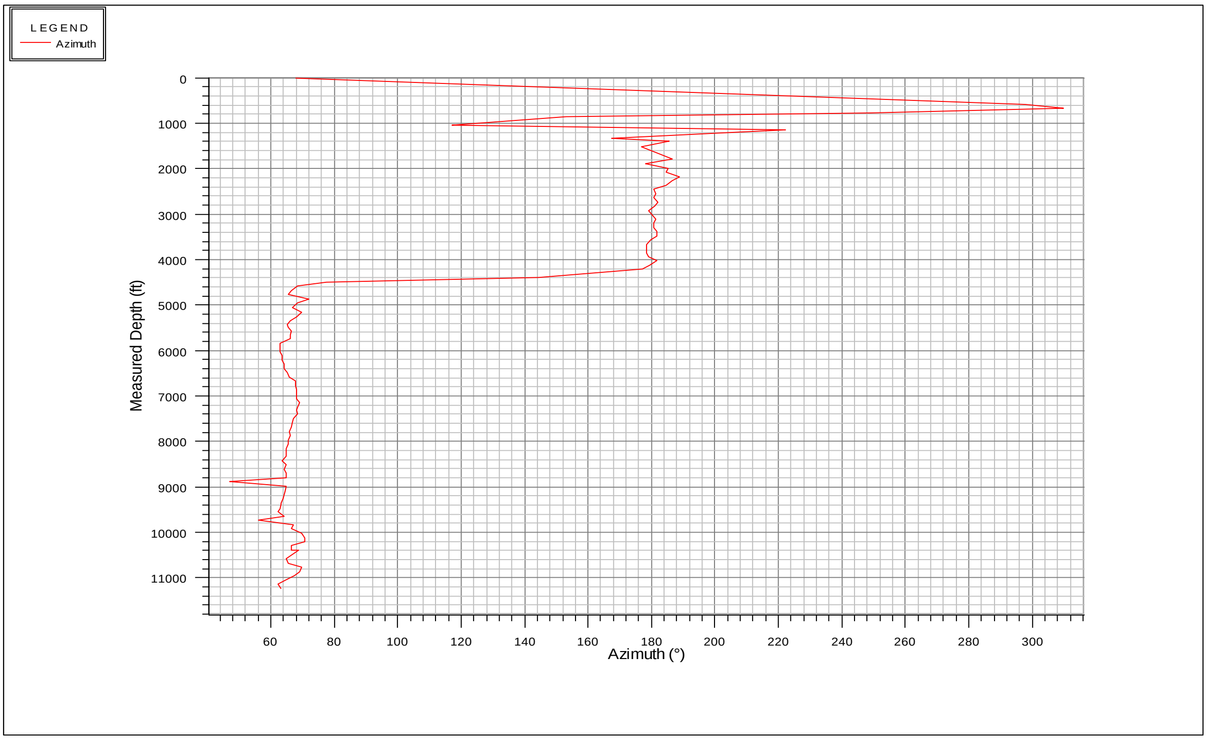

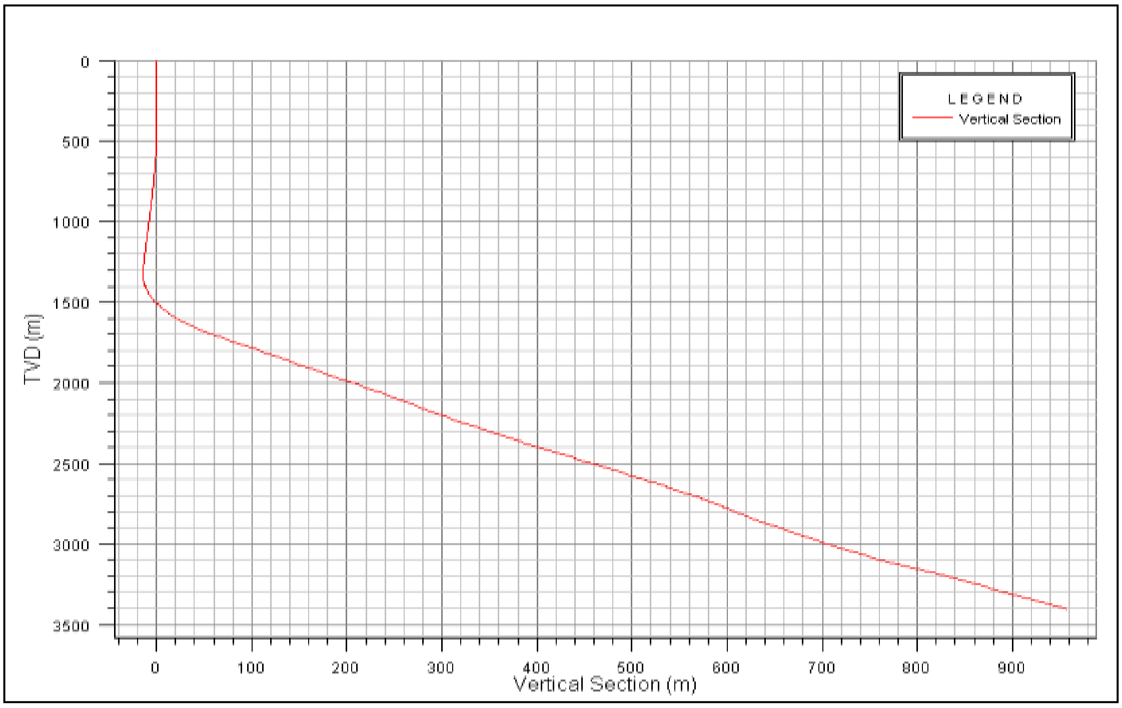

Vertical section

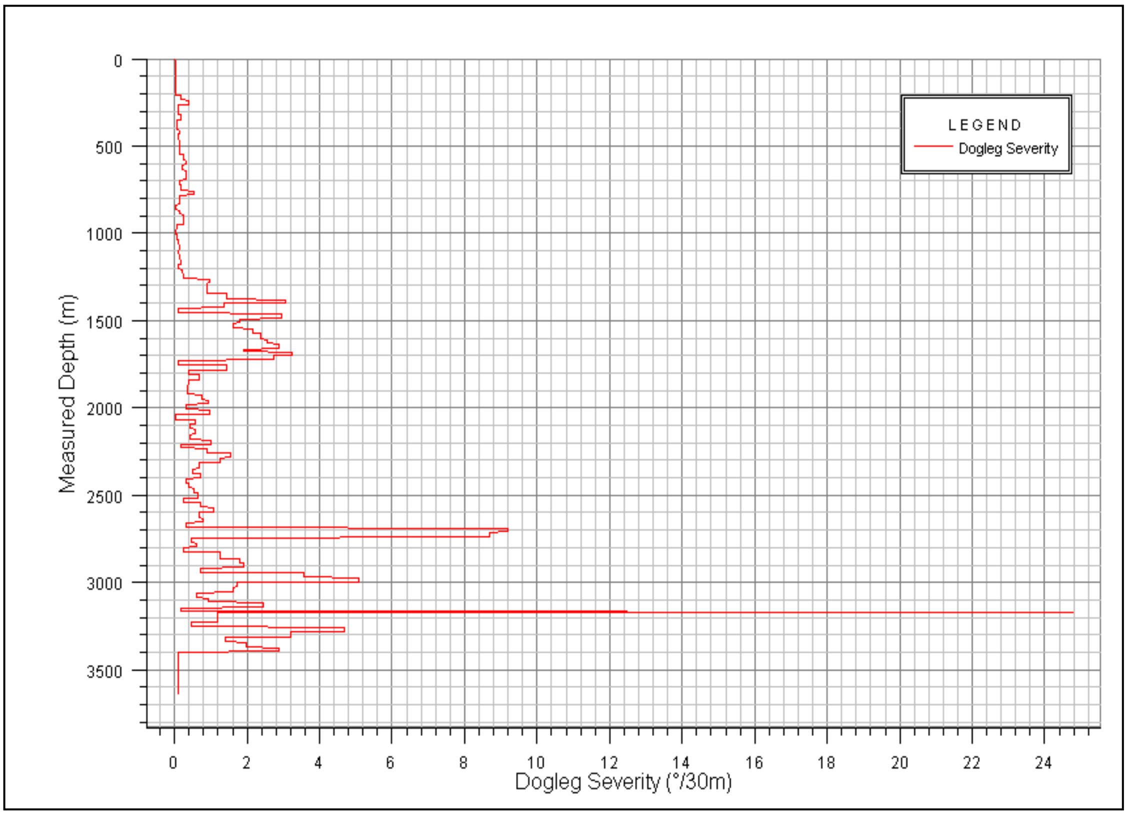

Dogleg severity

Appendix B: Well plan cutting transport models

Hole Cleaning Calculations

Calculate $n, K, \tau_y,$ and Reynold's Number

$$n = \frac{(3.32)(\log 10)(YP + 2PV)}{(YP + PV)}$$

$$K = \frac{(PV + YP)}{511}$$

$$\tau_y = (5.11K)^n$$

$$R_A = \frac{\rho V_a^{(2-n)}(D_H - D_P)^n}{(2/3)G_{fa}K}$$

Concentration Based on ROP in Flow Channel

$$C_o = \frac{\left(V_r D_B^{\ 2}/1471\right)}{\left(V_r D_B^{\ 2}/1471\right) + Q_m}$$

Fluid Velocity Based on Open Flow Channel

$$V_a = \frac{24.5Q_m}{D_H^{\ 2} - D_P^{\ 2}}$$

Coefficient of Drag around Sphere

If $R_e < 225$ then,

$$C_D = \frac{22}{\sqrt{R_a}}$$

else,

$$C_D = 1.5$$

Mud carrying capacity

$$C_M = \frac{4g\left(\frac{D_c}{12}\right)(\rho_c - \rho)}{3\rho C_D}$$

Slip Velocity

If $V_A < 53.0$, then $V_{SV} = (0.00516)V_A + 3.0006$

If $V_A \geq 53.0$, then $V_{SV} = (0.02554)(V_A - 53.0) + 3.28$

Settling Velocity in the Plug in a Mud with a Yield Stress

$$U_p = \left[\frac{4}{3}\frac{gD_c^{1+bn}(\rho_c - \rho}{aK_b\rho_c^{1-b}}\right]^{\frac{1}{2-b(2-n)}}$$

Where:

$$a = 42.9 - 23.9n$$

$$b = 1 - 0.33n$$

Angle of Inclination Correction Factor

$$C_a = (\sin(1.33\alpha))^{1.33}\left(\frac{5}{D_H}\right)^{0.65}$$

Cuttings Size Correction Factor

$$C_s = 1.286 - 1.04D_c$$

Mud Weight Correction Factor

If $(\rho < 7.7)$,then

$$C_m = 1.0$$

else

$$C_m = 1.0 - 0.0333(\rho - 7.7)$$

Critical Wall Shear Stress

$$\tau wc = [ag\sin(\alpha)(\rho_c - \rho)D_c^{1+b}\rho^{b/2}]\frac{2n}{2n - 2b + bn}$$

Where:

$$a = 1.732$$

$$b = -0.744$$

Critical Pressure Gradient

$$Pgc = \frac{2\tau wc}{r_h[1-(\frac{r_0}{r_h})^2]}$$

Total Cross Sectional Area of the Annulus without Cuttings Bed

$$A_A = \frac{\pi}{4}\frac{\left(D_H^2 - D_P^2\right)}{144}$$

Dimensionless Flow Rate

$$\Pi g_b = \Pi[8 \times \frac{\frac{n}{2(1+2n)}}{(a)\frac{1}{b}}]^{\frac{1}{2-(2-n)b}} \times (1-(\frac{r_p}{r_h})^2)(1-(\frac{r_p}{r_h})^{\frac{b}{2-(2-n)b}}]$$

Where:

a = 16

b = 1

Critical Flow Rate (CFR)

$$Q_{crit} = rh^2 \left[\frac{\rho g b^{\frac{1}{b}} r_h^{\left(\frac{1}{b+n}\right)}}{K\rho^{\left(\frac{1}{b-1}\right)}} \right]^{\frac{b}{2-b(2-n)}} \prod_{gb}$$

Correction Factor for Cuttings Concentration

$$C_{BED} = 0.97 - (0.00231\, \mu_a)$$

Cuttings Concentration for a Stationary Bed by Volume

$$C_{bconc} = C_{BED}\left(1.0 - \frac{Q_m}{Q_{crit}}\right)(1.0 - \phi_B)(100)$$

Where:

D_B = Bit diameter

D_H = Annulus diameter

D_P = Pipe diameter

D_{TJ} = Tool joint diameter

D_C = Cuttings diameter

τ_y = Mud yield stress

G_{fa} = Power law geometry factor

R_A = Reynolds number

R_e = Particle Reynolds number

ρ = Fluid density

ρ_c = Cuttings density

V_a = Average fluid velocity for annulus

V_R = Rate of penetration, ROP

V_{CTV} = Cuttings travel velocity

V_{so} = Original slip velocity

V_{SV} = Slip velocity

V_{CTFV} = Critical transport fluid velocity

V_{TC} = Total cuttings velocity

K = Consistency factor

n = Flow behavior index

a, b, c = Coefficients

YP = Yield point

PV = Plastic viscosity

Q_C = Volumetric cuttings flow rate

Q_m = Volumetric mud flow rate

Q_{crit} = Critical flow rate for bed to develop

C_o = Cuttings feed concentration

C_D = Drag coefficient

C_m = Mud carrying capacity

C_A = Angle of inclination correction factor

C_S = Cuttings size correction factor

C_{mud} = Mud weight correction factor

C_{BED} = Correction factor for cuttings concentration

C_{bmc} = Cuttings concentration for a stationary bed by volume

U_{sp} = Settling velocity

U_s = Average settling velocity in axial direction

U_{mix} = Average mixture velocity in the area open to flow

α = Wellbore angle

ϕ_B = Bed porosity

μ_a = Apparent viscosity

λ_p = Plug diameter ratio

g = Gravitational coefficient

r_0 = Radius of which shear stress is zero

r_p = Radius of drill pipe

r_h = Radius of wellbore or casing

P_{g} = Critical frictional pressure gradient

τ_{wc} = Critical wall shear stress

Appendix C: Effect of ex-situ salt –Na_2CO_3

1	0,4g Duovis, 0,3g CMC, 4g KCl, (0,2g nano, 0,75g Na2CO3 ex-situ)
2	0,95g Duovis, 0,35g CMC, 4g KCl,(0,2g nano, 0,75g Na2CO3 ex-situ)
3	0,4g Duovis, 0,3g CMC, 4g KCl
4	0,95g Duovis, 0,35g CMC, 4g KCl
5	Mud 5 0,2g nano-PAC

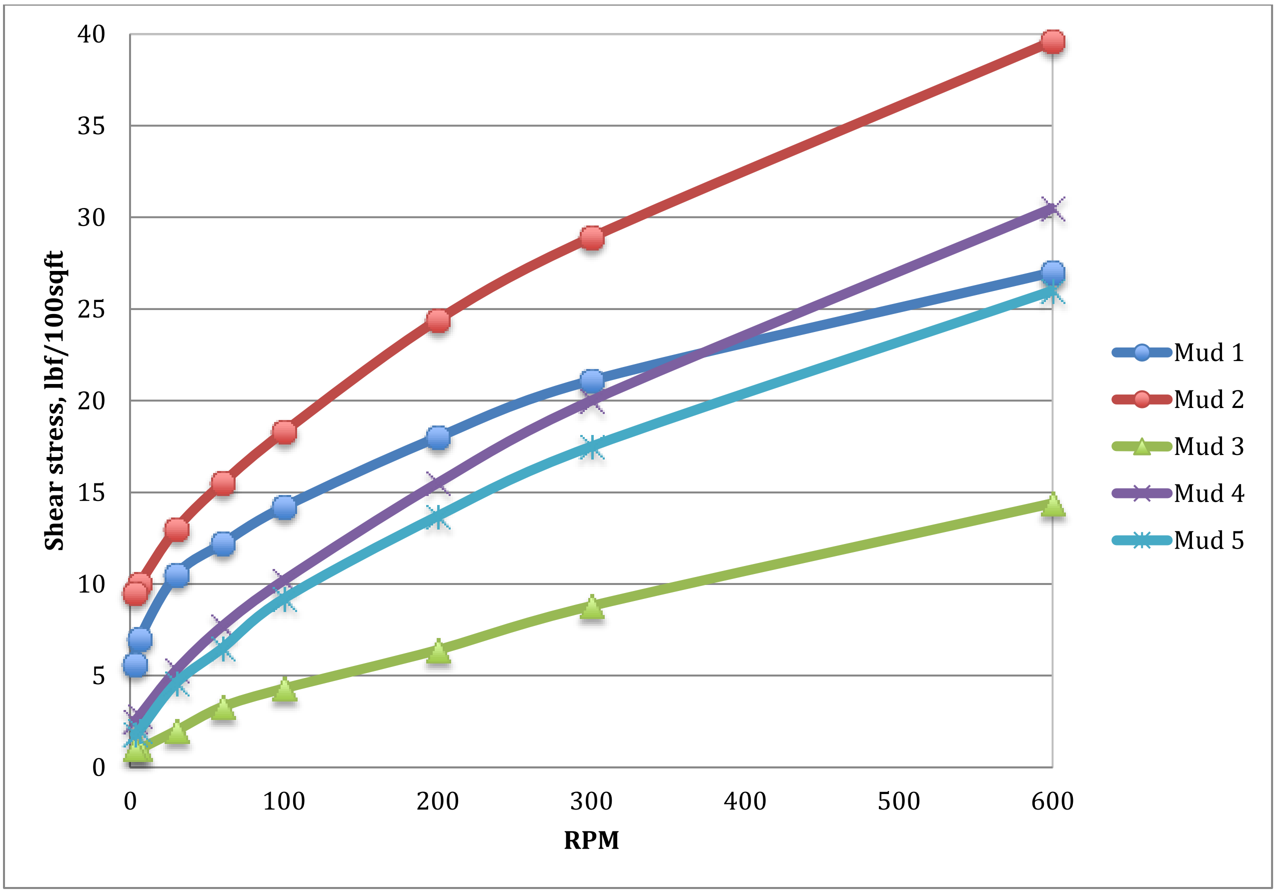

Parameters	Mud 1	Mud 2	Mud 3	Mud 4	Mud 5
PV (cP)	5.9	10.7	5.6	10.5	8.5
YS (lbf/100sqft)	15.2	18.2	3.2	9.5	9
LSYS(lbf/100sqft)	4.2	9	1	2.2	1.6
k(lbf.s^n/100sqft)	2.298	1.701	0.105	0.450	0.498
n []	0.356	0.454	0.710	0.608	0.571

Appendix D: Effect of ex-situ KCL salt

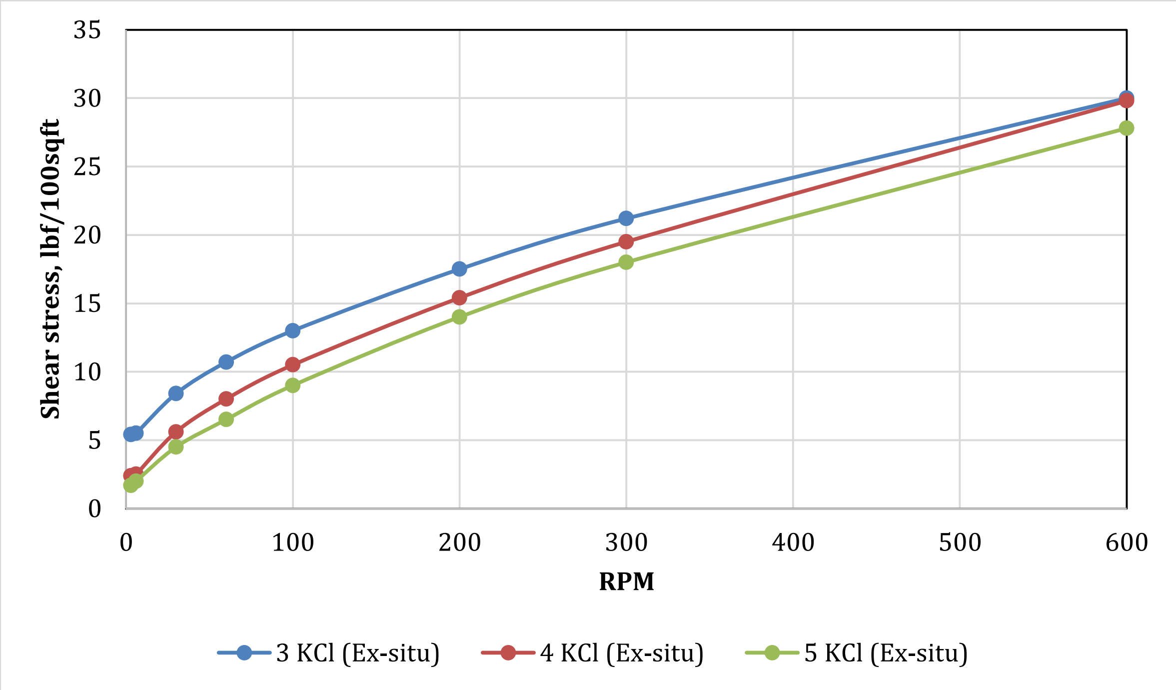

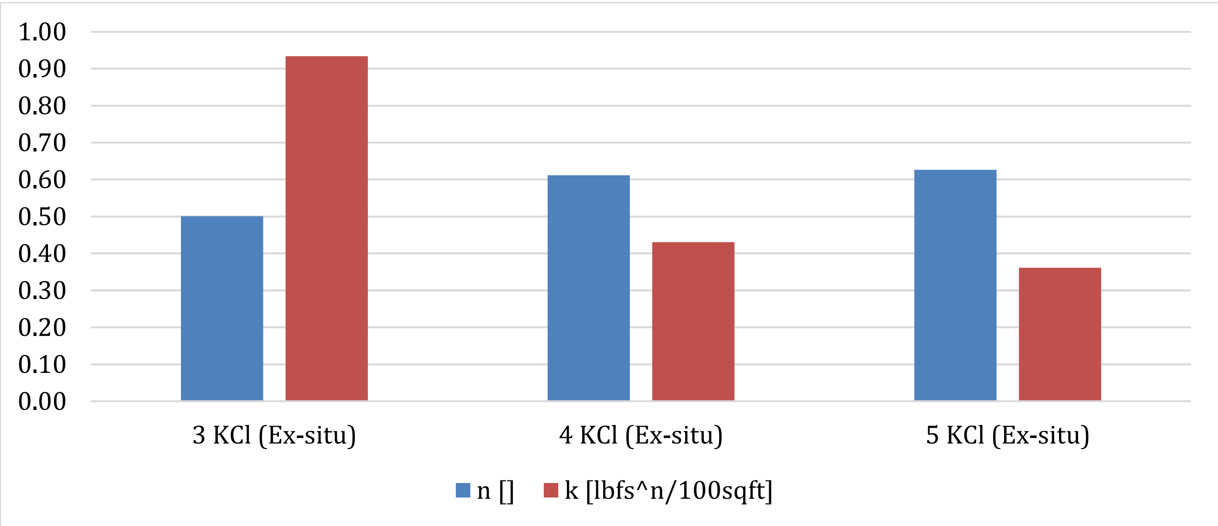

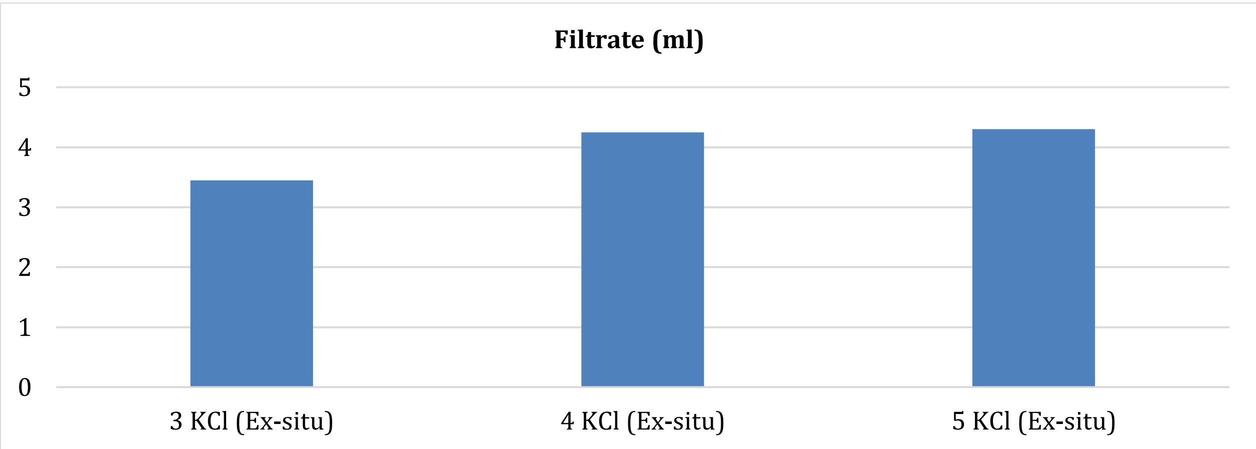

Appendix E: Effect of polymer concentration

1	0,95g Duovis, 0,35g CMC, 4g KCl
2	0,4g Duovis, 0,3g CMC, 4g KCl
3	0,95g Duovis, 4g KCl, 0,2g nano, (0,75g Na2CO3 ex situ)
4	0,95g Duovis, 0,35g PAC, 4g KCl, (2g Na2SO4 ex situ)
5	0,95g Duovis, 4g KCl, (0,5g NaHCO3 ex situ)

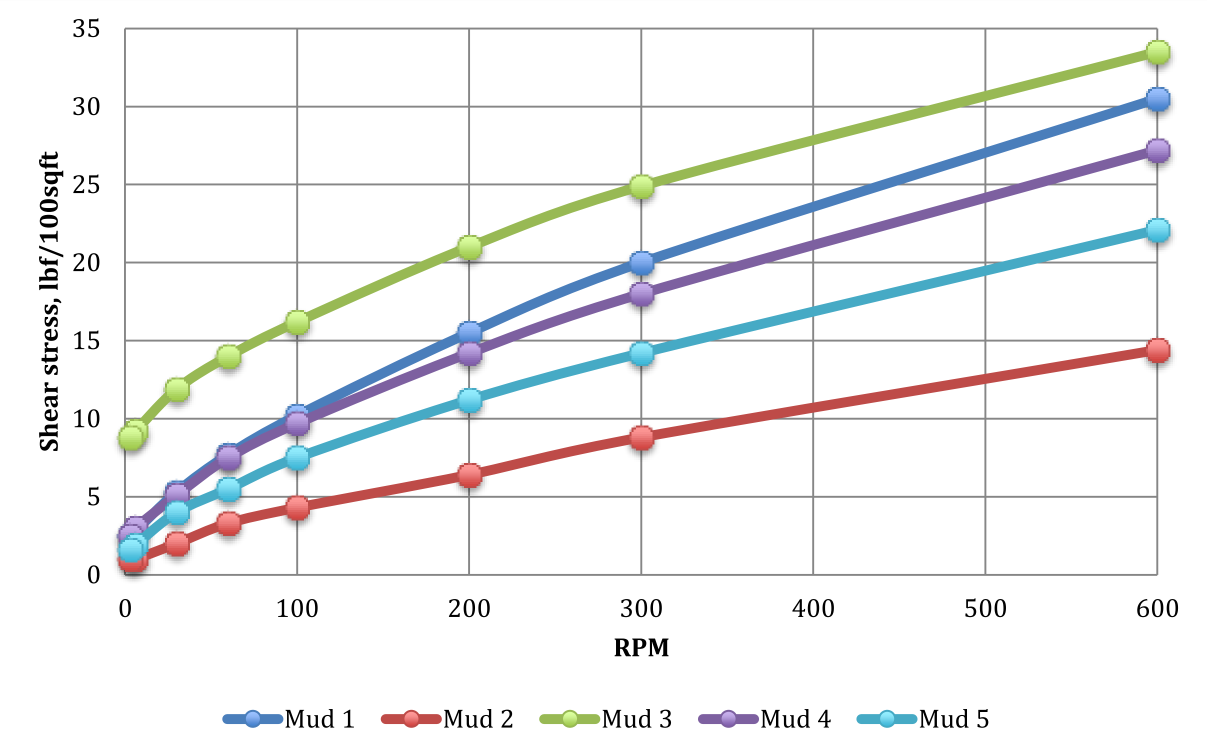

Parameters	Mud 1	Mud 2	Mud 3	Mud 4	Mud 5
PV (cP)	10.5	5.6	8.6	9.2	7.9
YS (lbf/100sqft)	9.5	3.2	16.3	8.8	6.3
LSYS(lbf/100sqft)	2.2	1	8.4	2	1.3
k(lbf.s^n/100sqft)	0.450	0.105	1.728	0.440	0.266
n []	0.608	0.710	0.428	0.595	0.638
pH	8.9	8.95	10	8.75	8.45
Filtrate loss [ml]	4.45	5.5	4.5	3.2	5.05

Appendix F: Effect of KCl/NaCl concentration

2gKCl+2gNaCl+0.2Nano+0.5PAC+25gBentonite
1,5gKCl+1,5gNaCl+0.2Nano+0.5PAC+25gBentonite

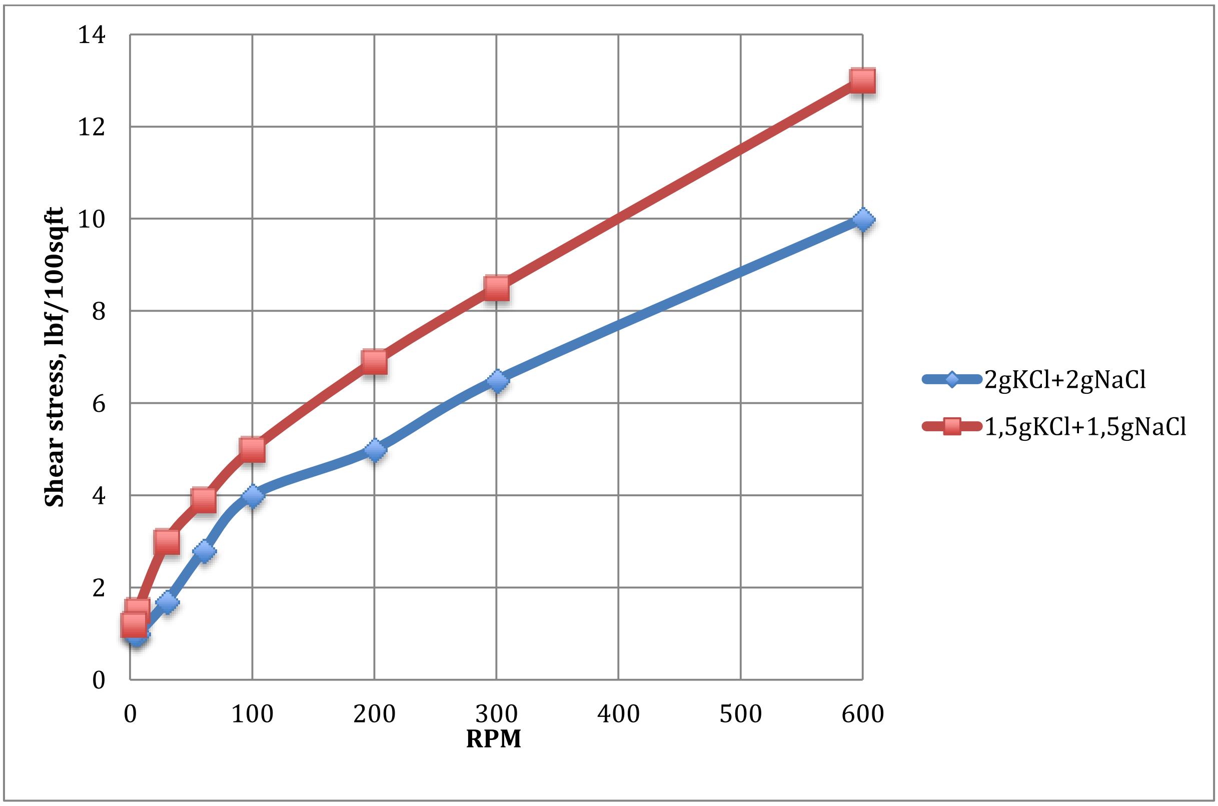

Ref: 500 ml H_2O, 25g bentonite, 0,5 PAC, 0,2g nano silica		
Parameters	**Ref + 2g KCl + 2g NaCl**	**Ref + 1,5g KCl + 1,5g NaCl**
PV (cP)	3,5	4,5
YS (lbf/100sqft)	3	4
LSYS(lbf/100sqft)	1	0,9
k(lbf.s^n/100sqft)	0,1	0,2
n []	0,6	0,6
Filtrate loss [ml]	5,5	5,4
pH	8,9	8,95

Appendix G: Effect of PAC concentration

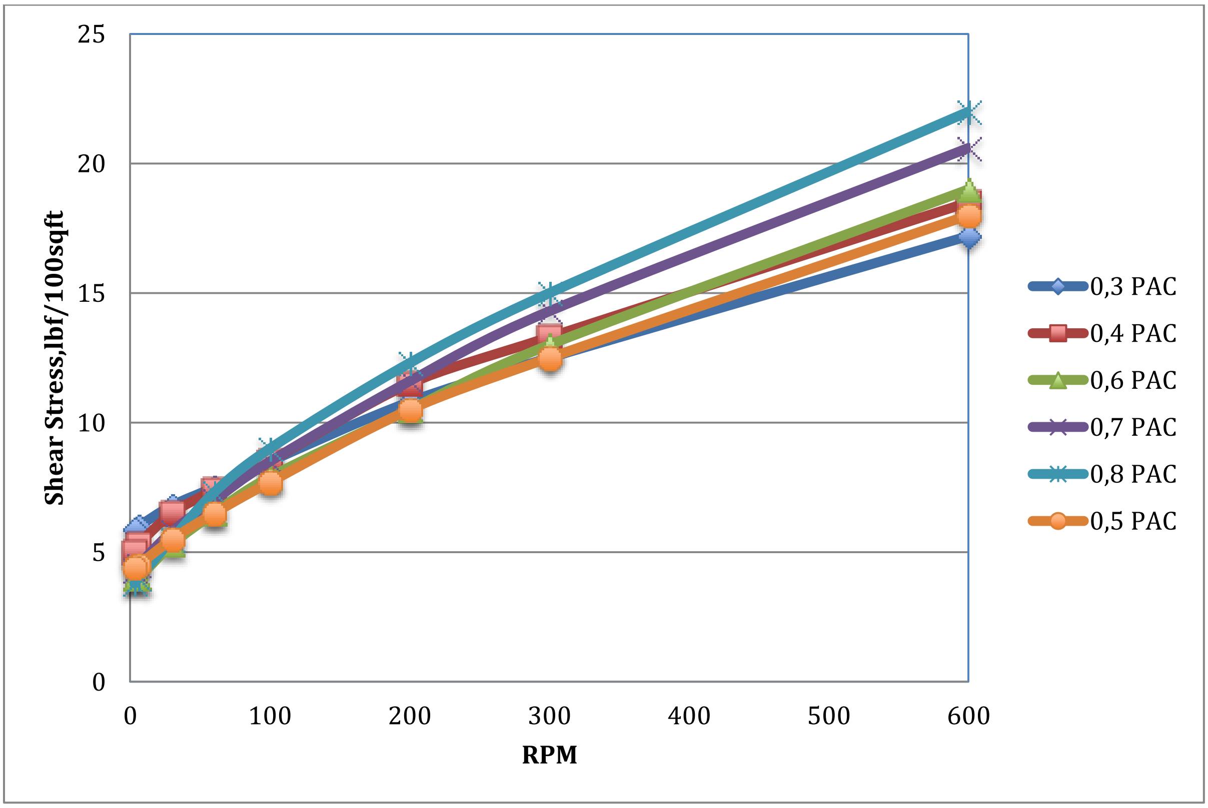

Ref: 500 ml H_2O, 25g Bentonite, 1g, KCl, 1g NaCl						
Parameters	**Ref +0,3g PAC**	**Ref +0,4g PAC**	**Ref +0,6g PAC**	**Ref +0,7g PAC**	**Ref +0,8g PAC**	**Ref +0,5g PAC**
PV (cP)	4,7	5,2	6	6,3	7	5,5
YS (lbf/100sqft)	7,8	8,1	7	8	8	7
LSYS(lbf/100sqft)	5,8	4,7	4	4,1	3,6	4,3
k(lbf.s^n/100sqft)	0,709	0,684	0,429	0,537	0,479	0,471
n []	0,460	0,476	0,547	0,526	0,552	0,526
Filtertap	5,5	5,25	4,5	4,3	4	5,2
PH	9	9,1	9,15	9,05	9,05	9,05

Appendix H: Effect of PAC concentration on ex-situ nano silica

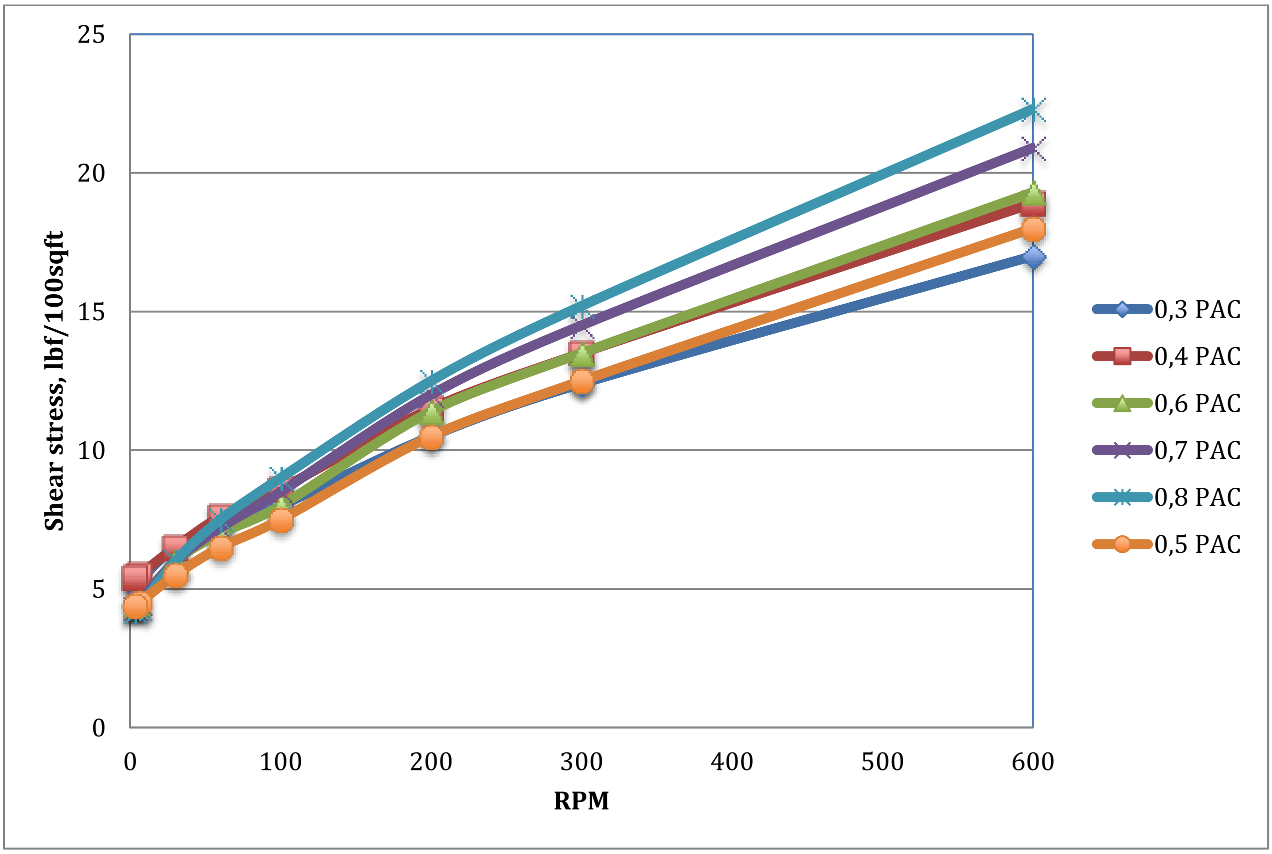

Ref: 500 ml water, 25 g bentonite, 1g Kcl, 1g NaCl, (+0,2g nano silica ex situ)						
Parameters	**0,3gm PAC**	**0,4gm PAC**	**0,6gm PAC**	**0,7gm PAC**	**0,8gm PAC**	**0,5gm PAC**
PV (cP)	4,6	5,4	5,8	6,4	7,1	5,5
YS (lbf/100sqft)	7,8	8,1	7,7	8,1	8,1	7
LSYS(lbf/100sqft)	5,1	5,3	4,3	4,1	4,1	4,3
k(lbf.s^n/100sqft)	0,727	0,655	0,543	0,542	0,484	0,471
n []	0,455	0,485	0,515	0,527	0,553	0,526
PH	8,7	8,85	8,85	8,75	8,75	9,1
Filtrate, ml	5	4,4	4,15	4	4	5,2

Appendix I: In situ nano, variating PAC concentration

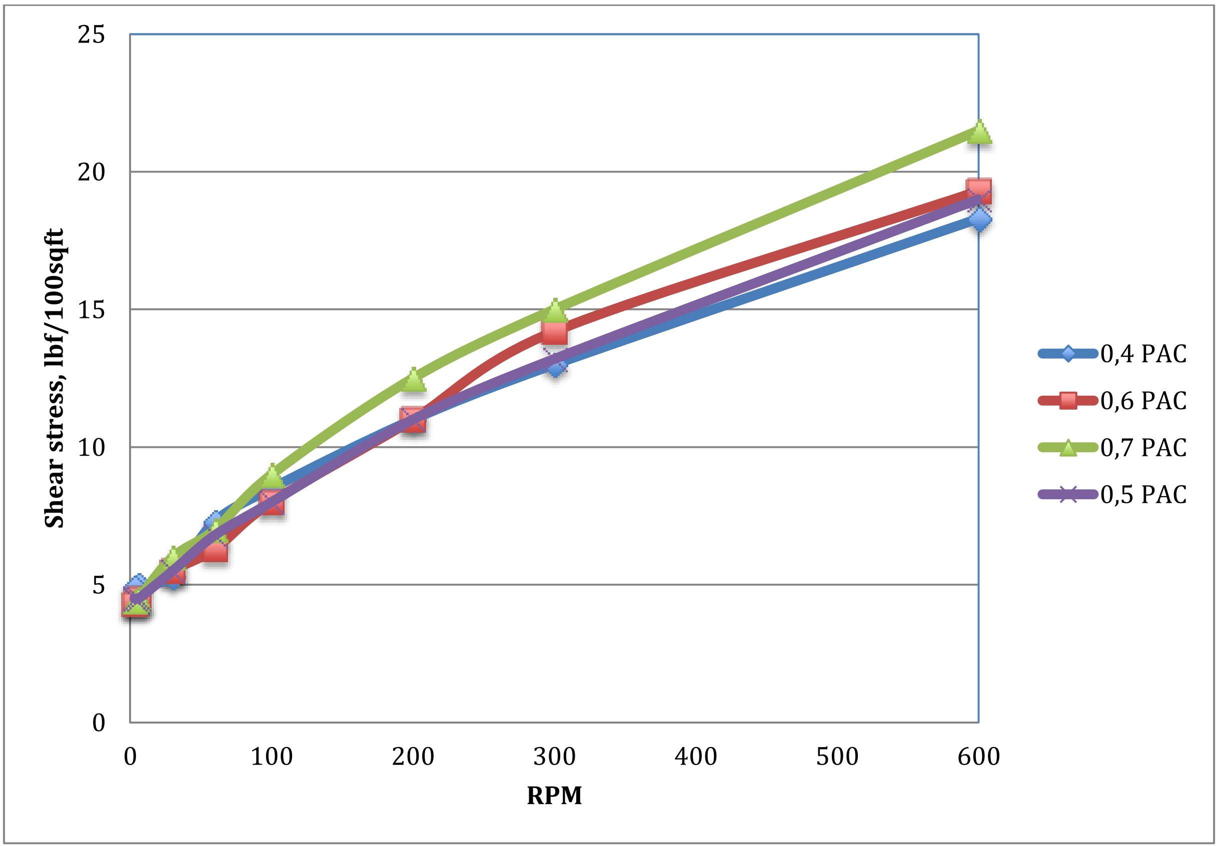

Ref: 500 ml water, 25g bentonite, 1g KCl, 1g NaCl, 0,2g Nano silica				
Parameters	**Ref +0,4g PAc**	**Ref +0,6g PAC**	**Ref +0,7g PAC**	**Ref +0,5g PAC**
PV (cP)	5,3	5,1	6,5	5,8
YS (lbf/100sqft)	7,7	9,1	8,5	7,4
LSYS(lbf/100sqft)	4,8	4,1	4,3	4,5
k(lbf.s^n/100sqft)	0,601	0,899	0,589	0,499
n []	0,493	0,442	0,519	0,525
Filtertap [ml]	4,6	4,40	4,5	4,75
PH	8,95	8,95	9	

Appendix J: Effect of nano silica concentration

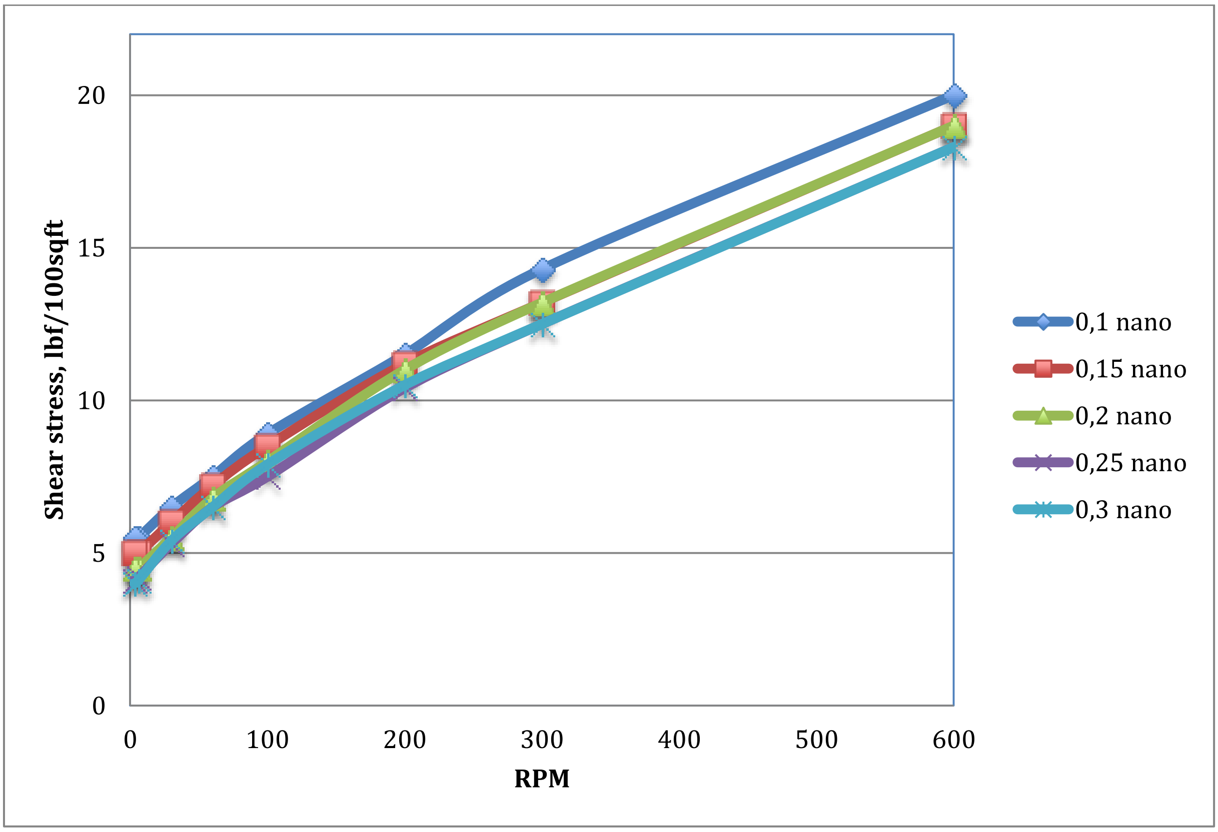

Ref: 500 ml Water, 25g Bentonite, 1g KCl, 1g NaCl, 0,5g PAC					
Parameters	**Ref +0,1 nano**	**Ref +0,15 nano**	**Ref +0,20 nano**	**Ref +0,25 nano**	**Ref + 0,30 nano**
PV (cP)	5,7	5,8	5,8	5,8	5,8
YS (lbf/100sqft)	8,6	7,4	7,4	6,7	6,7
LSYS(lbf/100sqft)	5,5	5	4,5	4	3,9
k(lbf.s^n/100sqft)	0,700	0,499	0,499	0,406	0,406
n []	0,484	0,525	0,525	0,550	0,550
pH	9,05	9,05	9,9	9,05	9
Filtrate loss [ml]	4,35	4,75	4,75	4,5	5

Appendix K: Effect of KCl concentration

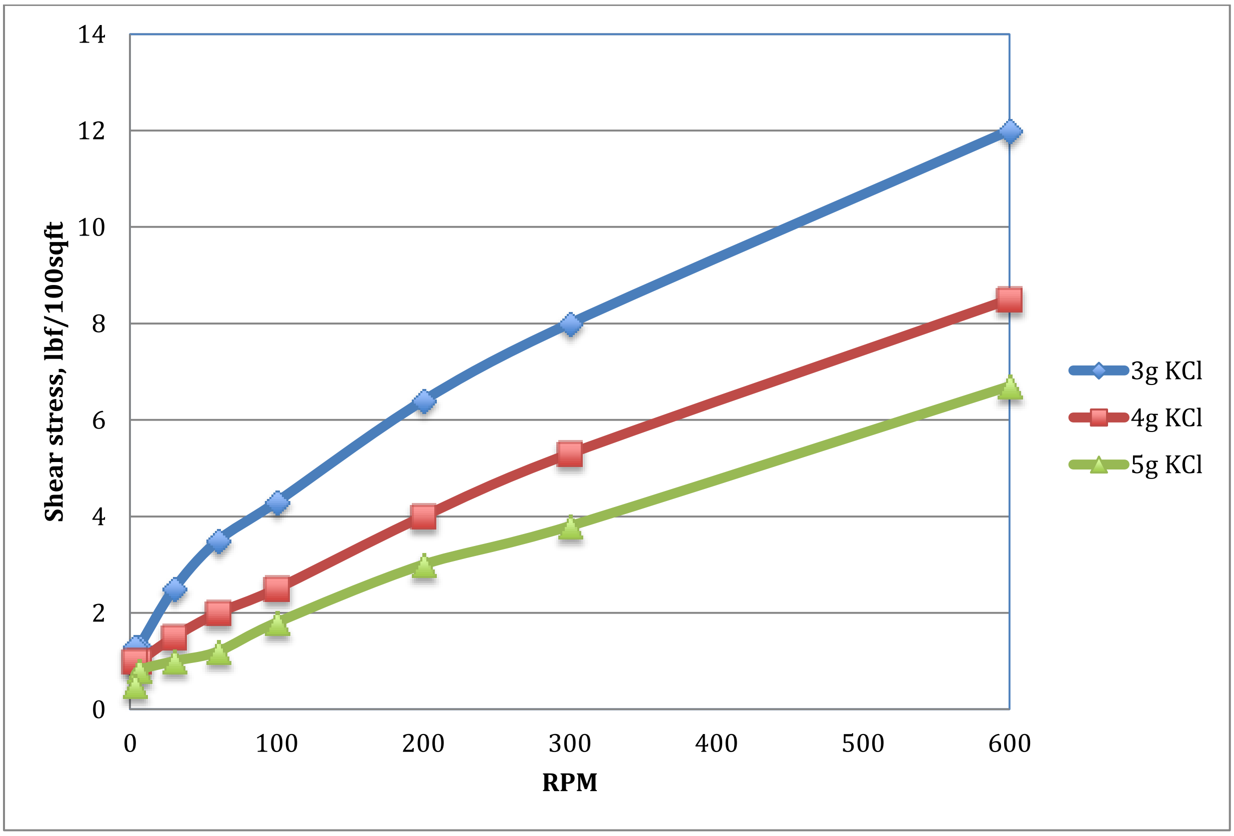

Ref: 500 ml water, 25g bentonite, 0,35g PAC, 0,15 duovis,			
Parameters	Ref +3 KCl	Ref + 4 KCl	Ref + 5 KCl
PV (cP)	4	3,2	2,9
YS (lbf/100sqft)	4	2,1	0,9
LSYS(lbf/100sqft)	1,3	1	0,2
k(lbf.s^n/100sqft)	0,209	0,076	0,023
n []	0,585	0,681	0,818
pH	8,9	8,75	8,7
Filtrate loss [ml]	5,3	5,5	5,5

Appendix L: Effect of ex-situ DUOVIS polymer additives

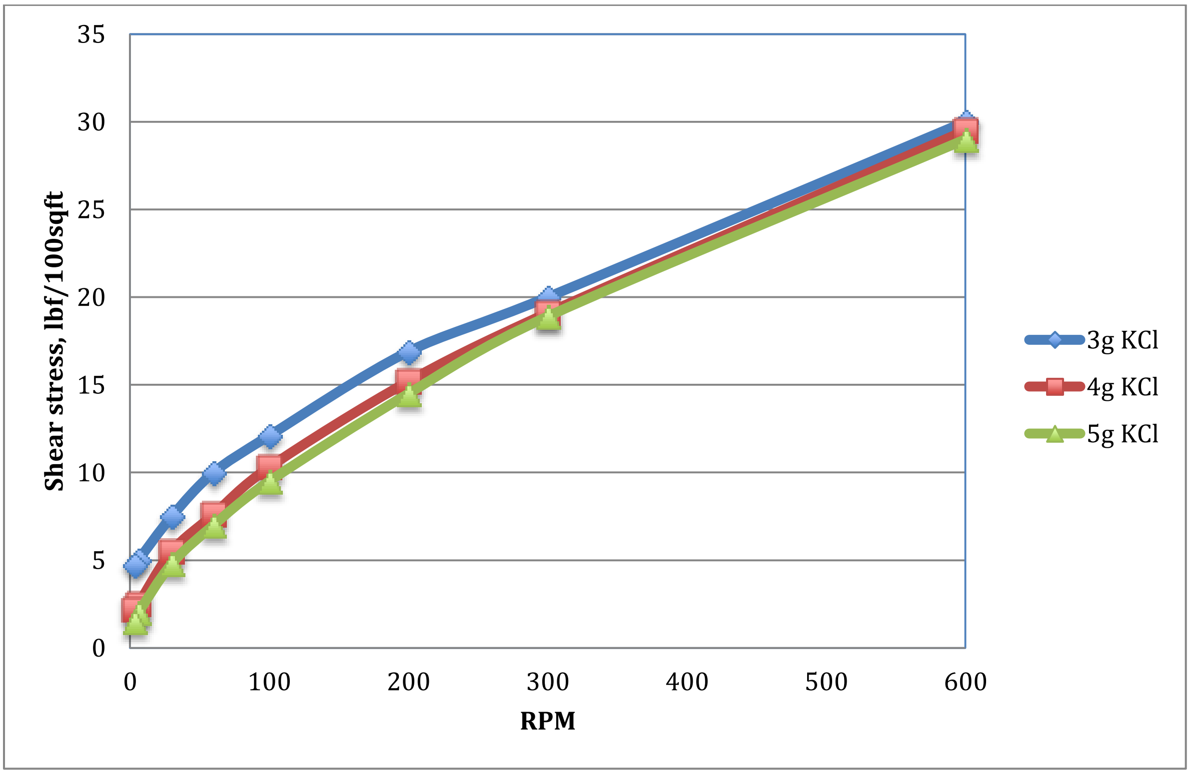

Ref: 500 ml water, 25 g bentonite, 0,15 duovis, 0,35 pac			
Parameters	Ref+ 3KCl+(0,5 g duovis, ex situ)	Ref + 4KCl+(0,8 g duovis, ex situ	Ref + 5KCl+(0,1 g duovis, ex situ
PV (cP)	10	10,4	10,1
YS (lbf/100sqft)	10	8,7	8,8
LSYS(lbf/100sqft)	4,4	1,9	1
k(lbf.s^n/100sqft)	0,522	0,383	0,402
n []	0,585	0,627	0,617
pH	8,6	8,5	8,5
Filtrate loss [ml]	4,45	3,5	4,6

Appendix M: Effect of Ex-situ Duovis and Ex-situ nano additives

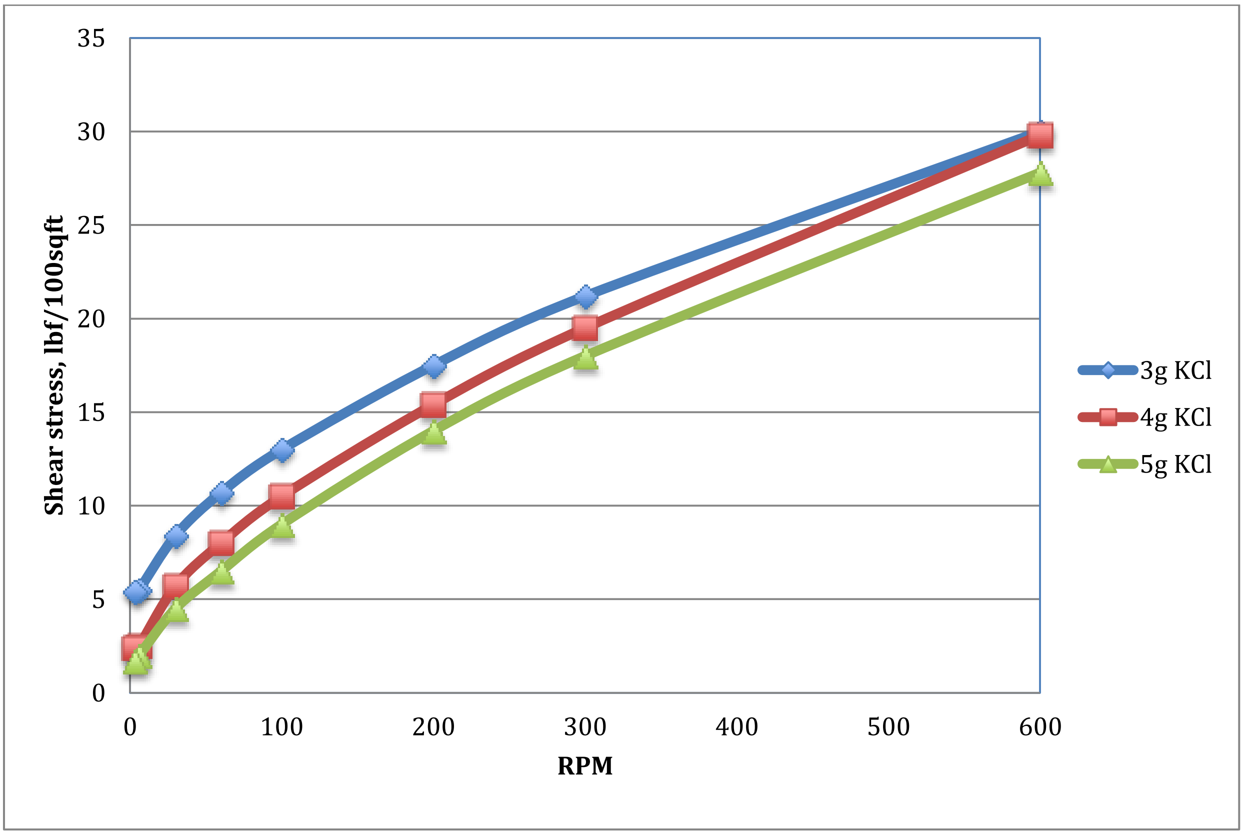

Ref:500 ml water, 25g bentonite, 0,15 duovis, 0,35 pac			
Parameters	**Ref+ 3 kcl, + (0,5gm duovis+ 0,2 nano ex situ)**	**Ref+ 4 kcl, + (0,8gm duovis+ 0,2 nano ex situ)**	**Ref+ 5 kcl, + (1gm duovis+ 0,2 nano ex situ)**
PV (cP)	8,8	10,3	9,8
YS (lbf/100sqft)	12,4	9,2	8,2
LSYS(lbf/100sqft)	5,3	2,3	1,4
k(lbf.s^n/100sqft)	0,934	0,430	0,361
n []	0,501	0,611	0,627
pH	8,45	8,4	8,3
Filtrate loss [ml]	3,45	4,25	4,3

Appendix N: Effect of DUOVIS/PAC, & KCl in various nano additives

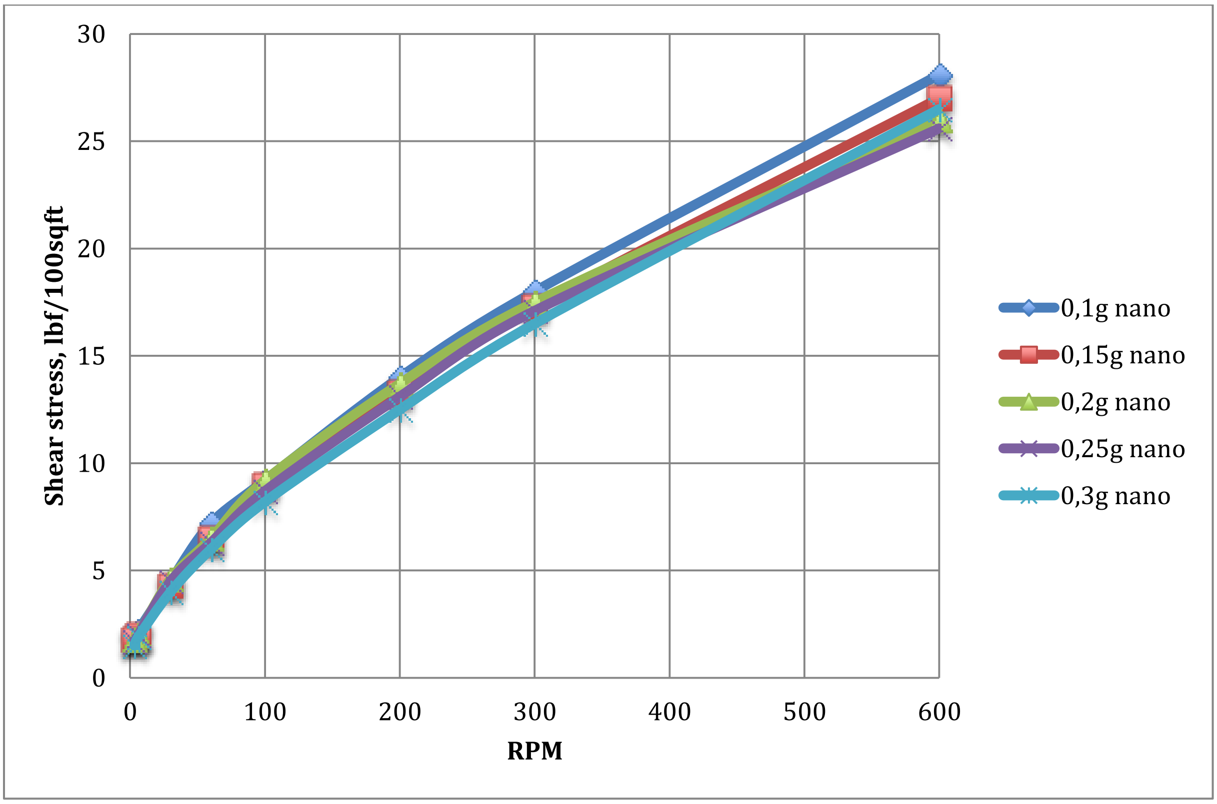

Ref: 500 ml water, 25g bentonite, 0,95g duovis, 0,35g PAC, 4g KCl					
Parameters	Ref+ 0,1g nano	Ref+ 0,15g nano	Ref+0,20g nano	Ref+0,25g nano	Ref+0,30g nano
PV (cP)	10,1	9,7	8,5	8,5	10
YS (lbf/100sqft)	7,9	7,6	9	8,6	6,5
LSYS(lbf/100sqft)	1,8	1,6	1,6	1,4	1,1
k(lbf.s^n/100sqft)	0,328	0,316	0,498	0,454	0,233
n []	0,642	0,642	0,571	0,582	0,683
pH	8,75	8,8	8,75	8,75	8,65
Filtrate loss [ml]	3,5	4,5	4,25	3,5	5

Appendix O: Effect of nano and PAC on DUOVIS mud system

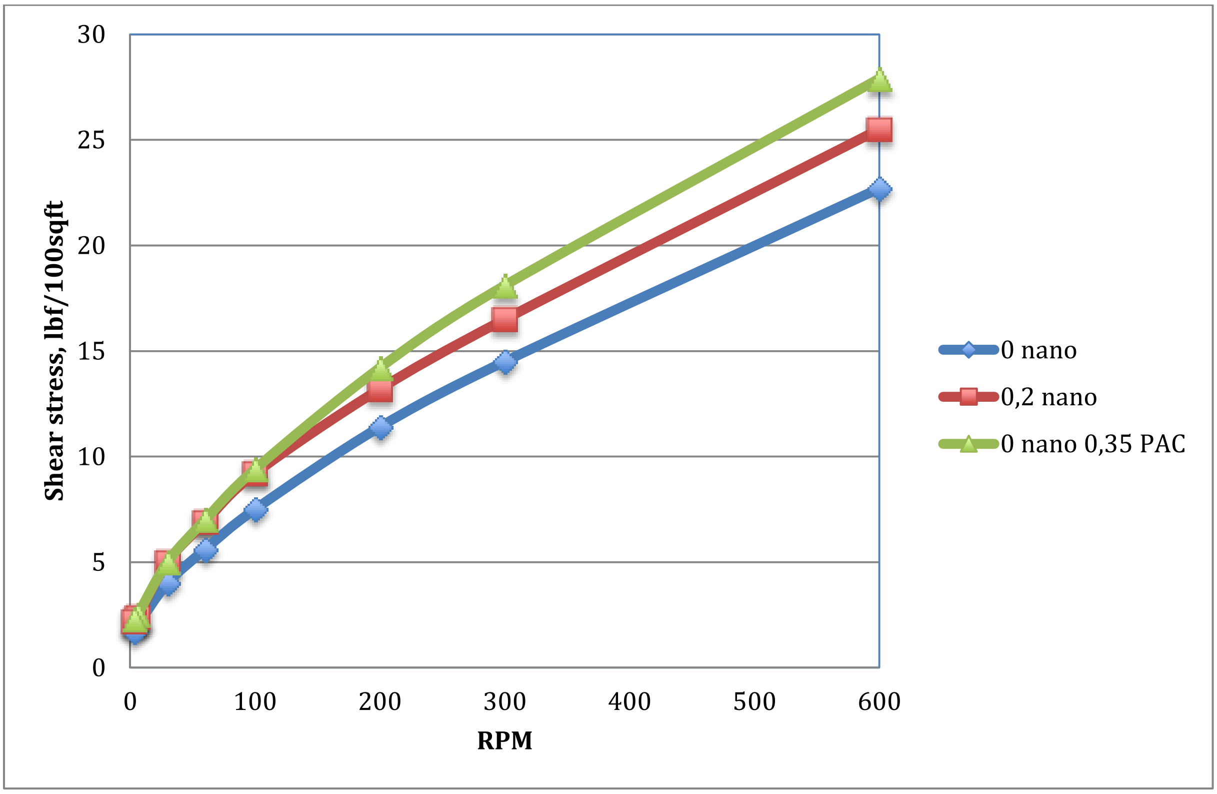

Ref: 500 ml water, 25gm bentonite, 0,95gm duovis, 4gm KCl			
Parameters	**Ref**	**Ref+0,2g nano**	**Ref+0,35g PAC**
PV (cP)	8,2	9	9,8
YS (lbf/100sqft)	6,3	7,5	8,3
LSYS(lbf/100sqft)	1,4	2	2,1
k(lbf.s^n/100sqft)	0,258	0,329	0,370
n []	0,646	0,628	0,624
pH	8,9	8,8	8,8
Filtrate loss [ml]	4,25	3,95	3,5

Appendix P: Various DUOVIS and CMC mud systems

#1	500ml water, 25g bentonite, 0,95g Duovis, 0,35g CMC, 4g KCl
#2	500ml water, 25g bentonite, 0,4g Duovis, 0,3g CMC, 4g KCl
#3	500ml water, 25g bentonite, 0,95g Duovis, 4g KCl, 0,2g nano, (0,75g Na2CO3 ex sithu)
#4	500ml water, 25g bentonite, 0,95g Duovis, 0,35g PAC, 4g KCl, (2g Na2SO4 ex sithu)
#5	500ml water, 25g bentonite, 0,95g Duovis, 4g KCl, (0,5g NaHCO3 ex sithu)

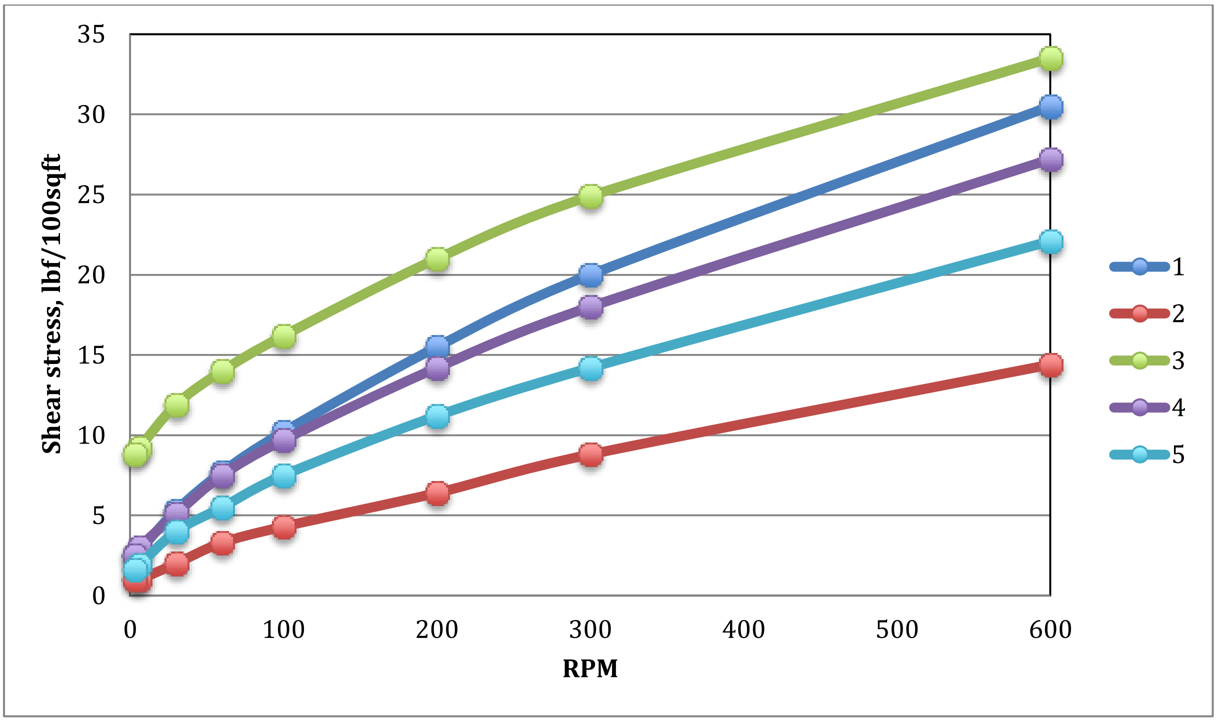

Parameters	Mud 1	Mud 2	Mud 3	Mud 4	Mud 5
PV (cP)	10,5	5,6	8,6	9,2	7,9
YS (lbf/100sqft)	9,5	3,2	16,3	8,8	6,3
LSYS(lbf/100sqft)	2,2	1	8,4	2	1,3
k(lbf.s^n/100sqft)	0,450	0,105	1,728	0,440	0,266
n []	0,608	0,710	0,428	0,595	0,638
pH	8,9	8,95	10	8,75	8,45
Filtrate loss [ml]	4,45	5,5	4,5	3,2	5,05

Appendix Q: Effect of Ex situ nano and Na_2CO_3

Mud#1	500ml water, 25g bentonite, 0,4g Duovis, 0,3g CMC, 4g KCl, (0,2g nano, 0,75g Na2CO3 ex sithu)	
Mud#2	500ml water, 25g bentonite,0,95g Duovis, 0,35g CMC, 4g KCl,(0,2g nano, 0,75g Na2CO3 ex sithu)	
Mud#3	500ml water, 25g bentonite,0,4g Duovis, 0,3g CMC, 4g KCl	(#2 from earlier)
Mud#4	500ml water, 25g bentonite,0,95g Duovis, 0,35g CMC, 4g KCl	(#1 from earlier)

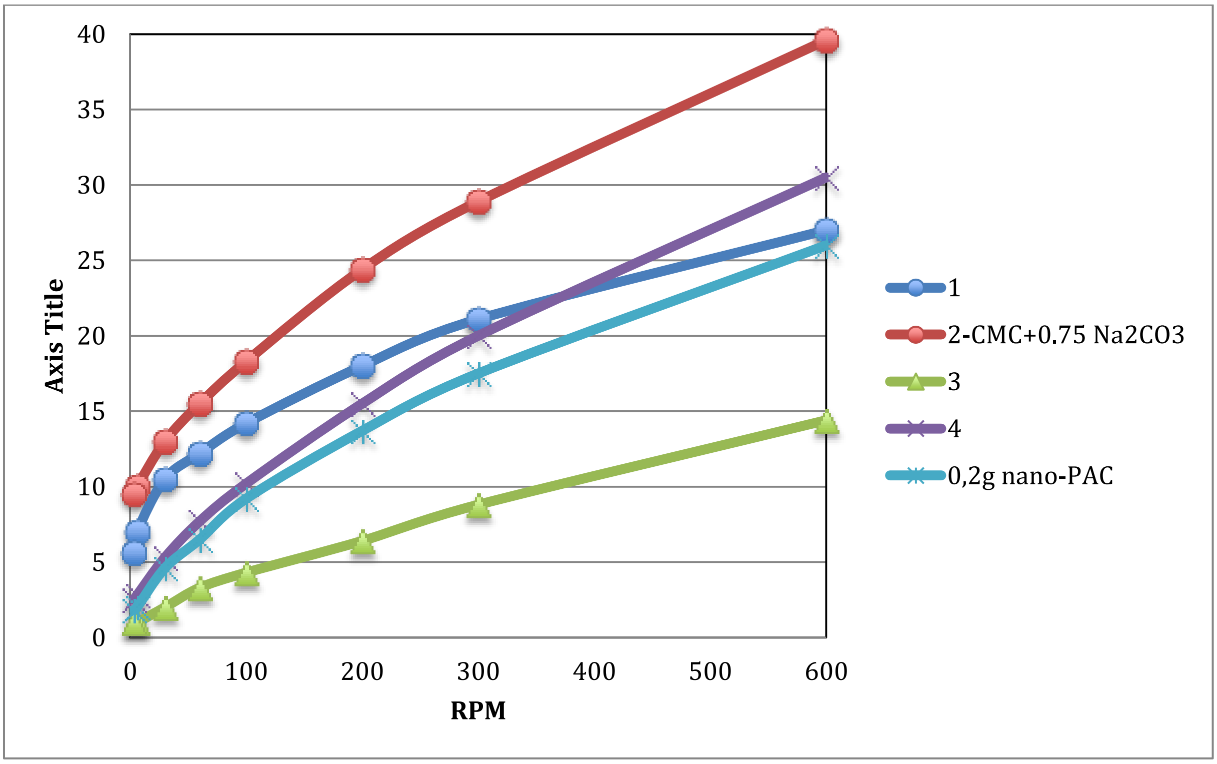

Parameters	Mud 1	Mud 2	Mud 3	Mud 4
PV (cP)	5,9	10,7	5,6	10,5
YS (lbf/100sqft)	15,2	18,2	3,2	9,5
LSYS(lbf/100sqft)	4,2	9	1	2,2
k(lbf.s^n/100sqft)	2,298	1,701	0,105	0,450
n []	0,356	0,454	0,710	0,608
pH	10	10,05	8,95	8,9
Filtrate loss [ml]	5,5	4	5,5	4,45

Appendix R: Effect of Xanthan gum (XC)

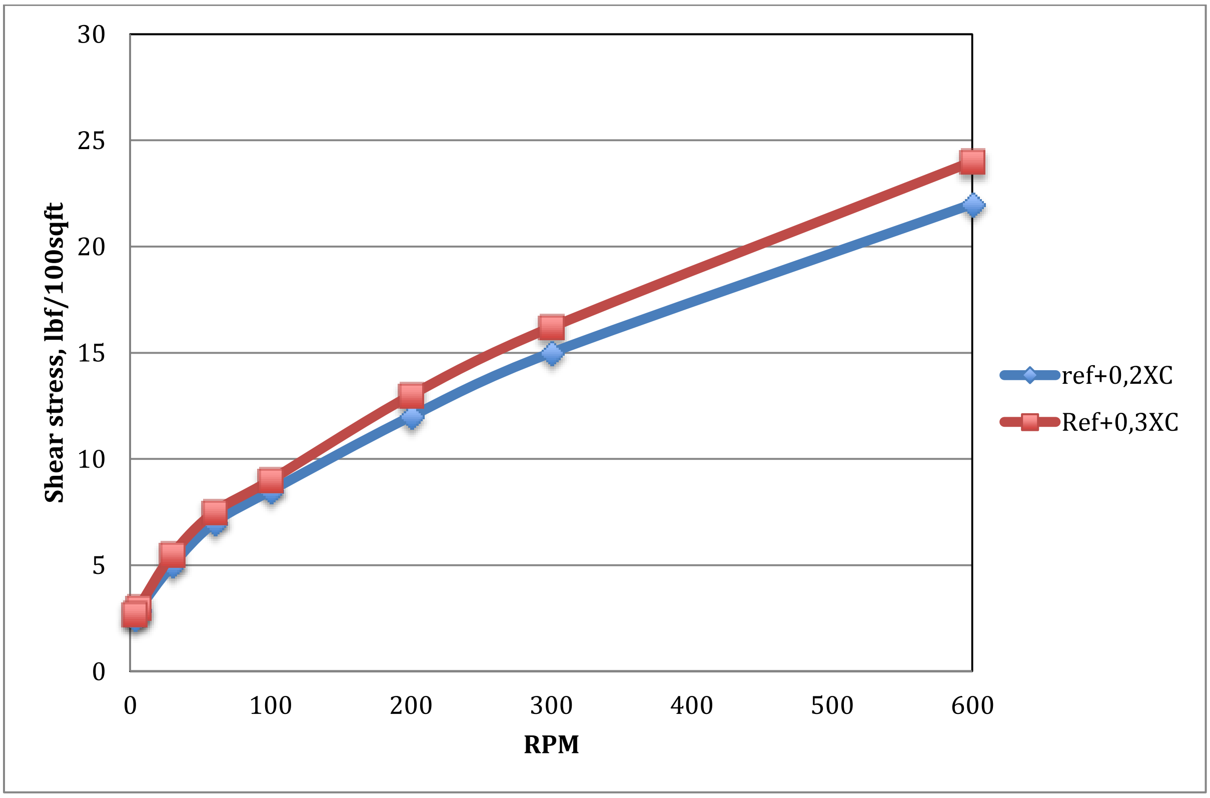

Ref: 500 ml water, 25g bentonite, 4g KCl, 0,95g Drispac, 0,75g na2co3		
Parameters	**Ref+0,2XC**	**Ref+0,3XC**
PV (cP)	7	7,8
YS (lbf/100sqft)	8	8,4
LSYS(lbf/100sqft)	2,1	2,4
k(lbf.s^n/100sqft)	0,479	0,473
n []	0,552	0,567
pH	10,1	10,1
Filtrate loss [ml]	4,5	4,5

Appendix S: Effect of Drispac and CMC in various nano silica and ex-situ Na_2CO_3

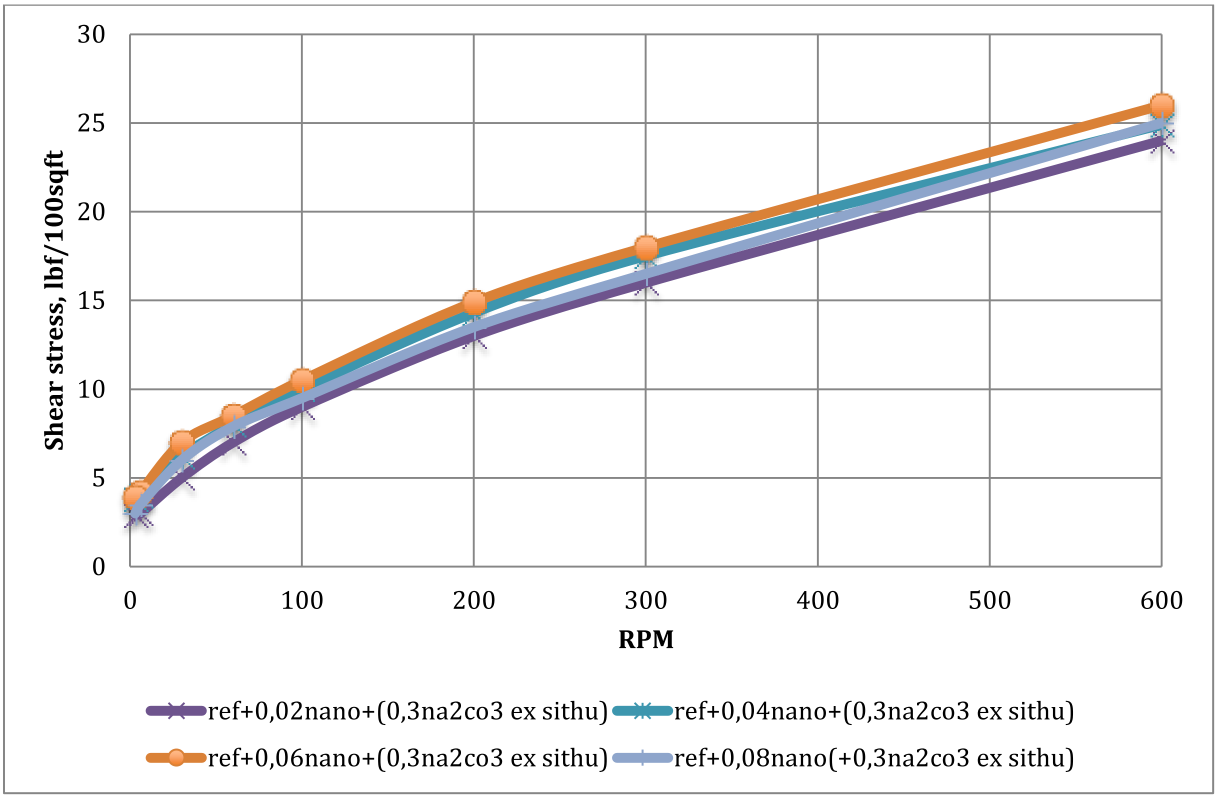

Ref:500 ml water, 25g bentonite, 4g KCl, 0,95g drispac, 0,35g CMC, (0,75+0,3 na2co3 ex situ)				
	Ref+0,02g nano ex situ	Ref+0,04g nano ex situ	Ref+0,06g nano ex situ	Ref+0,08g nano ex situ
PV (cP)	8	7,4	8	8,5
YS (lbf/100sqft)	8	10,1	10	8
LSYS(lbf/100sqft)	2,8	3,6	3,6	2,5
k(lbf.s^n/100sqft)	0,418	0,734	0,660	0,393
n []	0,585	0,508	0,530	0,599
pH	10,15	10,15	10,15	10,15
Filtrate loss [ml]	4,5	4,3	4	5,25

List of Figures

List of Tables

List of symbols

A	Surface area of cake, m^2
A	Static leak-off, $m^3/s^{0.5}$
B	*D*ynamic leak-off, m^3/s
C	Robertson and Stiff stain correction, 1/s
C_d	Bit discharge coefficient which is normally set equal to 0.95.
D	Hydraulic diameter of the pipe, m
G'	Elastic/storage modulus, Pa
G''	Loss /Viscous modulus, Pa
h_{mc}	Thickness of mud cake
k	Consistency factor, lbf/100sqft
n	Flow index, a power law exponent.
ΔP_a	Pressure loss, Pa
TVD	True vertical depth, m
k	Permeability of mud cake,
ΔP	Differential pressure across mud cake, Pa
t	time of filtrate testing, s
V_C	Cumulative filtrate volume per unit area, cm^3/cm^2
Vsp	Spurt loss, ml
$\bar{V}$	Mean fluid velocity, m/s
μ	Dynamic viscosity of the fluid (Pa·s or N·s/m² or kg/m·s)
ρ	Density of the fluid (kg/m^3)
ρ_{st}	Static mud density (ppg)
γ	Shear rate , 1/s
τ	Shear stress, lbf/100sqft
τ_y	Yield point, lbf/100sqft
μ_p	Plastic viscosity, cP
δ	Phase angle (degree)

List of Abbreviations

API	American Petroleum Institute
CMC	Carboxymethyl Cellulose
ECD	Equivalent circulation density
LVER	Linear Viscoelastic Region
PAC	Polyanionic cellulose
PV	Plastic viscosity
YS	Yield stress
LSYS	Lower shear yield stress
ROP	Rate of Penetration
RPM	Revolutions per minute
SEM	Scanning Electron Microscopy
TVD	True Vertical Depth
XC	Xanthan Gum
YP	Yield Point
ppb	Pounds per (oil) Barrel
ppg	Pounds per gallon
gpm	Gallon per minute